A Study on High-Resolution Direction-of-Arrival Estimation Algorithms for Array Antenna Systems

February 2017

Hirotaka Hayashi

A Thesis for the Degree of Ph.D. in Engineering

A Study on High-Resolution Direction-of-Arrival Estimation Algorithms for Array Antenna Systems

February 2017

Graduate School of Science and Technology
Keio University

Hirotaka Hayashi

Acknowledgments

First of all, I would like to express my special appreciation and thanks to my supervisor Prof. Tomoaki Ohtsuki whose support and encouragement made this research possible. I am deeply grateful for all his guidance and advice that helped improve the quality of this dissertation.

I would also like to thank my dissertation committee members, Prof. Iwao Sasase, Prof. Masaaki Ikehara, and Prof. Yukitoshi Sanada, for their encouragement and insightful comments.

I would like to thank all of Ohtsuki Lab members for all the help and great support. My sincere thanks also go to Assistant Prof. Kentaroh Toyoda for his advice writing this dissertation. I would also like to thank Dr. Jihoon Hong for his great support.

I would like to express my appreciation to Ministry of Defense and my colleagues for giving me this opportunity.

I would like to express my gratitude to Keio Leading Edge Laboratory (KLL) at Keio University, Ph.D. Student Research Support programs, for offering the research grants to support my research activities.

Last but not least, I would like to express my appreciation to my family. Most especially, I am very grateful to my wife, Yuko, who have always given me a great support and encouragement.

Contents

List of Figures

List of Tables

Acronyms

CBR

Cramér-Rao Bounds

CSSM

Coherent Signal Subspace Method

DBF

Digital Beam Forming

DFT

Discrete Fourier Transform

DML

Deterministic Maximum Likelihood

DOA

Direction of Arrival

DOF

Degree of Freedom

ESPRIT

Estimation of Signal Parameters via Rotational Invariance Techniques

EVD

Eigenvalue Decomposition

ISSM

Incoherent Signal Subspace Method

KR

Khatri-Rao

MIMO

Multiple Input Multiple Output

MODE

Method of Direction Estimation

MUSIC

Multiple Signal Classification

PRI

Pulse Repetition Interval

SML

Stochastic Maximum Likelihood

SSP

Spatial Smoothing Processing

TOFS

Test of Orthogonality Frequency Subspace

TOPS

Test of Orthogonality Projected Subspace

ULA

Uniform Linear Array

WAVES

Weighted Average of signal Subspaces

WSF

Weighted Subspace Fitting

Notation & Symbols

Notation

Bold faces lowercase letters : Vectors

Bold faces uppercase letters : Matrices

The superscripts T : Transpose

The superscripts H : Complex conjugate transpose

Symbols

$vec(\cdot)$

: vectorization operation

$\otimes$

: Kronecker delta product

$|\cdot|$

: Absolute value

$E[\cdot]$

: Expectation operator

Chapter 1

Introduction

1.1 Background

In recent years, remarkable enhancement of radio frequency (RF) devices has been seen with explosive popularization of communication systems [1]. Those technologies can improve not only communication systems but also RF sensor systems, e.g., radar systems, sonar systems, seismic systems, electronic surveillance systems, medical diagnosis, and treatment systems [2, 3]. However, radio environments in real world are very complicated and time-varying with increase in RF devices use [1, 2].

To realize high reliable RF sensor systems under the condition of the complicated radio environments described above, it is an important task to estimate the number and direction-of -arrival (DOA) of the incoming signal sources accurately without time delay. In particular, it follows that classifying closely spaced signal sources is the major work, to avoid interferences which cause negative effects on the performance of the RF sensor systems [2]. In general, RF sensor systems consist of an antenna (an array antenna or a single antenna), RF circuits, an analog-to-digital converter and a signal processor, etc. From perspective of improvement of DOA estimation performance, array signal processing is one of the most important research topics to distinguish the incoming multiple signal sources.

Actually, an array antenna has been widely used to solve direction finding [1–3]. Therefore DOA estimation methods with array antenna have received a significant

amount of attention for the decades, and many researches on DOA estimation have been deeply investigated from various perspectives, e.g., improving the DOA estimation accuracy, increasing degree-of-freedom (DOF), dealing with coherent signal sources, and reducing computational complexity [4–8].

The well-known nonparametric DOA estimation methods are beamforming [4–6], Capon [9], and subspace based approach e.g., multiple signal classification (MUSIC) [10]. Root-MUSIC [11] and estimation of signal parameters via. rotational invariance techniques (ESPRIT) [12], which require the assumption that the array is uniform linear array (ULA), are low complexity methods. The parametric approach based on maximum likelihood method [13, 14] shows higher estimation accuracy than that of nonparametric methods, however, they require high computational complexity. For each method, the lower bound of estimation accuracy has also been well investigated, e.g., Cramér-Rao Bounds (CRB) [15, 16].

In the radar community, multiple input multiple output (MIMO) array has received much attention from the aspect of DOA estimation performance, because MIMO radar presents several advantages compared to common phased array radars [17–23]. In particular, one of the advantages of MIMO radar is that the DOF can be greatly increased by the concept of virtual array [17, 18]. The virtual array formed by MIMO array where transmit antennas use orthogonal transmit waveforms can also expand the aperture size. Therefore, MIMO radar can also provide high estimation accuracy of the DOA owing to the virtual array [17, 24].

Recently, a novel approach to estimate DOA of incoming signal sources by using temporal spatial virtual array has been proposed with MIMO array [25]. Although the method has some issues that need to be solved, it can generate additional virtual array other than MIMO virtual array and improve DOA estimation performance.

Furthermore, to improve communication capacity, the communication devices dealing with wideband signals are pervasive [1]. Of course, in RF sensor systems, e.g., radar systems and electronic surveillance systems, wideband signals have been also applied to improve system performance such as range resolution [26, 27]. Therefore, DOA estimation method for wideband signal sources should be in consideration

to realize performance improvement of RF sensor systems in the environment with complex radio signals, which will behave as the interference signals for the user of the sensor systems.

As described above, because of its wide-ranging applications and difficulty of realizing an optimum estimator under the complex radio environment, researches on DOA estimation method will continue in the future [8].

Based on the background, this dissertation focuses on the two topics related to DOA estimation of multiple signal sources with an array antenna; The first topic is DOA estimation by using temporal spatial virtual array. The second topic is DOA estimation of wideband signal sources. The following subsection shows the detailed objective of each research topic.

1.2 Objectives

1.2.1 DOA Estimation by Using Temporal Spatial Virtual Array

As mentioned in Section 1.1, MIMO array has received much attention in recent years because of its high estimation accuracy of DOA [17, 24]. Also, high-resolution DOA estimation techniques for instance MUSIC [10], Root-MUSIC [11], and ESPRIT [12], have been applied to various RF sensor systems including MIMO radar [28, 29].

Researches on the optimization of array geometry have attracted attention to realize improvement of DOA estimation performance. The ULA which is the simplest and most-popular antenna array configuration has limitation of DOF which depends on the number of antenna elements. Therefore, non-uniform linear array configurations are proposed to increase DOF and improve DOA [30–33]. However, these approaches use the fixed array configuration and the DOA estimation performance of them depends on the configuration.

The limitation of resolution performance of MIMO radar with these high-resolution methods and array configuration are also well investigated [33–35]. Based on the facts,

the other approaches are required to realize further improvement of DOA estimation performance.

Recently, a novel approach to improve DOA estimation accuracy by using an additional virtual array which is referred to as temporal spatial virtual array was proposed [25]. The method provides the further enhancement of the DOA estimation accuracy. Temporal spatial virtual array is formed by using pulse responses received at different time as if they are received at same time. This method generates additional virtual arrays other than MIMO virtual array without modifying the actual array structure. However, to form temporal spatial virtual array and estimate the DOA of a target using it, the method requires the pre-estimated parameters of the target: its velocity and its direction. This means that the arrangement of the temporal spatial virtual array depends on the velocity and the direction of the single target on which we focus. Therefore, it is difficult to implement the method if there are several targets in the search space. There are other problems that remain to be solved. One is interference from other targets. Another is a mismatch between the steering vectors based on the pre-estimated target parameters and the received signal.

In this dissertation, to solve these problems, we propose a new DOA estimation method by using the temporal spatial virtual array based on output signals of Doppler filter with adaptive pulse repetition interval (PRI) control. The proposed method provides accurate DOA estimation by using output signals of Doppler filter with adaptive PRI control technique. The performance of the proposed method is compared with that of the conventional method via computer simulations with detailed performance analysis. The simulation results show that the new DOA estimation method performs better than the conventional method.

1.2.2 DOA Estimation for Wideband Signal Sources

DOA estimation for wideband signals has been also attracting much attention for decades, because wideband signals are commonly used in real world for such as signal source localization in wireless communication and radar systems [1, 3]. To improve DOF and accuracy of DOA estimation, many researches on wideband DOA estimation

have also been introduced over several decades [2]. DOA estimation methods for narrowband signals cannot be applied directly to wideband signals, because the phase difference between array antennas depends on not only the DOA of the signals but also the temporal frequency. Thus, the common pre-processing for wideband signal estimator decomposes a wideband signal into some narrowband signals using filter banks or discrete Fourier transform (DFT). Based on the method, many algorithms have been introduced and they are categorized into two groups: incoherent signal subspace method (ISSM) [36, 37] and coherent signal subspace method (CSSM) [38].

ISSM is one of the simplest wideband DOA estimation methods. ISSM uses several narrowband signals decomposed from wideband signal incoherently [37]. In particular, the method applies narrowband DOA estimation techniques, such as MUSIC [10], independently to the narrowband signals. Then, these results are averaged to estimate the DOA of incoming wideband signal sources. Although ISSM provides better estimation accuracy in high signal-to-noise ratio (SNR) regions, the performance deteriorates when the SNR of some frequency bands are low. In other words, the poor estimates from some frequency bands will degrade the final estimation accuracy.

To overcome these disadvantages and to improve DOA estimation performance, CSSM was proposed [38]. In CSSM processing, the correlation matrix of each frequency band is focused by transformation matrices and the focused matrices are averaged to generate a new correlation matrix. Then CSSM estimates the DOA of incoming wideband signal sources by applying a DOA estimation method for narrowband signals. The key point of CSSM algorithm is how to focus correlation matrices. Many techniques have been proposed to obtain a proper focusing matrix [39, 40]. However, each focusing technique requires the initial values, which means the pre-estimated direction of incoming signal sources, and the performance of CSSM is sensitive to the initial values [41]. Weighted average of signal subspaces (WAVES) [42] is also a well-known DOA estimation method for wideband signal sources. However, WAVES also needs the initial DOA estimates and its performance greatly depends on the accuracy of the initial values.

A novel wideband DOA estimation method, which is named test of orthogonality

of projected subspaces (TOPS), was proposed [43]. TOPS uses the signal and noise subspaces of several frequency bands and provides good DOA estimation performance without requiring the initial values. However, the method has a drawback that the spatial spectrum calculated by TOPS algorithm has some false peaks and they make it difficult to estimate the true DOA of signal sources.

Squared TOPS was proposed as an improvement method of TOPS [44]. Squared TOPS improves DOA estimation performance by using the squared matrix for orthogonality test instead of the matrix to be tested in the signal processing of TOPS. The method provides higher DOA estimation accuracy and better resolution performance than those of TOPS. However, the undesirable false peaks in spatial spectrum remain.

Test of orthogonality of frequency subspaces (TOFS) was proposed as a new wideband DOA estimation method [45]. TOFS uses the noise subspaces of multiple frequency bands with the steering vector and shows high estimation accuracy when SNR is high. However, TOFS cannot resolve closely spaced signal sources when SNR is low.

Recently, Khatri-Rao (KR) subspace approach was proposed as the method to expand the array structure and to increase DOF [46]. Applying KR subspace approach to CSSM algorithm, some DOA estimation methods of wideband signal sources were proposed [47]. The methods achieve higher DOA estimation accuracy and resolution performance than the conventional CSSM even if there are fewer sensors or antennas than the incoming signal sources. However, it also requires the initial DOA estimate of each signal source.

Furthermore, sparse signal representation algorithms have also been received much attention, which can provide new approaches for wideband DOA estimation [48–51]. These DOA estimation methods based on the sparse signal representation perform higher resolution than the conventional methods without knowing the number of sources. However, there are some difficulties in selecting parameters to calculate optimal solutions.

In this dissertation, we propose a new DOA estimation method for wideband

signals called weighted squared TOPS (WS-TOPS) based on Squared TOPS. WS-TOPS also uses signal subspace and noise subspace of each frequency like Squared TOPS and does not require any initial values. Using modified squared matrix and selective weighted averaging process, WS-TOPS can suppress all false peaks in spatial spectrum and improve DOA estimation accuracy of wideband signal sources and also keep the same resolution performance as Squared TOPS. We also consider the low complexity version of WS-TOPS. The performance of the proposed method is compared with that of the conventional method via computer simulations. Simulation results show that the proposed method can provide good resolution performance and DOA estimation accuracy with low computational complexity.

1.3 Contribution of Dissertation

The contributions of this dissertation are summarized in Table 1.1. This dissertation has contributions in DOA estimation by using temporal spatial virtual array and DOA estimation of wideband signal sources.

For the DOA estimation by using temporal spatial virtual array, this dissertation has two major contributions: The first contribution is the achievement of the stable temporal spatial virtual array by using adaptive PRI control algorithm which takes into account the target information to calculate the optimal virtual array position. The algorithm can keep the optimal array arrangement of the temporal-spatial virtual array without depending on target movement and realize stable performance of DOA estimation. The second contribution is to realize the DOA estimation with the temporal spatial virtual array in the situation where there are multiple targets. The algorithm which uses output signals of Doppler filter with adaptive PRI control technique can eliminate the mismatches between the steering vectors based on the pre-estimated target parameters and the received signal. Therefore, the proposed method can provide accurate DOA of the focused target without deterioration caused by the signals from the other targets.

For the DOA estimation of wideband signal sources, this dissertation has three

contributions: The first contribution is the DOA estimation with the complete suppression of false peaks in spatial spectrum of the conventional methods. Unlike the conventional methods based on TOPS which can estimate DOA of incoming signal sources without requiring initial estimates, the proposed method, WS-TOPS, can completely suppress the false peaks by modifying the orthogonality test matrix. The second contribution is the improvement of DOA estimation performance in terms of estimation accuracy and probability of resolution which denotes the probability that all signal sources are resolved. By using all the signals in multiple frequency bands with appropriate weight parameters, WS-TOPS can achieve the better DOA estimation performances than those of the conventional methods. Moreover, as the third contribution, this dissertation shows the low computational complexity approach of the aforementioned WS-TOPS. While WS-TOPS can provide high DOA estimation performance, it requires high computational costs. The proposed method can reduce computational complexity with minimizing deterioration on DOA estimation performance.

Table 1.1: Contribution of this dissertation.

Chapter 3	
Purpose	DOA estimation by using temporal spatial virtual array with adaptive PRI control
Issue [25]	Deterioration of the DOA estimation accuracy by using temporal spatial virtual array based on the conventional method, which is caused by the movement of the focused target and the undesirable signals from the other targets.
Proposal [52, 53]	We propose two algorithms. The first one is the construction method of the stable temporal spatial virtual array with PRI control algorithm which can calculate the optimal virtual array adaptively. The second one is to use output signals of Doppler filter with adaptive PRI control technique, which can eliminate the mismatches between the steering vectors based on the pre-estimated target parameters and the received signal.
Achievement	Improvement of the DOA estimation accuracy of the moving targets with temporal spatial virtual array under the condition that there are multiple targets simultaneously.
Chapter 4 & Chapter 5	
Purpose	DOA estimation of wideband signal sources by weighted Squared TOPS
Issue [44]	The conventional method has some false peaks which cause miss estimation of signal source directions in spatial spectrum and suffers the DOA estimation accuracy.
Proposal [54, 55]	Chapter 4: We propose a weighted orthogonality test matrix approach to prevent miss estimation due to false peaks in spatial spectrum, and also the algorithm to improve the DOA estimation accuracy by averaging output of each frequency bins. Chapter 5: We consider a low complexity signal processing approach based on modified orthogonality test matrix with a little deterioration of the DOA estimation performance in terms of estimation accuracy and probability of resolution.
Achievement	Chapter 4: Improvement of the DOA estimation performance of incoming wideband signal sources without false peaks in spatial spectrum. Chapter 5: Low computational complexity version of WS-TOPS with minimizing deterioration on DOA estimation performance.

1.4 Outline of Dissertation

As discussed in the previous sections, this dissertation focuses on DOA estimation of incoming RF signals sources using array antenna. The structure of this dissertation is summarized in Fig. 1-1.

Chapter 2 deals with the related work and fundamental technologies of this dissertation. Some DOA estimation methods related to this dissertation are introduced in the chapter. We also show basic and principle techniques of processing for DOA estimation as fundamental technologies. Moreover, we explain some DOA estimation related researches which could be applied to the proposed methods.

Chapter 3 deals with a temporal spatial virtual array with adaptive PRI control method. The method is suppose to be applied to active sensor systems, e.g, radar systems and sonar systems. The system model we assume in this chapter is described in Section 3.2. The conventional method to form temporal spatial virtual array is explained in Section 3.3. The proposed method is shown in Section 3.4. In Section 3.5 and 3.6, the performance analysis and summarized signal processing process are shown, respectively. In Section 3.7, simulation results are presented. The conclusion of this chapter is presented in Section 3.8.

Chapter 4 deals with a DOA estimation method for wideband signal sources based on Weighted Squared TOPS. The method is suppose to be applied to passive sensor systems, e.g. electronic surveillance systems. The summary of the conventional methods are shown in Section 4.2. The proposed method is described in Section 4.3. Simulation results and detailed performance evaluation are discussed in Section 4.4 and Section 4.5, respectively. The conclusion of the chapter is presented in Section 4.6.

Chapter 5 considers a low complexity signal processing method for WS-TOPS. The low complexity approach based on WS-TOPS is discussed in Section 5.2. Simulation results of the low complexity method is described in Section 5.3. The conclusion of the chapter is presented in Section 5.4.

Chapter 6 is the conclusion of this dissertation and summarizes the contribution of this work.

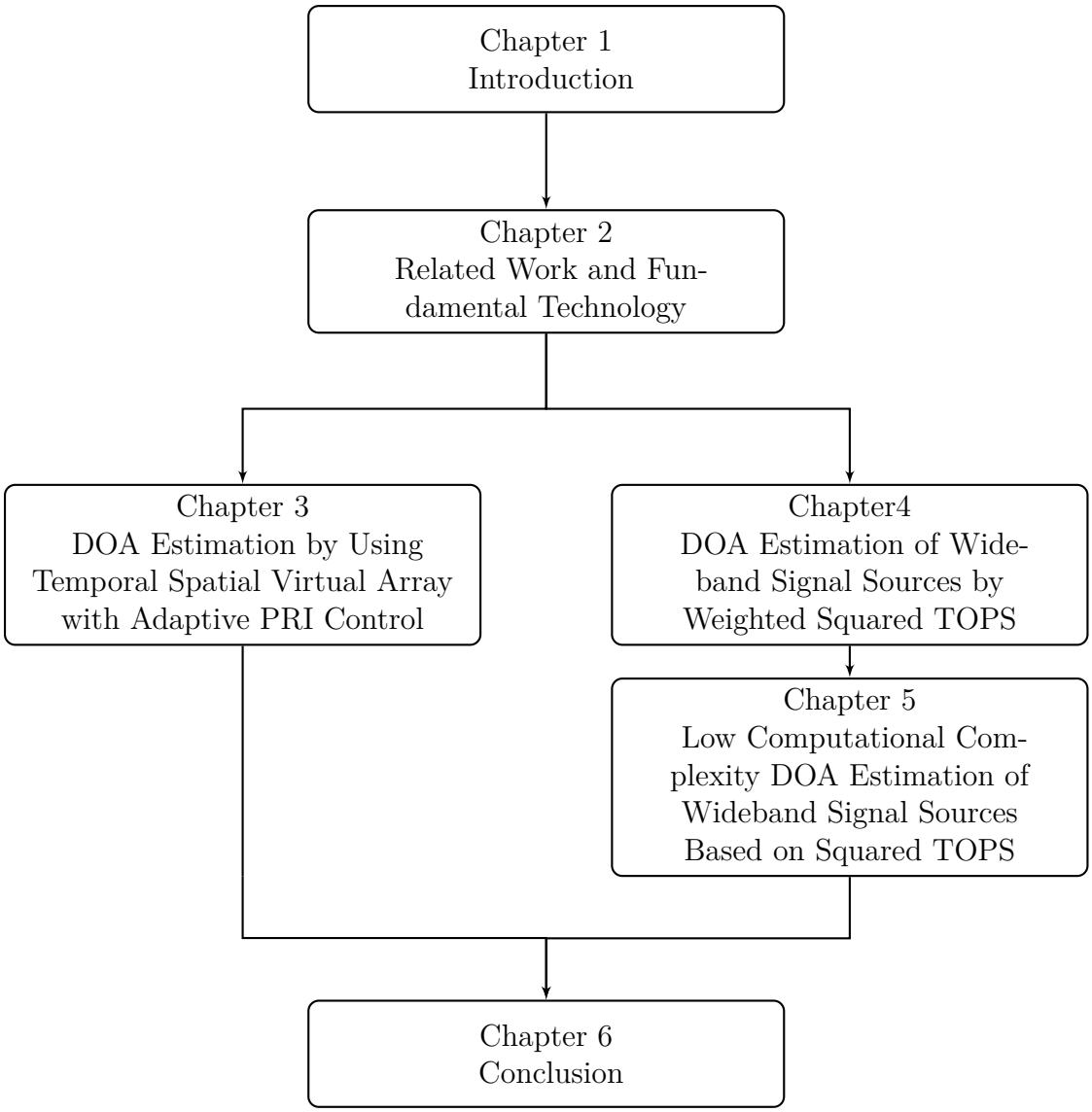

Figure 1-1: Structure of Dissertation.

Chapter 2

Related Work and Fundamental Technology

This chapter shows the fundamental technologies and the researches related to this dissertation. Section 2.1 starts with an introduction to array antenna. Section 2.2 overviews array configuration, including MIMO virtual array. Section 2.3 and 2.4 present DOA estimation method for narrowband signal sources and wideband signal sources, respectively.

2.1 Array Antenna

The array antenna has been applied to various kinds of applications ranging from military use to commercial use, e.g., ground based radar systems and airborne radar systems, base stations for mobile communication and radio astronomy observatory, etc [2]. Although the conventional phased array antenna in Fig. 2-1 (a) provides only single synthesized signal at single observation, we can obtain the digital data of received signals at every element antenna individually by using the adaptive array antenna as shown in Fig. 2-1 (b) and arbitrarily control the received gain of the array antenna [56]. Those are owing to the improvement of RF devices and electric devices in recent year. In what follows, we call the adaptive array antenna which can digitalize the received signal at every element antenna as simply “array antenna”.

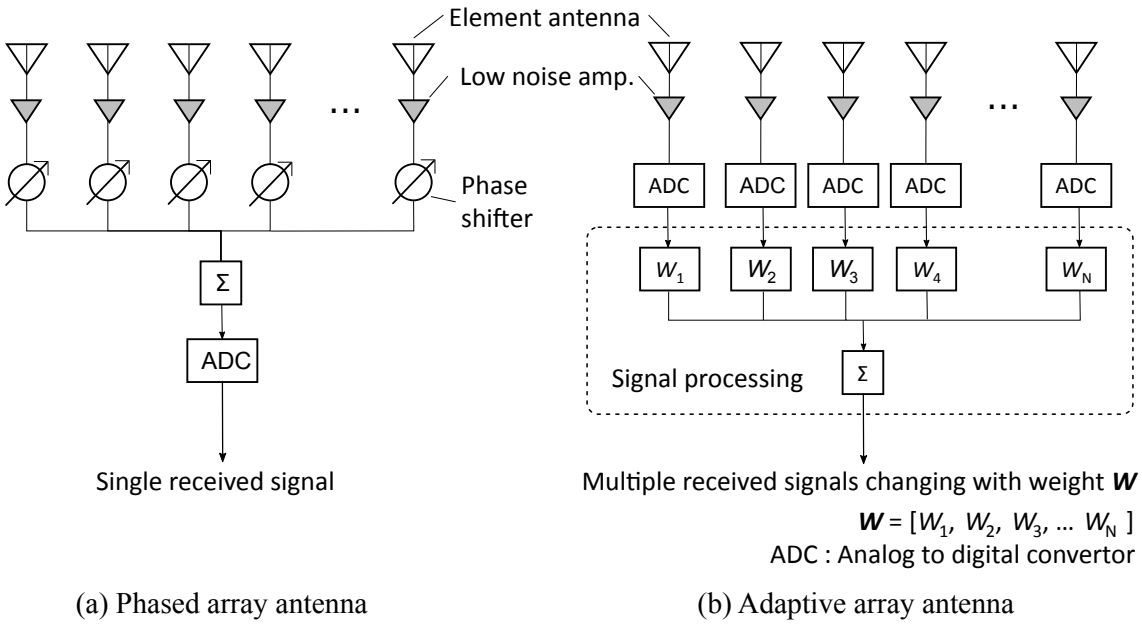

Figure 2-1: Phased array and adaptive array.

2.2 Array Configuration

Array antenna performs spatial sampling of incoming signal sources which are used to estimate DOA of the signal sources and/or the number of signal sources [57]. DOA estimation is one of the major applications of the array antenna. The number of sources that can be resolved depends on the DOF of array antenna which is related to array configuration. DOA estimation accuracy with array antenna also depends on the array configuration. Therefore, it is important to understand the fundamental relationship between array configuration and DOA estimation performance. In this section, we show the array configurations to be used in this dissertation.

2.2.1 ULA

The simplest and most frequently applied array structure is ULA because of its usefulness and easiness to apply to any RF devices to be used for DOA estimation [8]. ULA is defined as the uniform structure which consists of arbitrary number of element antennas where every spacing between each element is the same value d as shown in Fig. 2-2. In general, the spacing is less than the half wavelength corresponding to the

highest frequency of received or transmitting signal sources due to avoiding sidelobes in the spatial spectrum calculated by DOA estimation methods, some of which are described in section 2.3 and 2.4.

Both of DOF and DOA estimation accuracy have been mostly confined to the case of ULA [57]. For example, the number of sources that can be resolved with ULA where N element antennas with conventional subspace based method like MUSIC is $N-1$. The DOA estimation accuracy of a certain DOA estimation method can be improved by using large aperture, in other words, the number of antennas in ULA defines the DOA estimation performance.

Direction finding algorithms based on high-order statistics was proposed to remove the effect of the Gaussian noise and provide good DOA estimation performance [58, 59]. Using the concept of KR product has been also proposed as a new way to expand array structure, which can identify $2N-1$ signal sources using N antennas [46]. These methods, however, require certain signal characteristics e.g., Gaussian noise condition and quasi stationary sources.

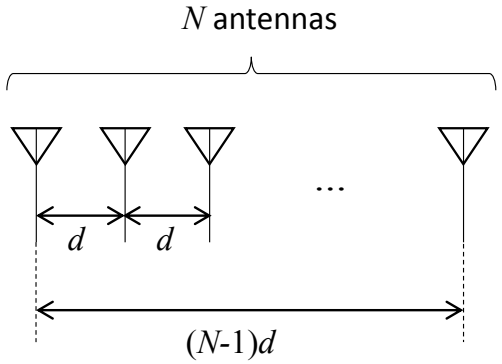

Figure 2-2: ULA structure.

2.2.2 Non-ULA Array Structures

Regarding the restriction described in Section 2.2.1, the issue of detecting more signal sources than the number of antennas has been addressed in some ways. To obtain more DOF required for detection of more than $N-1$ signal sources with N antennas, the use of minimum redundancy arrays [60], a transformation of this augmented

matrix into a suitable positive definite Toeplitz matrix [61, 62] was suggested. However, the optimum design of arrays is not an easy task and in most cases complicated iterative processing is required [63, 64], because there is no closed form expression for the array geometry.

Nested array is a novel design of array structure which can greatly increase the DOF in a completely passive scenario. The structure is obtained by systematically nesting two or more uniform linear arrays and can provide $O(N^2)$ degrees of freedom using only N actual antennas [31]. Although the nested array approach provides good DOF, DOA estimation accuracy using nested array is almost same as that using ULA, because DOA estimation accuracy mainly depends on array aperture size.

2.2.3 MIMO Array

MIMO array has some transmit antennas and receive antennas, where each transmit antenna transmits the orthogonal signal to the signals used for the other antennas. It is generally known that MIMO array produces the virtual array. Actually, we should consider waveform correlation and optimization issues to use MIMO array efficiently, because MIMO array requires high orthogonality of transmit signals [65–67]. Assuming we can design the optimal orthogonal waveform, Fig. 2-3 shows that the signal chain from transmission of signals to decoding of received signals. As we can see in Fig. 2-3, the combined steering vector, hereafter we call it as "MIMO steering vector", has MN length. It means that the length of MIMO steering vector M times bigger than that of the original received steering vector N.

The examples of some virtual array pattern are shown in Fig. 2-4. From Fig. 2-4, it is found that the virtual array constructed by using MIMO array can expand array structure in terms of the number of antennas and the aperture size. It means that MIMO array can improve not only DOF but also DOA estimation accuracy.

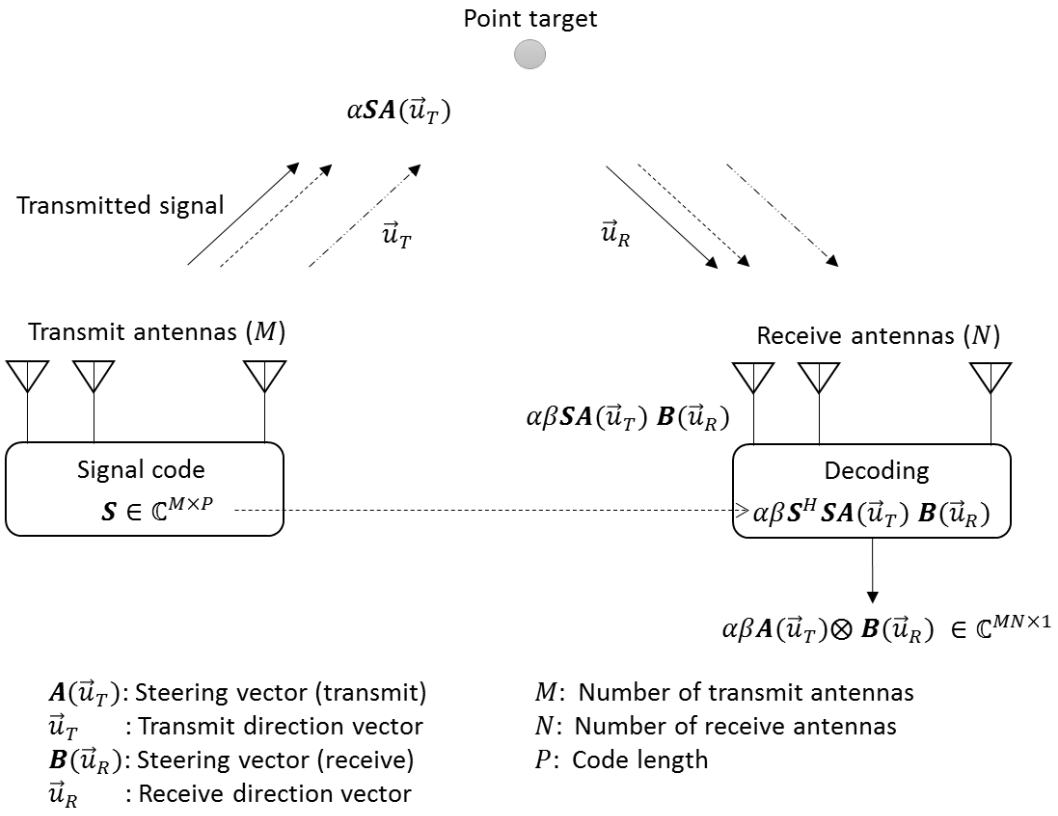

Figure 2-3: MIMO signal chain.

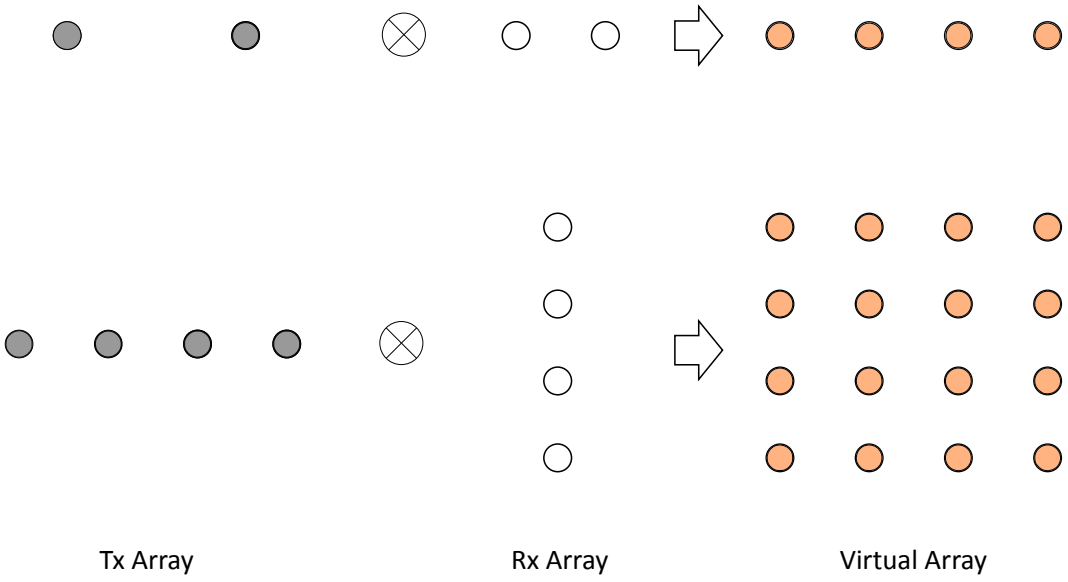

Figure 2-4: Examples of virtual array.

2.3 DOA Estimation Method for Narrowband Signal Sources

As mentioned earlier, DOA estimation method for narrowband signal sources has been well researched in prior decades [1, 2, 8]. Based on these researches, DOA estimation techniques can be classified into two main categories, non-parametric approaches and parametric approaches. In this section, we introduce several major methods, some of which are applied in this dissertation.

2.3.1 System Model

We assume that array antenna is an ULA with N antennas and antenna spacing d is equal to $\lambda/2$, where λ is the wavelength of carrier frequency. Then, we consider estimating the DOA of L incoming signal sources by using the ULA. Note that the number of signal sources L ($\leq N$) is either known a priori or can be estimated [68–72]. The received signal at the mth antenna can be expressed as

$$\boldsymbol{x}(t) = \boldsymbol{s}(t)\boldsymbol{A}(\boldsymbol{\theta}) + \boldsymbol{n}(t), \tag{2.1}$$

where, $\boldsymbol{s}(t) = [s_0(t), s_1(t), \cdots, s_{l-1}(t)]^T$ denotes the signal source vector, $\boldsymbol{n}$(t) denotes additive white Gaussian noise, and $\boldsymbol{A}(\boldsymbol{\theta})$ is the array manifold matrix which can be expressed as

$$\boldsymbol{A}(\boldsymbol{\theta}) = [\boldsymbol{a}(\theta_0), \boldsymbol{a}(\theta_1), \cdots, \boldsymbol{a}(\theta_{L-1})], \tag{2.2}$$

$$\boldsymbol{a}(\theta_l) = [1, \mathrm{e}^{-j\frac{2\pi}{\lambda}d\sin\theta_l}, \cdots, \mathrm{e}^{-j\frac{2\pi}{\lambda}d(n-1)\sin\theta_l}]^T. \tag{2.3}$$

Then, the correlation matrix of $\boldsymbol{x}(t)$ is expressed as

$$\boldsymbol{R}_{xx} = E[\boldsymbol{x}\boldsymbol{x}^H], \tag{2.4}$$

$$= \boldsymbol{A}_i(\boldsymbol{\theta})\boldsymbol{R}_{ss}\boldsymbol{A}_i^H(\boldsymbol{\theta}) + \sigma_n^2\boldsymbol{I}, \tag{2.5}$$

where $\boldsymbol{R}_{ss} = E[\boldsymbol{s}(t)\boldsymbol{s}(t)^H]$, σ_n^2 is noise power, where internal noises at all antennas are assumed to be independent of each other, and $\boldsymbol{I}$ is an $N \times N$ unit matrix. Assuming the L signal sources are uncorrelated, $\boldsymbol{R}_{ss}(\omega_i)$ has full rank.

2.3.2 Non-parametric Methods 1: Beamforming Method

Beamformer

Beamformer is the most basic approaches of spectral based approaches, and beamformer spectrum $P(\theta)_{bf}$ is calculated by following equation.

$$P(\theta)_{bf} = \frac{\boldsymbol{a}_i^H(\theta) R_{xx} \boldsymbol{a}_i(\theta)}{\boldsymbol{a}_i^H(\theta)\boldsymbol{a}_i(\theta)}. \tag{2.6}$$

Figure 2-5 shows the example of the spatial spectrum calculated by eq. (2.6), in which some peaks can be found as the DOA of incoming signal sources. As we can see from the figure, the conventional beamformer can not separate closely spaced signal sources. Therefore, to improve resolution performance, researchers have proposed various modifications based on beamformer. A well-known methods are, for example, Capon [9, 56, 73] and linear prediction (LP) method [74]. However, the DOA estimation performance of them are lower than those of subspace based methods described in the following section.

2.3.3 Non-parametric Methods 2: Subspace Based Method

MUSIC

As mentioned in the previous section, beamforming methods are basic techniques to estimate the DOA of incoming signal sources. Subspace based methods which have been proposed as super-resolution approach can provide better DOA estimation accuracy than those of the conventional beamformer methods. In particular, Multiple SIgnal Classification (MUSIC) algorithm is the most famous subspace based method [10]. Root-MUSIC [11] which is polynomial-rooting version of MUSIC technique can provide high resolution performance. ESPRIT [12] is a well-known subspace based

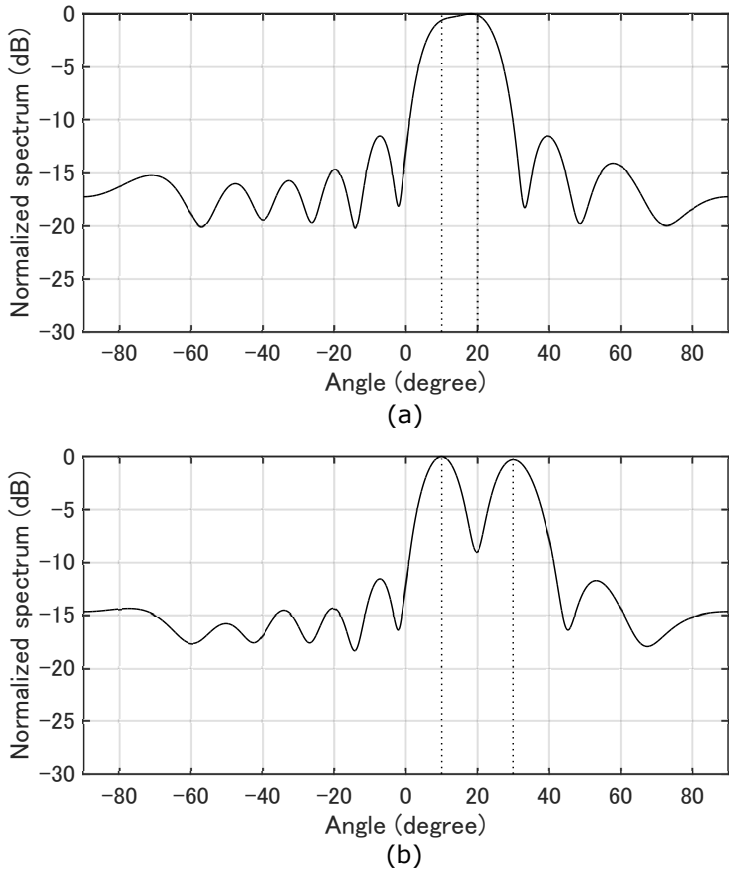

Figure 2-5: Example of normalized beamforming spectra with ULA, where the number of antennas = 10, $SNR = 0$ dB, and snapshot = 100. Dotted lines are the true direction of incoming signal sources. (a) The true direction of signal sources = {10 deg., 20 deg.} (b) The true direction of signal sources = {10 deg., 30 deg.}.

approach. However, the latter two techniques have require array structure to be ULA. The detail of MUSIC is as follows.

Since the matrix $\boldsymbol{R}_{xx}$ is a Hermitian matrix, the eigenvalue decomposition (EVD) of the matrix gives

$$\boldsymbol{R}_{xx} = \boldsymbol{E}_S \boldsymbol{\Lambda}_S \boldsymbol{E}_S^H + \boldsymbol{E}_N \boldsymbol{\Lambda}_N \boldsymbol{E}_N^H, \tag{2.7}$$

where $\boldsymbol{E}_S$ and $\boldsymbol{E}_N$ are the signal subspace matrix and the noise subspace matrix, respectively. $\boldsymbol{\Lambda}_S$ and $\boldsymbol{\Lambda}_N$ are the diagonal matrices corresponding to $\boldsymbol{E}_S$ and $\boldsymbol{E}_N$, respectively. These matrices are expressed as follows.

$$\boldsymbol{E}_S = [\boldsymbol{e}_1, \cdots, \boldsymbol{e}_L], \tag{2.8}$$

$$\boldsymbol{E}_N = [\boldsymbol{e}_{L+1}, \cdots, \boldsymbol{e}_N], \tag{2.9}$$

$$\boldsymbol{\Lambda}_S = \mathrm{diag}(\lambda_1, \cdots, \lambda_L), \tag{2.10}$$

$$\boldsymbol{\Lambda}_N = \mathrm{diag}(\lambda_{L+1}, \cdots, \lambda_N), \tag{2.11}$$

where $\lambda_k (k = 1, 2, \cdots, N)$ are eigenvalues of $\boldsymbol{R}_{xx}$, and they have the relation given by

$$\lambda_1 \geq \lambda_2 \geq \cdots \geq \lambda_L > \lambda_{L+1} = \cdots = \lambda_N = \sigma^2, \tag{2.12}$$

also, $\boldsymbol{e}_k (k = 1, 2, \cdots, M)$ are corresponding eigenvectors orthogonal to each other as shown below.

$$\boldsymbol{E}\boldsymbol{E}^H = \boldsymbol{E}^H\boldsymbol{E} = \boldsymbol{I}, \tag{2.13}$$

$$\boldsymbol{E} \equiv [\boldsymbol{E}_S \boldsymbol{E}_N]. \tag{2.14}$$

Then, using the noise subspace matrix $\boldsymbol{E}_N$, the MUSIC spectrum $P_{music}(\theta)$ can be expressed as

$$P_{music}(\theta) = \frac{\boldsymbol{a}^H(\theta)\boldsymbol{a}(\theta)}{\boldsymbol{a}^H(\theta)\boldsymbol{E}_N\boldsymbol{E}_N^H\boldsymbol{a}(\theta)}. \tag{2.15}$$

Figure 2-6 shows the example of the spatial spectrum calculated by eq. (2.6) and eq. (2.15). As we can see in the figure, MUSIC method can separate closely spaced signal sources while the conventional beamforming technique can not. Therefore, in this dissertation, we use MUSIC as the basic DOA estimation method.

Spatial Smoothing Processing (SSP)

If some of the received signals are coherent to each other, it causes a rank deficiency in the source covariance matrix. Then, $\boldsymbol{E}_N^H\boldsymbol{a} \neq 0$ for any θ and MUSIC will fail to detect accurate peak in spatial spectrum, which denotes the DOA of incoming signal sources. Spatial smoothing processing (SSP) is the method to restore the rank of the

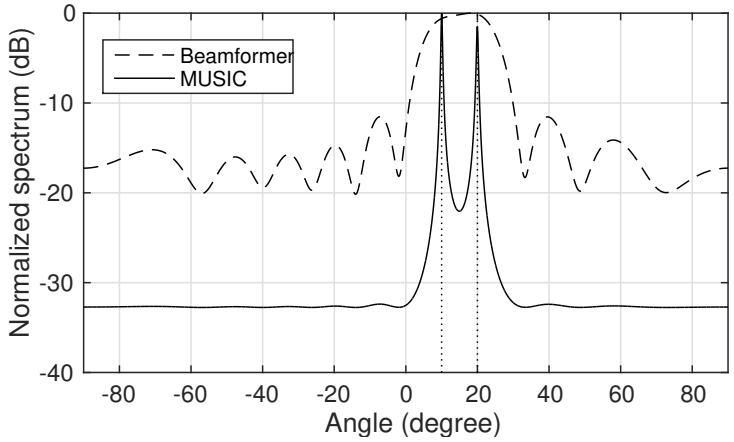

Figure 2-6: Example of normalized spectrum of beamformer and MUSIC with ULA, where the number of antennas = 10, $SNR = 0$ dB, and snapshot = 100. Dotted lines are the true direction of incoming signal sources from {10 deg. and 20 deg.}.

signal covariance matrix [75] when we use ULA. The key idea of SSP is that phase relationships among coherent signals are different from one element to another. First, splitting the ULA into a number of overlapping subarrays. Then the steering vectors of the subarrays are calculated and the subarray covariance matrices are averaged. Finally, the process de-correlates the signals that caused the rank deficiency. We assume that the ULA with N antennas is divided into P-elements subarrays and we get M subarrays, where $M = N - P + 1$, as shown in Fig. 2-7. The received signal vector of the mth subarrays can be expressed as

$$\boldsymbol{x}_m^f(t) = [x_m(t), \cdots, x_{m+P-1}(t)]^T. \tag{2.16}$$

Then, the averaged correlation matrix can be calculated by the following equation.

$$\boldsymbol{R}_{ssp}^f = \frac{1}{M} \sum_{m=1}^{M} E[\boldsymbol{x}_m^f(t) \boldsymbol{x}_m^f(t)^H]. \tag{2.17}$$

The basic approach described above has been extended [76,77], which is called the forward-backward SSP (FB-SSP). Using these SSP techniques, we can estimate the DOA of incoming signal sources even if there are coherent signals, while the process reduces the number of efficient antenna elements from N to P.

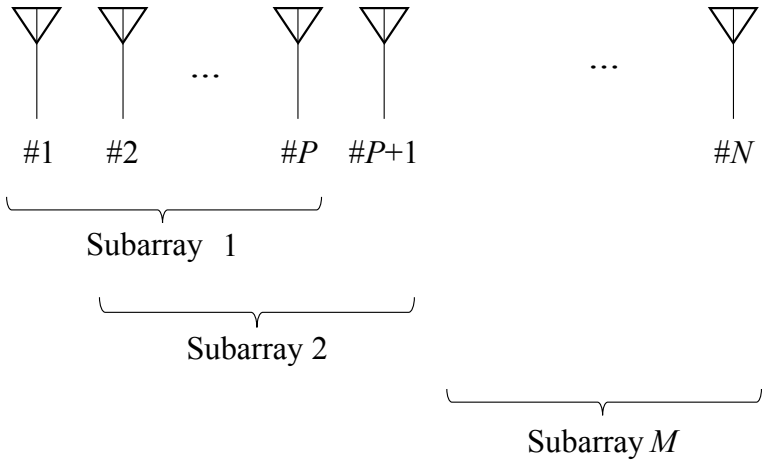

Figure 2-7: Original array structure and subarray structure.

2.3.4 Parametric Methods

Parametric based method can exploit underlying solution, which can handle coherent signals without any pre-processing technique. The DOA estimation accuracy of the method is much higher than that of the spectral based methods. The algorithms typically require solving a multidimensional non-linear optimization problem to find the estimates. Although, some kinds of techniques have been proposed, e.g., Weighted Subspace Fitting (WSF) [78,79], Deterministic Maximum Likelihood (DML) [80–82], Stochastic Maximum Likelihood (SML) [83] and Method of Direction Estimation (MODE) [84,85], the computational complexity of parametric DOA estimation methods is quit high.

Therefore, in this dissertation, we focus on the nonparametric methods shown in Senction 2.3.3 to realize further improvement in terms of DOA estimation performance.

2.4 DOA Estimation Methods for Wideband Signal Sources

To estimate DOA of wideband signal sources, we should consider that the diversity of frequency bands. In general, incoming signal sources are affected by the circumstance, which is time-varying and of course spatially varying, then, the characteristic of signal in each frequency bands is different from each other. Therefore, the key point of DOA estimation methods of wideband signal sources is how to deal with the signals in each frequency band. From the perspective, DOA estimation for wideband signal sources has been investigated [1, 2, 8].

As mentioned in Introduction, the conventional DOA estimation methods for wideband signal sources are categorized into two groups: incoherent signal subspace method (ISSM) [36, 37] and coherent signal subspace method (CSSM) [38]. From a different perspective, there are two types of DOA estimation methods: one requires the initial estimate of the DOAs and the other does not. CSSM, which is categorized in the former group, can provide higher estimation accuracy than that of the methods categorized in the latter group owing to use initial estimates. However, requiring initial estimates is the serious drawback because the requirement limits range of application. Therefore, in this dissertation, we focus on DOA estimation method which can estimate DOA of incoming signal sources without any pre-information.

In this section, we introduce the some conventional DOA estimation methods, some of which are compared to our proposed method described in Sections 4 and 5.

2.4.1 System Model

We consider estimating the DOA of L wideband signal sources using a uniform linear array that consists of M antennas. Let us assume that the number of signal sources L ($\leq M$) is either known or can be estimated [68–72]. We also assume that all signals are uncorrelated with each other and exist in the bandwidth between w_L and w_H.

Then, the received signal at the mth antenna can be expressed as

$$x_m(t) = \sum_{l=1}^{L} s_l(t - v_m \sin\theta_l) + n_m(t), \tag{2.18}$$

where $s_l(t)$ is the lth signal source, $n_m(t)$ is additive white Gaussian noise at the mth antenna, $v_m = (m-1)d/c$, where d is the distance between adjacent antennas, and c is the speed of light. θ_l is the DOA to be estimated. Then, the received wideband signals are decomposed into K narrowband signals. The DFT of the signal received at the mth antenna is

$$x_m(\omega) = \sum_{l=1}^{L} s_l(\omega) \exp(-j\omega v_m \sin\theta_l) + n_m(\omega). \tag{2.19}$$

Then, the output signals of the DFT can be written in vector form as follows.

$$\boldsymbol{x}(\omega_i) = \boldsymbol{A}(\omega_i, \boldsymbol{\theta})\boldsymbol{s}(\omega_i) + \boldsymbol{n}(\omega_i), i = 1, 2, \cdots, K, \tag{2.20}$$

where $\omega_L < \omega_i < \omega_H$ for $i = 1, 2, \cdots, K$,

$$\boldsymbol{A}(\omega_i, \boldsymbol{\theta}) = \left[\begin{array}{cccc} \boldsymbol{a}(\omega_i, \theta_1) & \boldsymbol{a}(\omega_i, \theta_2) & \cdots & \boldsymbol{a}(\omega_i, \theta_L) \end{array} \right], \tag{2.21}$$

$$\boldsymbol{a}(\omega_i, \theta_l) = [1, \mathrm{e}^{-j\omega_i v_1 \sin\theta_l}, \cdots, \mathrm{e}^{-j\omega_i v_{M-1} \sin\theta_l}]^T. \tag{2.22}$$

For simplicity, hereafter, $\boldsymbol{A}(\omega_i, \boldsymbol{\theta})$ and $\boldsymbol{a}(\omega_i, \theta_l)$ will be represented as $\boldsymbol{A}_i(\boldsymbol{\theta})$ and $\boldsymbol{a}_i(\theta_l)$, respectively. The correlation matrix is calculated as follows,

$$\begin{aligned} \boldsymbol{R}_{xx}(\omega_i) &= E[\boldsymbol{x}(\omega_i)\boldsymbol{x}^H(\omega_i)], & (2.23) \\ &= \boldsymbol{A}_i(\boldsymbol{\theta})\boldsymbol{R}_{ss}(\omega_i)\boldsymbol{A}_i^H(\boldsymbol{\theta}) + \sigma_n^2\boldsymbol{I}, & (2.24) \end{aligned}$$

where $\boldsymbol{R}_{ss}(\omega_i) = E[\boldsymbol{s}(\omega_i)\boldsymbol{s}^H(\omega_i)]$, σ_n^2 is noise power and $\boldsymbol{I}$ is an $M \times M$ unit matrix. Assuming the L signal sources are uncorrelated, $\boldsymbol{R}_{ss}(\omega_i)$ has full rank, then the signal subspace matrix $\boldsymbol{F}_i$ and the noise subspace matrix $\boldsymbol{W}_i$ at frequency ω_i can be formed

from the EVD of the correlation matrix as

$$\boldsymbol{F}_i = [\boldsymbol{e}_{i,1}, \boldsymbol{e}_{i,2}, \cdots, \boldsymbol{e}_{i,L}], \tag{2.25}$$

$$\boldsymbol{W}_i = [\boldsymbol{e}_{i,L+1}, \boldsymbol{e}_{i,L+2}, \cdots, \boldsymbol{e}_{i,M}], \tag{2.26}$$

where $\boldsymbol{e}_{i,1}, \cdots, \boldsymbol{e}_{i,M}$ are the orthogonal eigenvectors of $\boldsymbol{R}_{xx}(\omega_i)$ indexed in descending order with respect to their corresponding eigenvalues as follows.

$$\lambda_{i,1} \geq \lambda_{i,2} \geq \cdots \geq \lambda_{i,L} > \lambda_{i,L+1} = \cdots = \lambda_{i,M} = \sigma_n^2. \tag{2.27}$$

2.4.2 Incoherent Signal Subspace Method (ISSM)

IMUSIC, which is one of the simplest DOA estimation methods for wideband signals, applies narrowband signal subspace methods (e.g., MUSIC) to each frequency band independently [36,37]. Then, IMUSIC estimates the DOA of wideband signal sources by using the following equation.

$$\hat{\theta} = \arg\min_{\theta} \sum_{i=1}^{K} \boldsymbol{a}_i^H(\theta) \boldsymbol{W}_i \boldsymbol{W}_i^H \boldsymbol{a}_i(\theta). \tag{2.28}$$

Since the DOAs estimated by eq. (2.28) are averages of the result of each frequency band, the poor estimates from a single frequency band even degrades the final estimation accuracy.

2.4.3 Test of Orthogonality Frequency Subspaces (TOFS)

TOFS uses the noise subspace obtained from EVD of the correlation matrix of each frequency [45]. The DOA of each incoming wideband signal source is estimated by testing the orthogonality between the steering vector and the noise subspaces. If θ is the one DOA of incoming wideband signals, θ satisfies the following equation.

$$\boldsymbol{a}_i^H(\theta) \boldsymbol{W}_i \boldsymbol{W}_i^H \boldsymbol{a}_i(\theta) = 0. \tag{2.29}$$

Here, we define the vector $\boldsymbol{d}(\theta)$ as follows.

$$\begin{aligned}\boldsymbol{d}(\theta) = [&\boldsymbol{a}_1^H(\theta)\boldsymbol{W}_1\boldsymbol{W}_1^H\boldsymbol{a}_1(\theta) \\ &\boldsymbol{a}_2^H(\theta)\boldsymbol{W}_2\boldsymbol{W}_2^H\boldsymbol{a}_2(\theta) \\ \cdots &\boldsymbol{a}_K^H(\theta)\boldsymbol{W}_K\boldsymbol{W}_K^H\boldsymbol{a}_K(\theta)].\end{aligned} \tag{2.30}$$

All elements of the vector $\boldsymbol{d}(\theta)$ will be zero when θ is the DOA of incoming wideband signal sources. Then, we can estimate the DOAs by using the following equation.

$$\hat{\theta} = \arg\max_{\theta} \frac{1}{||\boldsymbol{d}(\theta)||}. \tag{2.31}$$

TOFS shows good DOA estimation accuracy in high SNR region by using the noise subspaces obtained from the correlation matrix of received signals. However, TOFS cannot resolve closely spaced signal sources when SNR is low.

2.4.4 Test of Orthogonality Projected Subspaces (TOPS)

TOPS uses both of the signal and noise subspaces of each frequency band to estimate the DOA of incoming wideband signal sources [43]. First, we obtain the signal subspace $\boldsymbol{F}_i$ and the noise subspace $\boldsymbol{W}_i$ from EVD of the correlation matrix of each frequency band. Then, one frequency band ω_i should be selected and the signal subspace $\boldsymbol{F}_i$ of the selected frequency band is transformed into other frequencies. TOPS uses a diagonal unitary transformation matrix. The mth term on the diagonal of the frequency transform matrix $\boldsymbol{\Phi}(\omega_i, \theta)$ is

$$[\boldsymbol{\Phi}(\omega_i, \theta)]_{(m,m)} = \exp\left(-j\omega_i \frac{md}{c}\sin\theta\right). \tag{2.32}$$

Using $\boldsymbol{\Phi}(\omega_i, \theta)$, the signal subspace $\boldsymbol{F}_i$ of the frequency band ω_i is transformed into the other frequency band ω_j, where we define the transformed signal subspace $\boldsymbol{U}_{ij}(\theta)$, as follows.

$$\boldsymbol{U}_{ij}(\theta) = \boldsymbol{\Phi}(\Delta\omega, \theta)\boldsymbol{F}_i, i \neq j, \tag{2.33}$$

where $\Delta\omega = \omega_j - \omega_i$.

The subspace projection technique is applied to reduce the signal subspace component leakage in the estimated noise subspace. The projection matrix $\boldsymbol{P}_i(\theta)$ is defined as

$$\boldsymbol{P}_i(\theta) = \boldsymbol{I} - (\boldsymbol{a}_i^H(\theta)\boldsymbol{a}_i(\theta))^{-1}\boldsymbol{a}_i(\theta)\boldsymbol{a}_i^H(\theta), \tag{2.34}$$

where $\boldsymbol{I}$ is an $M \times M$ unit matrix. Then, we obtain the transformed signal subspace matrix $\boldsymbol{U}'_{ij}(\theta)$.

$$\boldsymbol{U}'_{ij}(\theta) = \boldsymbol{P}_j(\theta)\boldsymbol{U}_{ij}(\theta). \tag{2.35}$$

Assuming that the selected frequency band is ω_1, the matrix $\boldsymbol{D}(\theta)$ is defined as

$$\boldsymbol{D}(\theta) = [\ \boldsymbol{U}'^H_{12}(\theta)\boldsymbol{W}_2 \quad \cdots \quad \boldsymbol{U}'^H_{1K}(\theta)\boldsymbol{W}_K\ ]. \tag{2.36}$$

We can estimate the DOA of the incoming wideband signal sources from spatial spectrum calculated by the following equation since the rank of the matrix $\boldsymbol{D}'(\theta)$ also decreases when θ is the one DOA of incoming wideband signal sources.

$$\hat{\theta} = \arg\max_{\theta} \frac{1}{\sigma_{min}(\theta)}, \tag{2.37}$$

where $\sigma_{min}(\theta)$ is a minimum singular value of $\boldsymbol{D}(\theta)$.

2.4.5 Squared TOPS

Squared TOPS [44] uses the frequency band where the difference between the smallest signal eigenvalue $\lambda_{i,L}$ and the largest noise eigenvalue $\lambda_{i,L+1}$ is maximum. Hereafter we call it as the reference frequency.

Then, the signal subspace of the reference frequency band is transformed into the other frequency bands by eq. 4.6. Let us assume that the frequency band ω_i is selected and the signal subspace $\boldsymbol{F}_i$ is transformed to the other frequency bands ω_j. Using $\boldsymbol{U}'_{ij}(\theta)$ and $\boldsymbol{W}_j$, we construct the squared matrix $\boldsymbol{Z}_i(\theta)$ for the test of orthogonality

of projected subspaces as follows.

$$\boldsymbol{Z}_i(\theta) = [\ \cdots\ \ \boldsymbol{U}_{ij}^{'H}(\theta)\boldsymbol{W}_j\boldsymbol{W}_j^H\boldsymbol{U}_{ij}'(\theta)\ \ \cdots\ ], i \neq j. \tag{2.38}$$

Squared TOPS estimates the DOA of wideband signals using the minimum singular value $\sigma_{zi_{min}}(\theta)$ of $\boldsymbol{Z}_i(\theta)$.

$$\hat{\theta} = \arg\max_{\theta} \frac{1}{\sigma_{zi_{min}}(\theta)}. \tag{2.39}$$

Chapter 3

DOA Estimation by Using Temporal Spatial Virtual Array with Adaptive PRI Control

3.1 Introduction

In Section 2.2, we have briefly reviewed array configuration including MIMO array. Some of DOA estimation methods for narrowband signal sources have also been introduced in Section 2.3. Although the conventional method in [25] can improve DOA estimation performance using temporal spatial virtual array, its performance deteriorates with changing parameters of the target; velocity and direction. Moreover, the conventional method can not address DOA estimation of the multiple targets, hence, it is difficult to implement the method in actual situation.

In this chapter, we propose a new DOA estimation method by using the temporal-spatial virtual array. The proposed method provides accurate DOA estimation by using output signals of Doppler filter with adaptive PRI control technique. The performance of the proposed method is compared with that of the conventional method via computer simulations. The simulations show that the new DOA estimation method performs better than the conventional method.

The rest of this chapter is organized as follows. In Section 3.2, the MIMO radar model is described, and the DOA estimation method using MUSIC algorithm is explained. The conventional method to form temporal spatial virtual array is explained in Section 3.3. In Section 3.4, the new method of DOA estimation using temporal spatial virtual array based on Doppler shift with adaptive PRI control is proposed. In Sections 3.5 and 3.6, the performance analysis and the signal processing process are shown, respectively. In Section 3.7, simulation results are presented. Finally conclusions are provided in Section 3.8.

3.2 System Model

We consider the MIMO radar model with N transmit antennas and M receive antennas described in Fig. 3-1. d_t and d_r denote the spacing of the transmit antennas and that of the receive antennas, respectively. We assume that Q ($< MN$) targets are present in the search space. Let θ_q and v_q represent the direction and the relative velocity of the q th target, respectively. Here, we also assume that the direction and the velocity of each target are constant within array signal processing period. The received signal of the m th antenna can be expressed as

$$\begin{aligned} & x_m\left(pT_{PRI}+\tau+\frac{2r}{c}\right) \\ & \quad = \sum_{q=1}^{Q}\sum_{n=0}^{N-1}\beta_q a_n(\theta_q)b_m(\theta_q)s_n(\tau)d(v_q)+n_{awgn}, \end{aligned} \tag{3.1}$$

$$a_n(\theta_q)=\exp\left(-j\frac{2\pi}{\lambda}nd_t\sin\theta_q\right), \tag{3.2}$$

$$b_m(\theta_q)=\exp\left(-j\frac{2\pi}{\lambda}md_r\sin\theta_q\right), \tag{3.3}$$

$$d(v_q)=\exp\left(-j\frac{2\pi}{\lambda}2v_q pT_{PRI}\right), \tag{3.4}$$

$$q=1,\cdots,Q,\quad p=1,\cdots,P,$$

$$m=0,\cdots,M-1,\quad n=0,\cdots,N-1,$$

where p indicates the index of transmitting pulse, T_{PRI} denotes PRI, r denotes the distance of the range bin of interest, β_q denotes the amplitude of the signal reflected by the q th target and λ denotes the wavelength of the carrier frequency. $s_n(\tau)$ denotes the transmitting signal from the n th transmit antenna and τ denotes the time length of transmitting signal. n_{awgn} denotes the additive white Gaussian noise. c is speed of light. In the MIMO radar, the transmitting signals $s_n(\tau)$ satisfy the following orthogonality. It means that N orthogonal signals are transmitted from Tx antennas individually.

$$\int s_i(\tau)s_j^H(\tau)d\tau = \begin{cases} \delta, & (i=j) \\ 0, & (i \neq j) \end{cases}, \tag{3.5}$$

$$i = 0, \cdots, N-1, \quad j = 0, \cdots, N-1.$$

We divide the received signal into N signals using matched filter and extract the signal of the range of interest. The extracted signal is expressed as

$$x_{r,m,n}(p) \equiv \int x_m(pT_{PRI} + \tau + \tfrac{2r}{c})s_n^H(\tau)d\tau$$

$$= \sum_{q=1}^{Q} \beta_q \exp\left\{-j\frac{2\pi}{\lambda}(\sin\theta_q(nd_t + md_r) + 2v_q pT_{PRI})\right\} + n_{awgn}. \tag{3.6}$$

Stacking the received signal in eq. (3.6), we get the vector $\boldsymbol{x}_r$.

$$\boldsymbol{x}_r(p) = [x_{r,0,0}(p), x_{r,1,0}(p), \cdots, x_{r,M-1,N-1}(p)]^T. \tag{3.7}$$

The vector length of the signal $\boldsymbol{x}_r(p)$ is MN. It shows that the convolution of real arrays in MIMO radar produces a virtual array. Here, we refer to the virtual array as the spatial virtual array to distinguish it from the temporal spatial virtual array described in Sect. 3. The correlation matrix of $\boldsymbol{x}_r$ is defined as

$$\boldsymbol{R}_{xx} = E[\boldsymbol{x}_r \boldsymbol{x}_r^H], \tag{3.8}$$

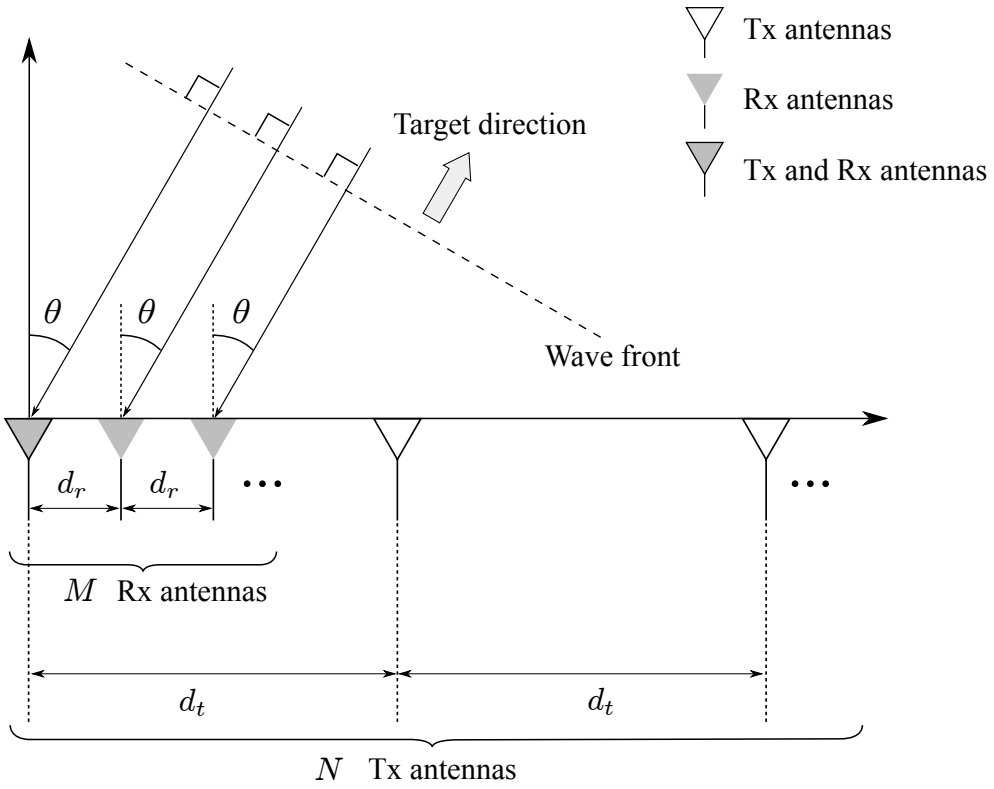

Figure 3-1: Configuration of a MIMO radar model.

where $E[\cdot]$ denotes expectation.

Here, internal noises at all antennas are assumed to be independent of each other with an equal power of σ^2. Also, for simplicity, echo signal from each target is assumed to be uncorrelated with each other, which means that every target has a different relative velocity. Then, we obtain the noise subspace matrix $\boldsymbol{E}_N$ by EVD as shown in Section 2.3.3.

Using the noise subspace matrix $\boldsymbol{E}_N$, the MUSIC spectrum $P_{MU}(\theta)$ with MIMO array can be expressed as

$$P_{MU}(\theta) = \frac{\boldsymbol{z}^H(\theta)\boldsymbol{z}(\theta)}{\boldsymbol{z}^H(\theta)\boldsymbol{E}_N\boldsymbol{E}_N^H\boldsymbol{z}(\theta)}, \tag{3.9}$$

where $\boldsymbol{z}(\theta)$ denotes the steering vector which can be expressed as

$$\boldsymbol{z}(\theta) = \boldsymbol{b}(\theta) \otimes \boldsymbol{a}(\theta), \tag{3.10}$$

$$\boldsymbol{a}(\theta) = [a_0(\theta), a_1(\theta), \cdots, a_{N-1}(\theta)]^T, \tag{3.11}$$

$$\boldsymbol{b}(\theta) = [b_0(\theta), b_1(\theta), \cdots, b_{M-1}(\theta)]^T. \tag{3.12}$$

Hereafter we refer the DOA estimation method using eq. (3.9) as the MUSIC.

3.3 Conventional Method to Form Temporal Spatial Virtual Array

In this section, we explain the conventional method to form temporal spatial virtual array [25]. First, we obtain the matrix $\tilde{\boldsymbol{X}}_r$ combining the received signal vectors $\boldsymbol{x}_r(p)$ observed by transmitting P pulses. Then, the new echo signal vector $\tilde{\boldsymbol{x}}_r$ is obtained by vectorizing it as follows.

$$\tilde{\boldsymbol{X}}_r = [\boldsymbol{x}_r(1), \boldsymbol{x}_r(2), \cdots, \boldsymbol{x}_r(P)], \tag{3.13}$$

$$\tilde{\boldsymbol{x}}_r = \mathrm{vec}(\tilde{\boldsymbol{X}}_{\mathrm{r}}). \tag{3.14}$$

As shown in eq. (3.14), the length of vector $\tilde{\boldsymbol{x}}_r$ is MNP. It means that this process expands the vector length P times the original size. The resulting new correlation matrix $\tilde{\boldsymbol{R}}_{xx}$ is defined as follows.

$$\tilde{\boldsymbol{R}}_{xx} = \tilde{\boldsymbol{x}}_r \tilde{\boldsymbol{x}}_r^H. \tag{3.15}$$

Next, the new steering vector corresponding to the vector $\tilde{\boldsymbol{x}}_r$ and its correlation matrix $\tilde{\boldsymbol{R}}_{xx}$ is defined. Here, $\tilde{v}_q$ represents the relative velocity of the target of which the DOA is to be estimated. Then, the distance that the target has traveled along the line of sight during the period of time between the first and the p th pulse, d_p, can be expressed as

$$d_p = 2\tilde{v}_q T_{PRI}(p-1). \tag{3.16}$$

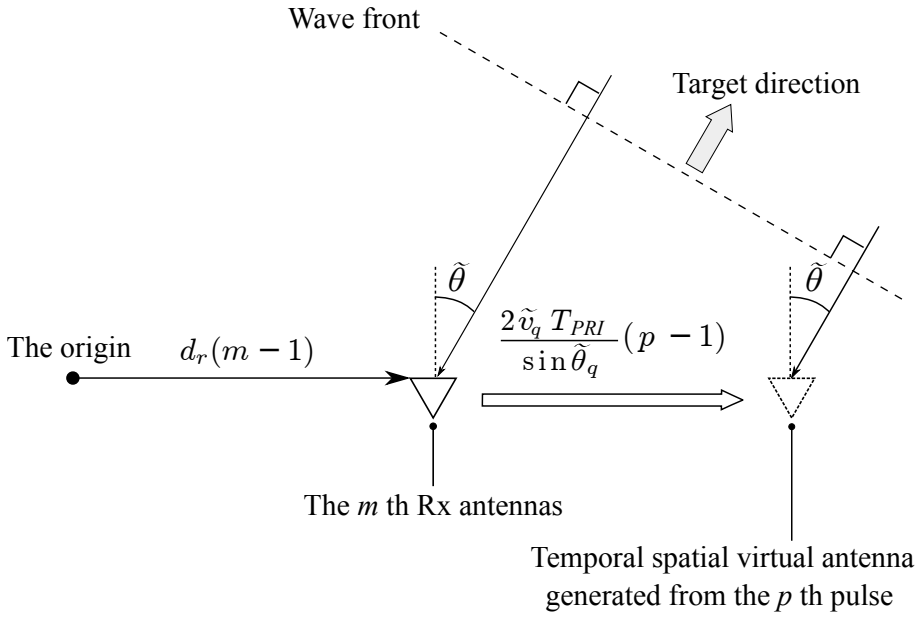

Figure 3-2: Temporal spatial virtual antenna.

Figure 3-2 shows the temporal spatial virtual antenna generated by the received signal of the existing antenna m at the pulse p. The position of the temporal spatial virtual antenna $d_v(m,p)$ can be expressed as

$$d_v(m,p) = d_r(m-1) + \frac{2\tilde{v}_q T_{PRI}}{\sin\tilde{\theta}_q}(p-1), \tag{3.17}$$

where $\tilde{\theta}_q$ and $\tilde{v}_q$ denote the pre-estimated direction and relative velocity of the target calculated by the common radar signal processing. In particular, we obtain each initial estimate $\tilde{\theta}_q$ by using the received signal $\boldsymbol{x}_r$ and the steering vector $\tilde{\boldsymbol{z}}$ based on the digital beam forming technique and also calculate each initial estimate $\tilde{v}_q$ by using eq. (3.18) with the Doppler frequency of the target $\tilde{\omega}_{d,q}$, which is indicated as a peak in the frequency spectrum obtained by digital Fourier transform of the received signal $\boldsymbol{x}_r$ [6].

$$\tilde{\boldsymbol{v}}_q = \frac{\tilde{\omega}_{d,q}}{4\pi}\lambda. \tag{3.18}$$

Then, we detect targets with pre-estimated target information; the direction $\tilde{\theta}_q$ and the relative velocity $\tilde{v}_q$. As already mentioned in Section 3.2, θ and v are assumed

to be constant within array signal processing period. Moreover the moving direction of each target affects DOA estimation accuracy. Therefore, in this paper, we also assume that the moving direction of each target is constant within the array signal processing period and is not orthogonal to the direction of the target (it means $\tilde{v}_q \neq 0$).

Using eqs. (3.10) and (3.17), we can generate the temporal spatial steering vector $\tilde{\boldsymbol{z}}(\theta)$ corresponding to the received signal vector $\tilde{\boldsymbol{x}}_r$ as follows.

$$\tilde{\boldsymbol{z}}(\theta) = [z_{1,1,1}(\theta), z_{1,1,2}(\theta), \cdots, z_{m,n,p}(\theta), \cdots, z_{M,N,P}(\theta)]^T, \tag{3.19}$$

$$z_{m,n,p}(\theta) = \exp\left[-j\frac{2\pi \sin\theta}{\lambda}\left\{d_t(n-1)+d_r(m-1)+\frac{2\tilde{v}_q T_{PRI}}{\sin\tilde{\theta}_q}(p-1)\right\}\right]. \tag{3.20}$$

Based on eqs. (3.15) and (3.20), the MUSIC spectrum $P_C(\theta)$ using the temporal spatial virtual array formed by conventional method is defined as follows.

$$P_C(\theta) = \frac{\tilde{\boldsymbol{z}}^H(\theta)\tilde{\boldsymbol{z}}(\theta)}{\tilde{\boldsymbol{z}}^H(\theta)\tilde{\boldsymbol{E}}_N\tilde{\boldsymbol{E}}_N^H\tilde{\boldsymbol{z}}(\theta)}, \tag{3.21}$$

where $\tilde{\boldsymbol{E}}_N$ is the noise subspace matrix of $\tilde{\boldsymbol{R}}_{xx}$.

3.4 Proposed Method

Equation (3.20) shows that the steering vector $\tilde{\boldsymbol{z}}(\theta)$ changes with the direction and the relative velocity of the target on which we focus. Moreover, there are mismatches between the steering vector $\tilde{\boldsymbol{z}}(\theta)$ for each target and the echo signals from the other targets. The mismatches cause the deterioration of the DOA estimation accuracy of the conventional method.

To prevent the degradation, we propose the new method of DOA estimation using the temporal spatial virtual array based on Doppler shift with adaptive PRI control as follows. First, we transmit pulses at a certain PRI (T_{PRI_ob}) and obtain the received signals. Secondly, we detect targets with the pre-estimated direction and relative velocity of each target by using the DBF technique and the Doppler analysis shown in Section 3.3. If there are several targets that have different relative velocities in same direction, they are associated with the same direction with different velocities. Then, we determine the optimal PRI (T_{PRI_opt}) for each target based on the pre-estimated target parameters to form temporal spatial virtual array. Next, we reconstruct received data matrix based on T_{PRI_opt} and extract the signal of the focused target by using Doppler filter. Finally, we estimate the direction of the target using the temporal spatial virtual array. Details are described as follows.

Note that in this dissertation, we consider short range human detection. Therefore, we assume that the maximum velocity and the maximum range of targets are 5 m/s and several hundred meters, respectively. To prevent grating lobes, we also assume that the original MIMO array is ULA and antenna spacing parameters are as follows: $d_r = \lambda/2$ and $d_t = Md_r$.

3.4.1 Observation

First of all, we obtain the received data matrix $\tilde{\boldsymbol{X}}_r$ transmitting pulses at T_{PRI_ob} interval. Then, we detect targets and obtain the initial estimates ($\tilde{\theta}_q$ and $\tilde{v}_q$) of targets using the common radar signal processing. T_{PRI_ob} is determined based on eqs. (3.22) and (3.23), which are required to eliminate range ambiguity and velocity ambiguity,

respectively.

$$T_{PRI\_ob} > 2R_{max}/c, \tag{3.22}$$

$$T_{PRI\_ob} < \lambda/(4|v_{max}|), \tag{3.23}$$

where, R_{max} and v_{max} denote the maximum range and the maximum velocity required by the system to eliminate the mentioned ambiguities, respectively.

3.4.2 Determine Optimal PRI to Arrange Temporal Spatial Virtual Array

For the arrangement of the temporal spatial virtual array, the parameters in eq. (3.20) that we can control are T_{PRI} and P. Therefore, we adjust the temporal spatial virtual array arrangement by controlling these two parameters. To achieve stable and high estimation accuracy of DOA, we need a constant array arrangement independent of the movement of targets. Figure 3 shows the arrangement of the temporal spatial virtual array generated by the received signals of P pulses. To keep constant array structure consisting of the original MIMO array and the temporal spatial virtual array without overlaps of them, we set d_a equal to d_{min}. Therefore, as shown in Fig. 3-3, satisfying eq. (3.24) is required.

$$d_{min} = \left| \frac{2\tilde{v}_q T_{PRI}}{\sin\tilde{\theta}_q} \right| - d_{max}, \tag{3.24}$$

where d_{min} denotes the minimum distance between arbitrary existing antennas, and d_{max} denotes the array length of the spatial virtual array as shown in Fig. 3-3. Here, we set $d_r = \lambda/2$ and $d_t = Md_r$, $\hat{T}_{PRI\_opt}$ can be calculated by eq. (3.25).

$$\hat{T}_{PRI\_opt} = \left| \frac{MN\lambda}{4\tilde{v}_q} \sin\tilde{\theta}_q \right|. \tag{3.25}$$

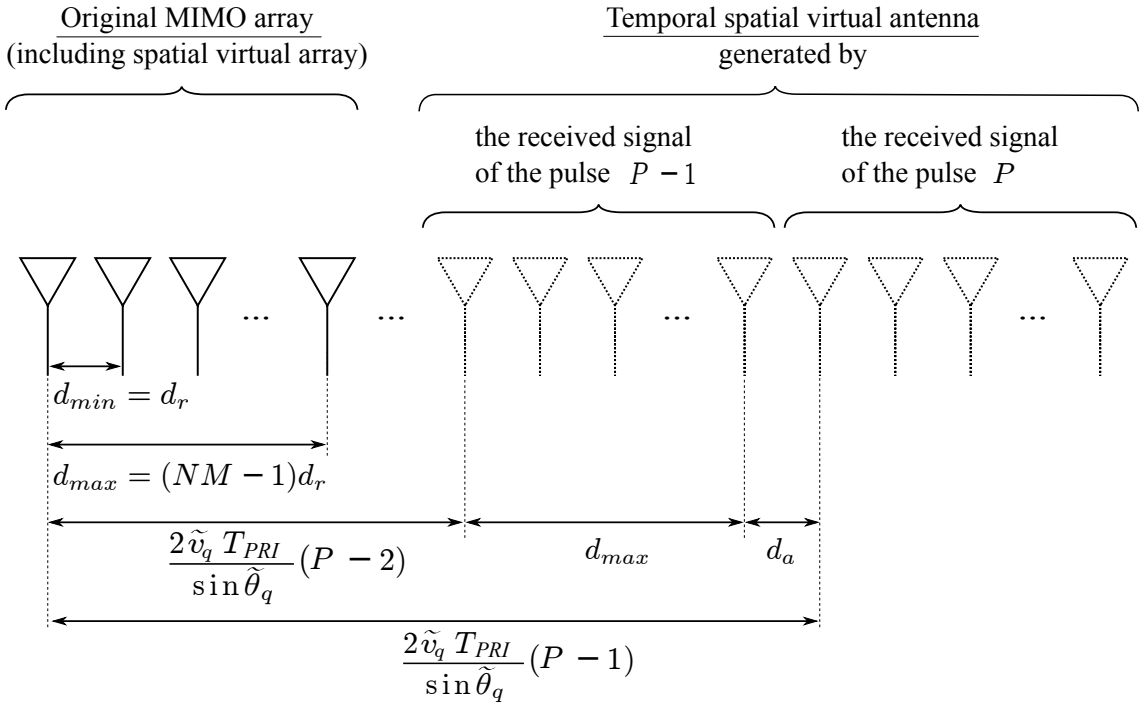

Figure 3-3: Arrangement of the temporal spatial virtual array.

3.4.3 Reconstruct the Received Data Matrix Based on the Optimal PRI

In this section, we explain how to obtain the data matrix to be used for adaptive forming the temporal spatial virtual array based on $\hat{T}_{PRI\_opt}$ from the original received data $\tilde{\boldsymbol{X}}_r$.

Figure 3-4 (a) shows the original received data matrix $\tilde{\boldsymbol{X}}_r$ and Fig. 3-4 (b) shows the reconstructed data matrix $\tilde{\boldsymbol{X}}'_r$ based on $\hat{T}_{PRI\_opt}$. Here, we define an $MN \times W$ matrix described in Fig. 3-4 (a) as the signal processing matrix unit. First, we extract P signal processing matrices at $\hat{T}_{PRI\_opt}$ interval from the original received data matrix $\tilde{\boldsymbol{X}}_r$ which is obtained by transmitting $K(P-1)+W$ pulses, as described in Fig. 3-4 (a). Then, we reconstruct the new received data matrix $\tilde{\boldsymbol{X}}'_r$ by using P signal processing matrices as shown in Fig. 3-4 (b). K denotes natural number that satisfies

$$T_{PRI\_ob}K \approx \hat{T}_{PRI\_opt}, \tag{3.26}$$

therefore we need to select the minimum T_{PRI_ob} satisfying eq. (3.22) to reduce the mismatch between $\tilde{\boldsymbol{X}}_r'$ based on $T_{PRI\_ob}K$ and $\tilde{\boldsymbol{z}}(\theta)$ based on $\hat{T}_{PRI\_opt}$. W denotes data length to be used for signal processing on each antenna.

Although large W provides high signal to noise ratio (SNR), the array signal processing period $\{K(P-1)+W\}T_{PRI\_ob}$ should be less than the period in which the focused target does not walk out of a range bin. Therefore, W should satisfy eq. (3.27).

$$\{K(P-1)+W\}T_{PRI\_ob} < R_{bin}/(2|\tilde{v}_q|), \tag{3.27}$$

where R_{bin} denotes size of a range bin which is expressed as

$$R_{bin} \approx c/(2B), \tag{3.28}$$

where B denotes the band width of transmitting signal.

Based on eqs. (3.25), (3.26), and (3.27), the relation between W, K, and P can be described as follows.

$$W < K\left(\frac{2R_{bin}}{MN\lambda|\sin\tilde{\theta}_q|}+1-P\right). \tag{3.29}$$

Since W and K should be natural numbers and the maximum value of $|\sin\tilde{\theta}_q|$ is 1, we set P to a natural number that satisfies

$$P < \frac{2R_{bin}}{MN\lambda}. \tag{3.30}$$

In practical situations, we determine the parameter P based on eq. (3.30) considering the system parameters.

3.4.4 Temporal Spatial Virtual Array Based on Doppler Shift with Adaptive PRI Control

After reconstructing received data matrix, we calculate digital Fourier transform of pulse train of $\tilde{\boldsymbol{X}}_r^{'} \in \mathbb{C}^{MNP \times W}$ shown in Fig. 3-4 (b). The output signal of the u th Doppler filter bank, $\boldsymbol{y}_r(u)$, is given by

$$\boldsymbol{y}_r(u) = \sum_{h=1}^{W} \tilde{\boldsymbol{x}}_r'(h) \exp(-j2\pi(u-1)(h-1)/W), \tag{3.31}$$

$$u = 1, \cdots, W,$$

where $\tilde{\boldsymbol{x}}_r'(h), (h = 1, \cdots, W)$, denotes the h th column of the matrix $\tilde{\boldsymbol{X}}_r^{'}$.

Since we already know the pre-estimated Doppler frequency $\tilde{\omega}_{d,q}$ as described in Section 3.3, we can obtain the index of Doppler filter bank D_q which represents the Doppler frequency of the q th target by using eq. (3.32). Finally, we extract the output signal of the D_q th Doppler filter bank $\boldsymbol{y}_r(D_q)$.

$$D_q = \lceil (\tilde{\omega}_{d,q} W T_{PRI\_opt})/2\pi \rceil, \tag{3.32}$$

where $\lceil \cdot \rceil$ denotes the ceiling function.

$\boldsymbol{y}_r(D_q)$ is the individual signal vector of the focused target unless there are multiple targets in the same range bin and the same Doppler filter bank. Therefore, using $\boldsymbol{y}_r(D_q)$ instead of $\tilde{\boldsymbol{x}}_r$, we can obtain the new correlation matrix of echo signal from the q th target. The resulting correlation matrix $\tilde{\boldsymbol{R}}_{yy}$ of $\boldsymbol{y}_r(D_q)$ is defined as follows.

$$\tilde{\boldsymbol{R}}_{yy} = \boldsymbol{y}_r(D_q)\boldsymbol{y}_r^H(D_q). \tag{3.33}$$

Finally, the new spectrum function $P_{Prop}(\theta)$ for each target is defined using the temporal spatial virtual array based on Doppler shift with adaptive PRI control as follows.

$$P_{Prop}(\theta) = \frac{\tilde{\boldsymbol{z}}^H(\theta)\tilde{\boldsymbol{z}}(\theta)}{\tilde{\boldsymbol{z}}^H(\theta)\tilde{\boldsymbol{E}}_N^{'}\tilde{\boldsymbol{E}}_N^{'H}\tilde{\boldsymbol{z}}(\theta)}, \tag{3.34}$$

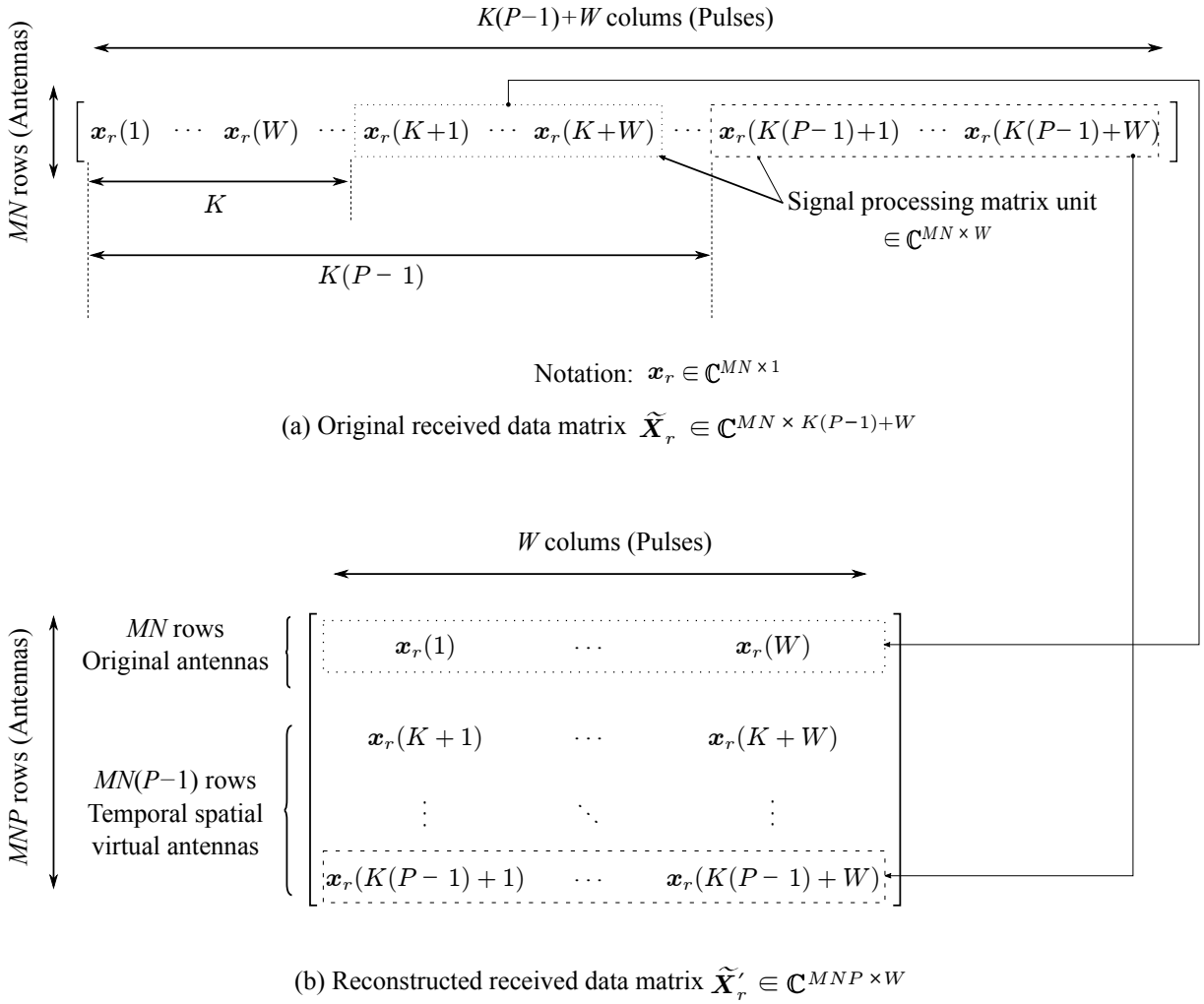

Figure 3-4: Original data matrix $\tilde{\boldsymbol{X}}_r$ and reconstructed data matrix $\tilde{\boldsymbol{X}}'_r$.

where $\tilde{\boldsymbol{E}}'_N$ is the noise subspace matrix of $\tilde{\boldsymbol{R}}_{yy}$.

3.5 Analysis of DOA Estimation Accuracy

As mentioned in the previous section, the proposed method requires the pre-estimation of the direction and the velocity of targets. These parameters are estimated by the common radar signal processing and these parameters have some errors, hereinafter we refer to the errors as the initial estimation error. Since $\hat{T}_{PRI\_opt}$ is calculated by using the pre-estimated parameters that include initial estimation errors, $\hat{T}_{PRI\_opt}$ obviously has some errors. Also, a reconstructed data matrix based on $\hat{T}_{PRI\_opt}$ us-

ing T_{PRI_ob} as a minimal unit has offset error within T_{PRI_ob}. Therefore, the initial estimation error and the offset error cause the mismatches between the steering vectors of the temporal spatial virtual array and the reconstructed data matrix. The mismatches degrade the DOA estimation accuracy of the proposed method. Thus, in this section, we clarify the impact of these errors on the DOA estimation accuracy of the proposed method with error evaluation and discuss how to reduce the negative effect.

For the error evaluation, we assume that ULA MIMO array consists of four Tx antennas and four Rx antennas with the structure shown in Fig. 3-1. In addition, we set the common parameters as follows; the carrier frequency is 24.1 GHz, the bandwidth is 200 MHz, and the spacing of antennas is $\lambda/2$ where λ is the wavelength of the carrier frequency. In this case, the range bin size can be calculated approximately 0.75 m by using eq. (3.28). Assuming 5 m/s for the maximum velocity of human target, the array signal processing period $\{K(P-1)+W\}T_{PRI\_ob}$ should be less than approximately 75 ms from eq. (3.27). Then, we set array signal processing period is 50 ms considering the margin for the maximum velocity of human targets.

First, we evaluate the impact of the offset error on the DOA estimation accuracy of the proposed method. In the analysis, to clarify the influence of the offset error, we assume that there are no initial estimation errors. Note that the number of transmit pulses will change depending on T_{PRI_ob}, because the fixed array signal processing period discussed above is applied to the simulation. R_{max} is assumed to be larger than several hundreds meters as mentioned previously, and it is determined by T_{PRI_ob} as shown in eq. (3.22) (for example, when T_{PRI_ob} is 0.005 ms, R_{max} is 750 m). Considering that the offset error depends on T_{PRI_ob}, we use several T_{PRI_ob} of which the lowest value is 0.005 ms. Table 3.1 lists the parameters to be used for the error evaluation.

Figures 3-5 and 3-6 show the root mean square error (RMSE) of the DOAs estimated by eq. (3.34) on each T_{PRI_ob} using $P=5$ and $P=2$, respectively. The RMSE of the MUSIC is also shown in these figures for comparison. Since we set the signal processing period to 50 ms and minimum T_{PRI_ob} to 0.005 ms, the maximum number

Table 3.1: Simulation parameters for the offset error evaluation.

Item	Symbol	Quantity
PRI for observation	T_{PRI_ob}	0.005, 0.01, 0.05, 0.1 ms
Direction of target	θ	10 deg.
Velocity of target	v	2.0 m/s

of transmitting pulses is 10000. Therefore, we also set the number of snapshots for MUSIC to 10000, to compare the proposed method with the best performance of MUSIC under the same condition. The parameter W of the proposed method for each condition is set to the maximum value that satisfies eq. (3.29). Obviously, the smaller the T_{PRI_ob} is, the less the DOA estimation error becomes. Since the offset error of $\hat{T}_{PRI\_opt}$ is subject to T_{PRI_ob} as mentioned previously, using small T_{PRI_ob} improves the DOA estimation accuracy of the proposed method. Here, we should mention that these results correspond to the lower bounds of RMSE of the proposed method on each T_{PRI_ob}, because they are calculated with no initial estimation errors. Based on the results, hereafter we set T_{PRI_ob} to 0.005 ms (in this case, $R_{max} = 750$ m from eq. (3.22)), which realizes much higher DOA estimation accuracy than one of the MUSIC as shown in Figs. 3-5 and 3-6.

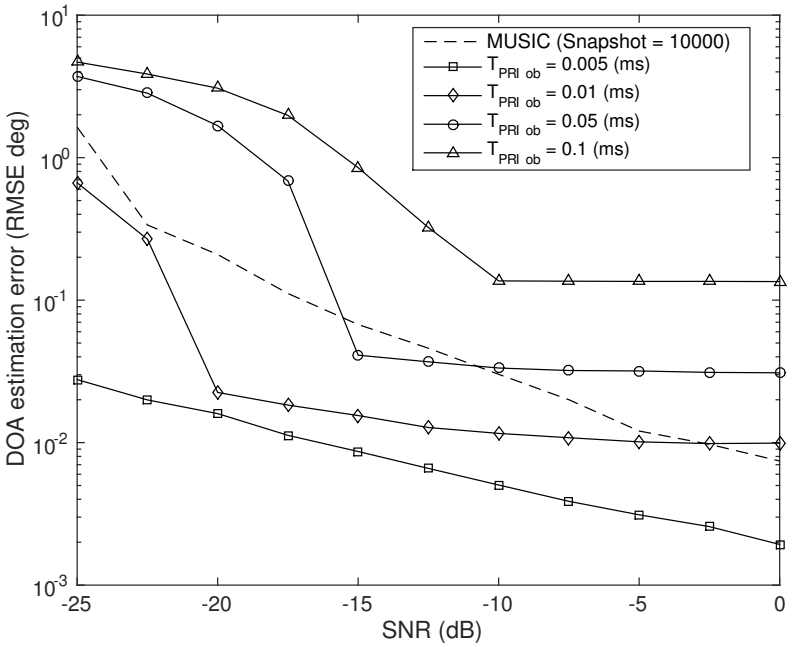

Figure 3-5: RMSE of the DOAs estimated by eq. (3.34) on each T_{PRI_ob} without initial estimation errors (P=5).

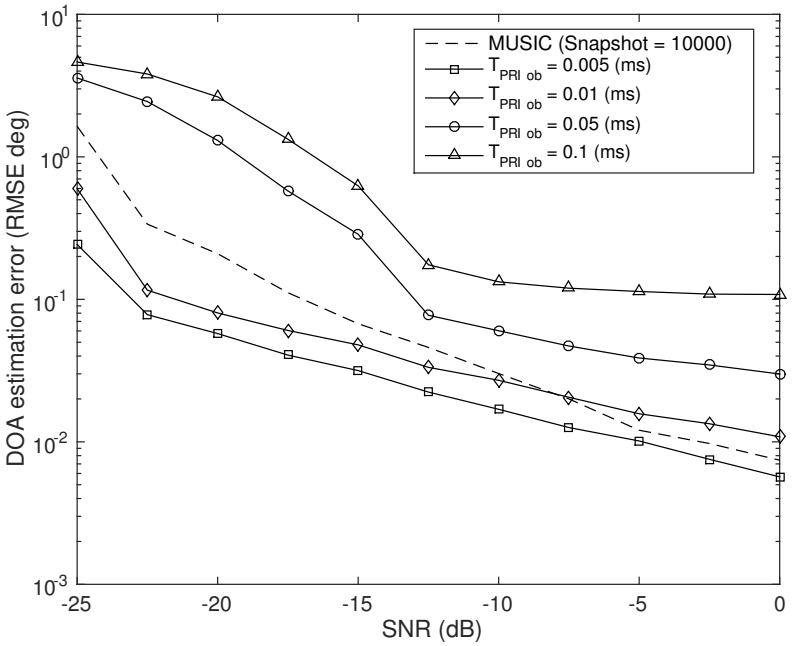

Figure 3-6: RMSE of the DOAs estimated by eq. (3.34) on each T_{PRI_ob} without initial estimation errors (P=2).

Table 3.2: Simulation parameters for the initial estimation error evaluation.

Item	Symbol	Quantity
PRI for observation	T_{PRI_ob}	0.005 ms
Variance of initial estimation error of target direction	σ_θ^2	0.25, 1.0, 4.0
Variance of initial estimation error of target velocity	σ_v^2	0.0025

Next, we evaluate the relation between the initial estimation errors and the DOA estimation accuracy of the proposed method using $T_{PRI\_ob} = 0.005$ ms. We use several values of variance of the initial estimation errors of directions for the simulation, because the accuracy of the pre-estimated direction of targets depends on many kinds of factors such as performance of element antennas, DOA estimation technique and so on. Here, to analyze the performance of the proposed method with the large initial estimation errors, we assume that the variances of the initial estimation errors of target direction (σ_θ^2) to be used in the simulation are 0.25, 1.0 and 4.0 degrees^2 ($\sigma_\theta = 0.5, 1.0$ and 2.0 deg.), of which the largest one is larger than the worst mean square errors of the MUSIC shown in Figs. 3-5 and 3-6. Note that the accuracy of the pre-estimated velocity of targets by Doppler analysis depends on array signal processing period, T_{PRI_ob} and carrier frequency. In this case, the variance of the error of the pre-estimated velocity σ_v^2 is calculated to be approximately 0.0025 (m/s)^2 ($\sigma_v = 0.05$ m/s) based on the parameters described above. Table 3.2 lists the parameters to be used for the evaluation. The parameters of the target are the same values shown in Table 3.1.

Figures 3-7 and 3-8 show the RMSE of the DOAs estimated by eq. (3.34) as a function of SNR using $P = 5$ and $P = 2$, respectively. The mismatch of the steering vector and reconstructed data matrix based on $\hat{T}_{PRI\_opt}$ causes degradations of the DOA estimation accuracy. These results show that the low initial estimation error yields the low RMSE of DOA estimation, vice versa. These figures also indicate that RMSE degrades with increasing the number of P. Since P represents ratio of the number of the temporal spatial virtual antennas to the number of the spatial virtual

antennas, the temporal spatial virtual antennas have predominant influence on RMSE in the case of using large P.

From the simulation results, the improvements of DOA estimation accuracy by using the proposed method disappear due to the initial estimation errors. Thus, we need to suppress the degradation caused by the initial estimation errors. Below we present a scheme that improves DOA estimation accuracy of the proposed method suppressing the negative effect of the initial estimation errors.

The weight w is used for compensation of errors of the 3rd term in eq. (3.20), which is in charge of forming the temporal spatial virtual array. Here we obtain the new steering vector $\tilde{z}'(\theta, w)$ and the spatial spectrum function $P'_{Prop}(\theta, w)$ as shown in eqs. (3.35) $\sim$ (3.37). Then, we search simultaneously $\hat{\theta}$ and $\hat{w}$ which maximize $P'_{Prop}(\theta, w)$ as shown in eq. (3.38). The scheme suppresses influences of the mismatch between the steering vector and the reconstructed data matrix caused by the initial estimation errors and provides improved spatial spectra. Note that the process requires $|\tilde{v}_q| - 3\sigma_v > 0$ and $|\tilde{\theta}_q| - 3\sigma_\theta > 0$.

$$\tilde{\boldsymbol{z}}'(\theta, w) =$$

$$[z'_{1,1,1}(\theta,w), z'_{1,1,2}(\theta,w), \cdots, z'_{m,n,p}(\theta,w), \cdots, z'_{M,N,P}(\theta,w)]^T, \tag{3.35}$$

$$z'_{m,n,p}(\theta, w) =$$

$$\exp\left[-j\frac{2\pi \sin\theta}{\lambda}\left\{d_t(n-1)+d_r(m-1)+w\frac{MN\lambda}{2}(p-1)\right\}\right], \tag{3.36}$$

$$P'_{Prop}(\theta, w) = \frac{\tilde{\boldsymbol{z}}'^H(\theta, w)\tilde{\boldsymbol{z}}'(\theta, w)}{\tilde{\boldsymbol{z}}'^H(\theta, w)\tilde{\boldsymbol{E}}'_N\tilde{\boldsymbol{E}}'^H_N\tilde{\boldsymbol{z}}'(\theta, w)}, \tag{3.37}$$

$$\{\hat{\theta}, \hat{w}\} = \arg\max_{\theta, w}\{\max(P'_{Prop}(\theta, w))\}, \tag{3.38}$$

$$\hat{\theta} \in \{\tilde{\theta}_q - 3\sigma_\theta \le \hat{\theta} \le \tilde{\theta}_q + 3\sigma_\theta\},$$

$$\hat{w} \in \left\{\frac{|\tilde{v}_q|\sin(|\tilde{\theta}_q|-3\sigma_\theta)}{(|\tilde{v}_q|+3\sigma_v)\sin|\tilde{\theta}_q|} \le \hat{w} \le \frac{|\tilde{v}_q|\sin(|\tilde{\theta}_q|+3\sigma_\theta)}{(|\tilde{v}_q|-3\sigma_v)\sin|\tilde{\theta}_q|}\right\}.$$

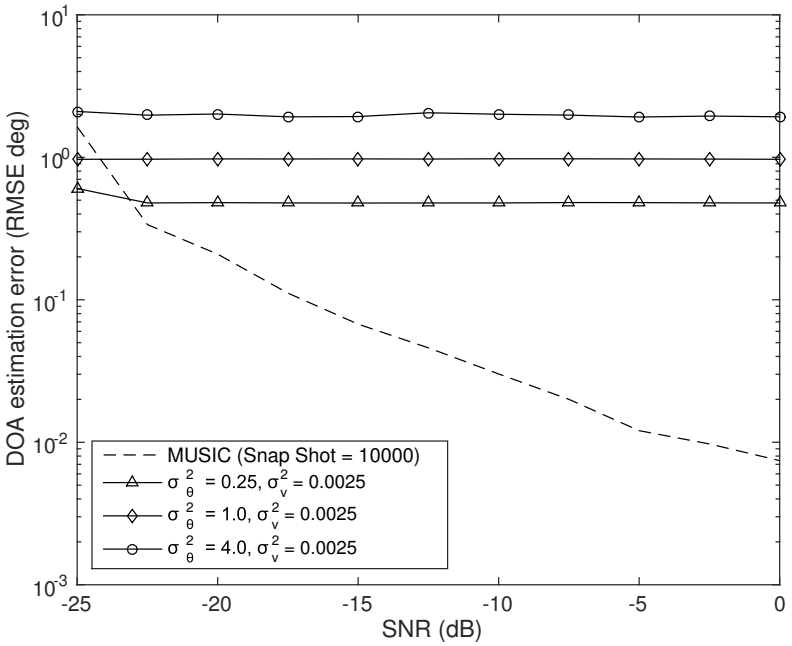

Figure 3-7: RMSE of the DOAs estimated by eq. (3.34) with initial estimation errors (P=5).

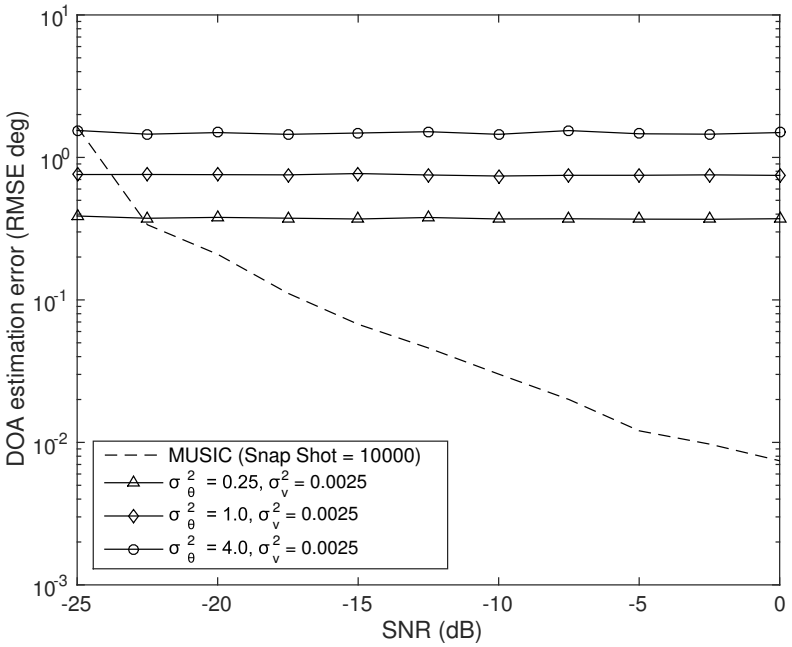

Figure 3-8: RMSE of the DOAs estimated by eq. (3.34) with initial estimation errors (P=2).

3.6 Summarized Signal Processing Process

Figure 3-9 shows the summarized flowchart of the signal processing process of the proposed method. As indicated in the flowchart, the steps from 5 to 8 are repeated Q times, which is the number of targets.

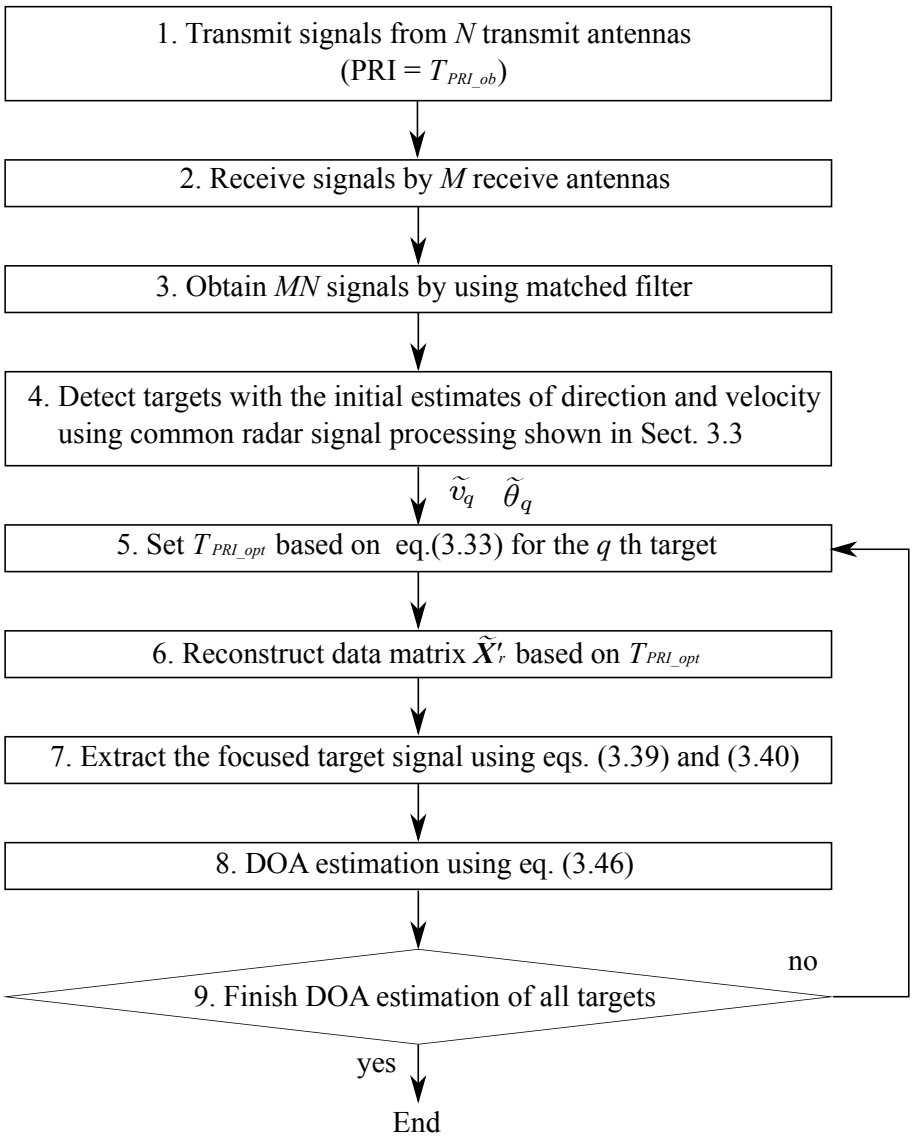

Figure 3-9: Signal processing flowchart of the proposed method.

3.7 Numerical Results

In this section, we demonstrate that the proposed method achieves high estimation accuracy of DOAs even if multiple targets exist in the search space. For this, we run following two simulations; first one is the evaluation of the DOA estimation of two targets which are close to each other in azimuth angle, and second one is the evaluation of the DOA estimation accuracy of the proposed method.

3.7.1 Simulation Parameters

The MUSIC and the conventional method were tested for comparison. As described previously, we consider the MIMO radar consisting of ULA with four transmit antennas and four receive ones. We select 24 GHz as a carrier frequency which is the commonly used frequency band in commercial based RF sensor systems. Since the conventional method requires the fixed PRI (T_{PRI_c}) to form temporal spatial virtual array, we set T_{PRI_c} equal to T_{PRI_ob}. As described in the previous section, we also set T_{PRI_ob} to 0.005 ms and array signal processing period to 50 ms. Thus, the number of snapshots to be used for the MUSIC is set to 10000. Note that W is calculated based on eq. (3.29). The parameters for each simulation are summarized in Table 3.3. In the case of the system parameters shown in table 3.3, T_{PRI_opt} is approx. tens of milliseconds.

3.7.2 Simulation 1: DOA Estimation of Two Closely Spaced Targets

In this simulation, we evaluate the performance of the DOA estimation of two closely spaced targets listed in Table 4.

Figures 3-10 and 3-11 show the resulting spatial spectra, where SNR of the echo signal from each target is 10 dB, calculated by focusing on the target A and calculated by focusing on the target B, respectively. In general, the MUSIC spectrum has the same number of peaks as the number of targets existing in the search space as far

Table 3.3: Simulation parameters.

Item	Symbol	Quantity	Remarks
Carrier frequency	f_c	24.1 GHz	$\lambda = 12.4$ mm
Band width	B	200 MHz	Range bin = 0.75 m
Array signal processing period	-	50 ms	
PRI for observation	T_{PRI_ob}	0.005 ms	$= T_{PRI\_c}$
Number of snapshots	-	10000	for MUSIC
Number of Tx antennas	-	4	
Number of Rx antennas	-	4	
Tx antenna spacing	d_t	2λ	$= 4d_r$
Rx antenna spacing	d_r	$\lambda/2$	

Table 3.4: Target parameters.

Item	Symbol	Quantity	Remarks
Direction of Target A	θ_a	10 deg.	$\sigma_\theta^2 = 4.0$(simulation 1)
Velocity of Target A	v_a	2.0 m/s	$\sigma_v^2 = 0.0025$(simulation 1)
Direction of Target B	θ_b	11 deg.	$\sigma_\theta^2 = 4.0$(simulation 1)
Velocity of Target B	v_b	1.0 m/s	$\sigma_v^2 = 0.0025$(simulation 1)
Range of both targets	r	20 m	

as echo signal from each target is uncorrelated to each other. We can see that the MUSIC spectrum has two peaks in Figs. 3-10 and 3-11. These figures also show that both the proposed method with $P = 1$ and the proposed method with $P = 5$, can estimate the DOA of each target individually, while the conventional method with $P = 5$ cannot estimate directions of two targets separately. It is also found that the proposed method with $P = 5$ yields a sharp peak compared to other methods.

The improvements result from expansion of array structure by using the temporal spatial virtual array. There are two reasons that the conventional method with $P = 5$ cannot provide the direction of each target. One reason is that the echo signal from each target behaves like interference signal to each other. Another reason is that the temporal spatial virtual antenna generated by the conventional method receives the echo signal from the same target as if correlated signal from other direction. These

factors cause the mismatches between the steering vector and the correlation matrix $\tilde{\boldsymbol{R}}_{xx}$. Therefore, the conventional method cannot provide the direction of targets.

Figures 3-12 and 3-13 show the resulting spatial spectra, where SNR of the echo signal from each target is 0 dB, calculated by focusing on the target A and calculated by focusing on the target B, respectively. These figures also show that the proposed method with $P = 5$ improves the performance of DOA estimation, while the MUSIC and the conventional method cannot estimate the direction of two targets. In the comparison between these simulations, it is found that the proposed method is more effective to improve the spatial spectrum in the low SNR case. As already discussed, the improvement is attributed to the expansion of array structure by using the temporal spatial virtual array with Doppler filter and adaptive PRI control technique.

The simulation results show that the proposed method can estimate the direction of targets accurately even if there are multiple targets. Moreover, it can clearly separate two targets, while the MUSIC and the conventional method cannot provide DOA of each target in the low SNR case.

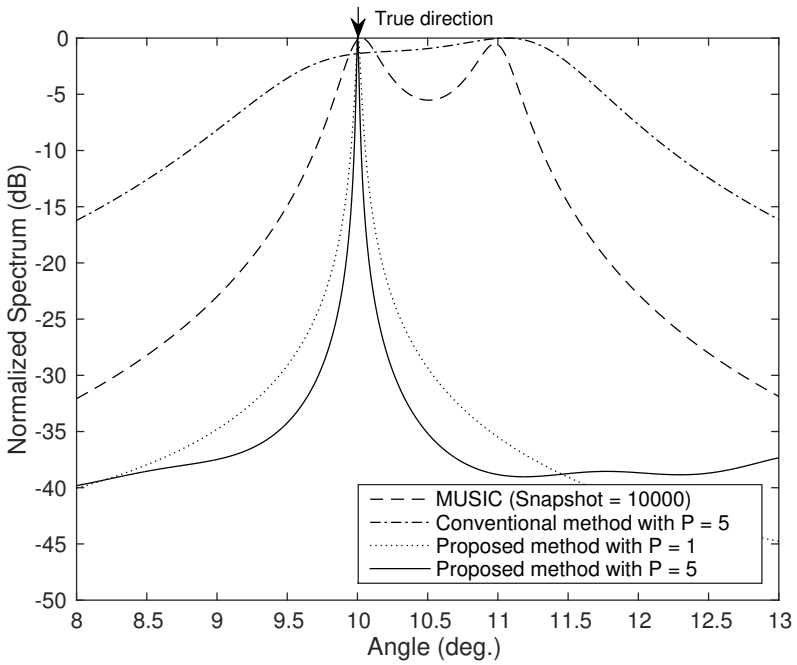

Figure 3-10: MUSIC spectrum focusing on the target A (true direction is 10 deg.), where SNR of the echo signal from each target is 10 dB.

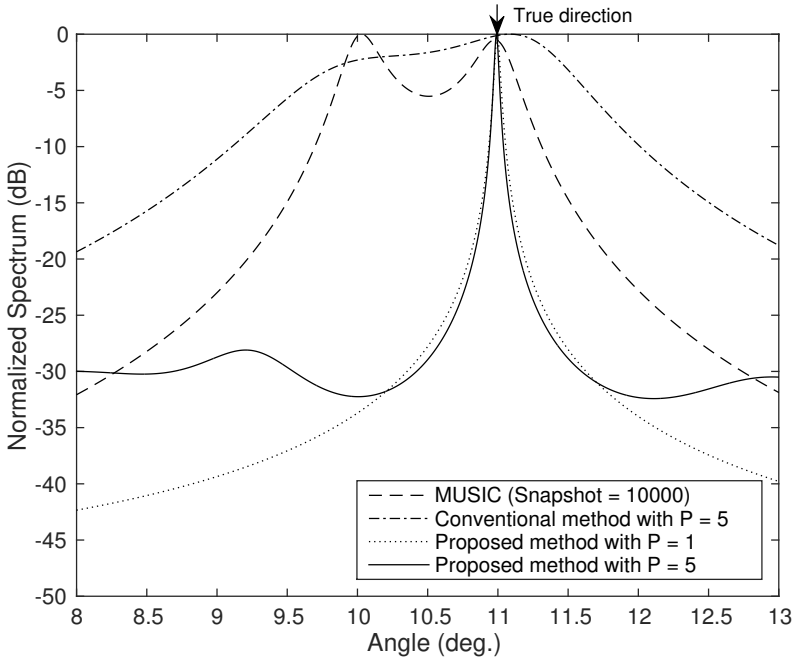

Figure 3-11: MUSIC spectrum focusing on the target B (true direction is 11 deg.), where SNR of the echo signal from each target is 10 dB.

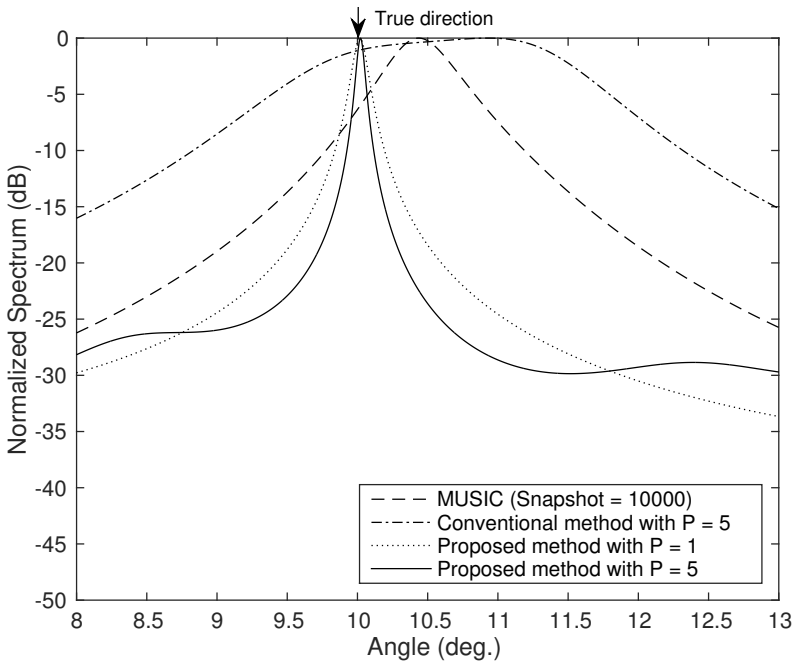

Figure 3-12: MUSIC spectrum focusing on the target A (true direction is 10 deg.), where SNR of the echo signal from each target is 0 dB.

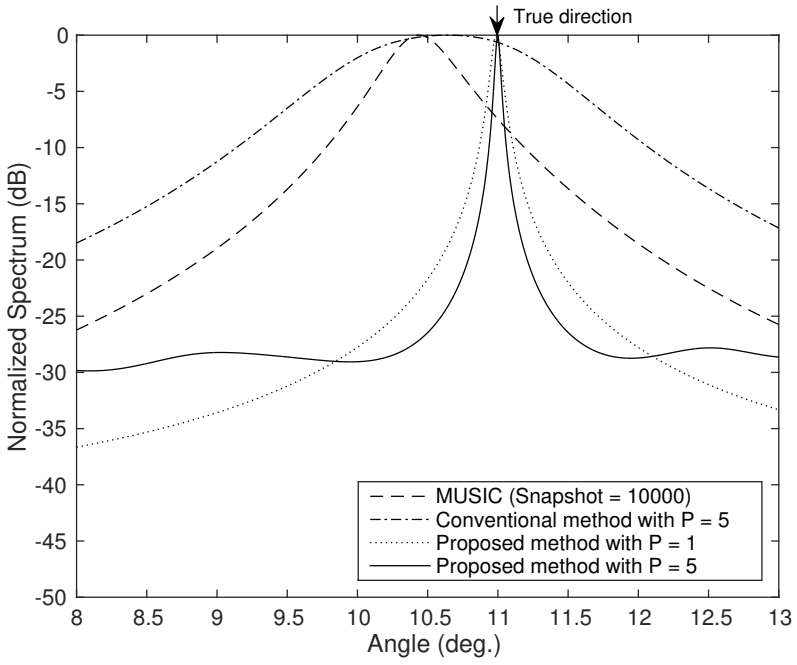

Figure 3-13: MUSIC spectrum focusing on the target B (true direction is 11 deg.), where SNR of the echo signal from each target is 0 dB.

3.7.3 Simulation 2: DOA Estimation Accuracy

In this section, we evaluate the DOA estimation accuracy of the proposed method with $P = 5$ using a single target. Two targets listed in Table 4 are used individually with several variance parameters. Figures 3-14 and 3-15 show the RMSEs of the estimated DOA of the target A and the target B, respectively.

These results show that the proposed method achieves higher accuracy of DOA estimation than the MUSIC. In comparison with Fig. 3-7, it is found that the proposed method can suppress the negative effect of the initial estimation errors and the RMSE of the proposed method in each figure is close to the lower bound shown in Fig. 3-5. The simulation results prove that the proposed method is effective to improve the DOA estimation accuracy without dependence on the velocity and the direction of targets even if the initial estimation errors exist.

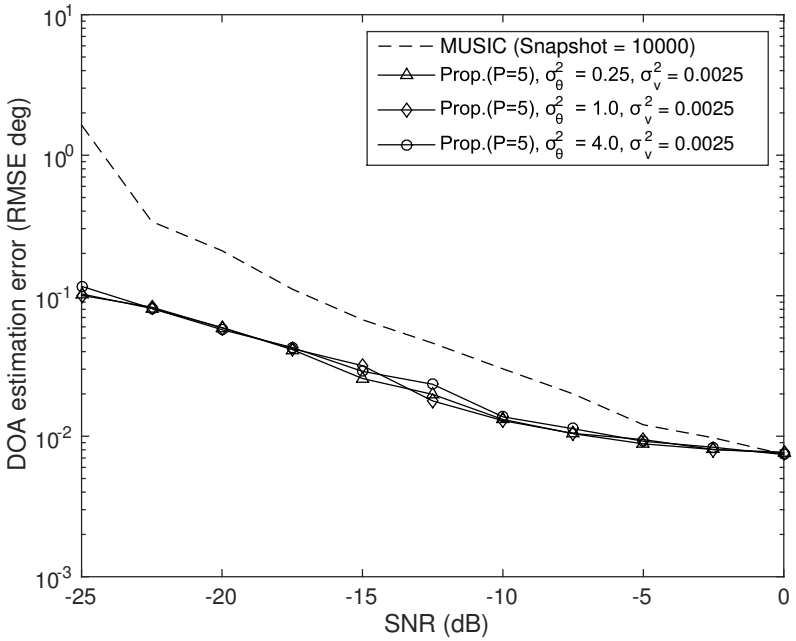

Figure 3-14: The RMSE of the estimated DOA of the target A (θ_a=10 deg.,v_a=2.0 m/s) versus SNR.

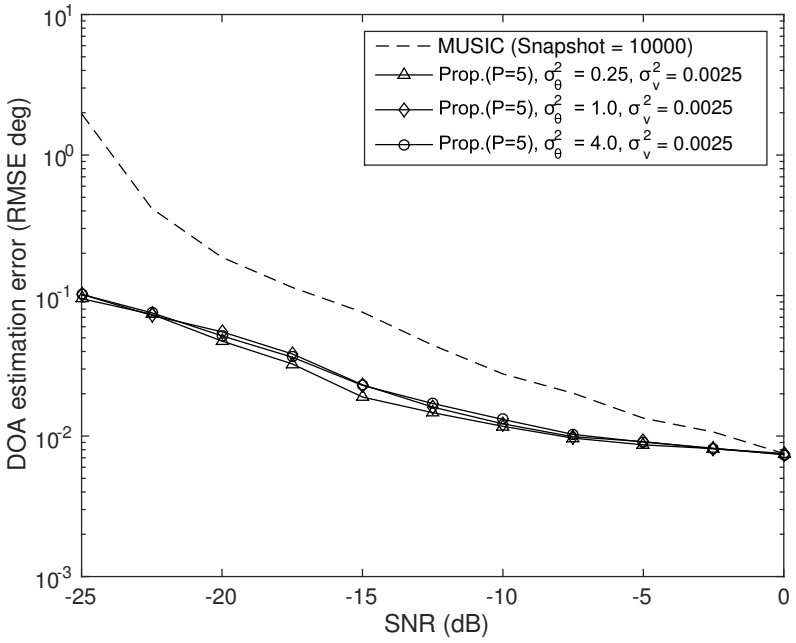

Figure 3-15: The RMSE of the estimated DOA of the target B (θ_b=11 deg.,v_b=1.0 m/s) versus SNR.

3.8 Conclusion

In this chapter, we have proposed a new DOA estimation method by using the temporal spatial virtual array based on Doppler shift with adaptive PRI control. The proposed method is effective for any sensor systems with an array antenna because it is the basic approach to arrange the virtual array structure. The numerical results show that our proposed method can provide the improved spatial spectrum for each target and estimate the DOA of target accurately even if multiple moving targets exist in the search area. The simulation results also prove that the proposed method can achieve high accuracy of DOA estimation without dependence on the target parameters even if the initial estimation errors exist.

Chapter 4

DOA Estimation of Wideband Signal Sources by Weighted Squared TOPS

4.1 Introduction

In the previous chapter, we have proposed a DOA estimation method for narrowband signal sources. Next, we shift our research topic to wideband signal sources, as shown in Fig. 1-1. In this chapter, we discuss a new DOA estimation method of wideband signal sources based on Squared TOPS. As mentioned in section 2.4, Squared TOPS can provide better DOA estimation accuracy and resolution performance than those of the other conventional methods e.g. ISSM, TOPS. The method, however, has the serious drawback: The spatial spectrum calculated by Squared TOPS has some false peaks.

To overcome the shortcoming, we propose a new DOA estimation method for wideband signals called WS-TOPS to improve Squared TOPS by modifying the orthogonality test matrix in the conventional method. Moreover, the algorithm averaging output of each frequency bin with appropriate weight is also applied to improve DOA estimation accuracy. WS-TOPS can suppress all false peaks in spatial spectrum and

improve DOA estimation performance of wideband signal sources. The performances of the proposed method are compared with those of the conventional one via computer simulation. From the simulation results, it is found that the proposed method can achieve better resolution performance and DOA estimation accuracy than those of the conventional one. Note that we consider the same system model described in section 2.4.1.

The rest of chapter is organized as follows. The conventional DOA estimation algorithms are explained in Section 4.2. In Section 4.3, WS-TOPS is proposed. Simulation results and detailed performance evaluation are discussed in Section 4.4 and Section 4.5, respectively. Finally, conclusion of this chapter is presented in Section 4.6.

4.2 Summarization of Conventional Methods

In this section, we summarize the conventional methods for wideband DOA estimation described in section 2.4, which are compared to our proposed method in the following sections.

ISSM (IMUSIC)

IMUSIC, which is one of the simplest DOA estimation methods for wideband signals, applies narrowband signal subspace methods, for example MUSIC, to each frequency band independently [36, 37]. Then, IMUSIC estimates the DOA of wideband signal sources by using the following equation.

$$\hat{\theta} = \arg\min_{\theta} \sum_{i=1}^{K} \boldsymbol{a}_i^H(\theta) \boldsymbol{W}_i \boldsymbol{W}_i^H \boldsymbol{a}_i(\theta). \tag{4.1}$$

TOFS

TOFS uses the noise subspace obtained from EVD of the correlation matrix of each frequency [45]. The DOA of each incoming wideband signal source is estimated by testing the orthogonality between the steering vector and the noise subspaces. If θ is

the one DOA of incoming wideband signals, θ satisfies the following equation.

$$\boldsymbol{a}_i^H(\theta)\boldsymbol{W}_i\boldsymbol{W}_i^H\boldsymbol{a}_i(\theta) = 0. \tag{4.2}$$

Here, we define the vector $\boldsymbol{d}(\theta)$ as follows.

$$\boldsymbol{d}(\theta) = [\boldsymbol{a}_1^H(\theta)\boldsymbol{W}_1\boldsymbol{W}_1^H\boldsymbol{a}_1(\theta) \quad \cdots \quad \boldsymbol{a}_K^H(\theta)\boldsymbol{W}_K\boldsymbol{W}_K^H\boldsymbol{a}_K(\theta)]. \tag{4.3}$$

All elements of the vector $\boldsymbol{d}(\theta)$ will be zero when θ is the DOA of incoming wideband signal sources. Then, we can estimate the DOAs by using the following equation.

$$\hat{\theta} = \arg\max_{\theta} \frac{1}{||\boldsymbol{d}(\theta)||}. \tag{4.4}$$

TOFS shows good DOA estimation accuracy in high SNR region by using the noise subspaces obtained from the correlation matrix of received signals. However, TOFS cannot resolve closely spaced signal sources when SNR is low.

TOPS

TOPS uses both of the signal and noise subspaces of each frequency band to estimate the DOA of incoming wideband signal sources [43]. First, we obtain the signal subspace $\boldsymbol{F}_i$ and the noise subspace $\boldsymbol{W}_i$ from EVD of the correlation matrix of each frequency band. Then, one frequency band ω_i should be selected and the signal subspace $\boldsymbol{F}_i$ of the selected frequency band is transformed into other frequencies. TOPS uses a diagonal unitary transformation matrix. The mth term on the diagonal of the frequency transform matrix $\boldsymbol{\Phi}(\omega_i, \theta)$ is

$$[\boldsymbol{\Phi}(\omega_i, \theta)]_{(m,m)} = \exp(-j\omega_i \frac{md}{c} \sin\theta). \tag{4.5}$$

Using $\boldsymbol{\Phi}(\omega_i, \theta)$, the signal subspace $\boldsymbol{F}_i$ of the frequency band ω_i is transformed into the other frequency band ω_j, where we define the transformed signal subspace $\boldsymbol{U}_{ij}(\theta)$, as follows.

$$\boldsymbol{U}_{ij}(\theta) = \boldsymbol{\Phi}(\Delta\omega, \theta)\boldsymbol{F}_i, \quad i \neq j, \tag{4.6}$$

where $\Delta\omega = \omega_j - \omega_i$.

The subspace projection technique is applied to reduce the signal subspace component leakage in the estimated noise subspace. The projection matrix $\boldsymbol{P}_i(\theta)$ is defined as

$$\boldsymbol{P}_i(\theta) = \boldsymbol{I} - (\boldsymbol{a}_i^H(\theta)\boldsymbol{a}_i(\theta))^{-1}\boldsymbol{a}_i(\theta)\boldsymbol{a}_i^H(\theta), \tag{4.7}$$

where $\boldsymbol{I}$ is an $M \times M$ unit matrix. Then, we obtain the transformed signal subspace matrix $\boldsymbol{U}'_{ij}(\theta)$.

$$\boldsymbol{U}'_{ij}(\theta) = \boldsymbol{P}_j(\theta)\boldsymbol{U}_{ij}(\theta). \tag{4.8}$$

Assuming that the selected frequency band is ω_1, the matrix $\boldsymbol{D}(\theta)$ is defined as

$$\boldsymbol{D}(\theta) = [\ \boldsymbol{U}'^H_{12}(\theta)\boldsymbol{W}_2 \quad \cdots \quad \boldsymbol{U}'^H_{1K}(\theta)\boldsymbol{W}_K\ ]. \tag{4.9}$$

We can estimate the DOA of the incoming wideband signal sources from spatial spectrum calculated by the following equation since the rank of the matrix $\boldsymbol{D}'(\theta)$ also decreases when θ is the one DOA of incoming wideband signal sources.

$$\hat{\theta} = \arg\max_{\theta} \frac{1}{\sigma_{min}(\theta)}. \tag{4.10}$$

where $\sigma_{min}(\theta)$ is a minimum singular value of $\boldsymbol{D}(\theta)$.

Squared TOPS

Squared TOPS [44] uses the frequency band where the difference between the smallest signal eigenvalue $\lambda_{i,L}$ and the largest noise eigenvalue $\lambda_{i,L+1}$ is maximum. Hereafter we call it as the reference frequency.

Then, the signal subspace of the reference frequency band is transformed into the other frequency bands by eq. (13). Let us assume that the frequency band ω_i is selected and the signal subspace $\boldsymbol{F}_i$ is transformed to the other frequency bands

ω_j. Using $\boldsymbol{U}'_{ij}(\theta)$ and $\boldsymbol{W}_j$, we construct the squared matrix $\boldsymbol{Z}_i(\theta)$ for the test of orthogonality of projected subspaces as follows.

$$\boldsymbol{Z}_i(\theta) = [\ \cdots\ \ \boldsymbol{U}'^{H}_{ij}(\theta)\boldsymbol{W}_j\boldsymbol{W}_j^{H}\boldsymbol{U}'_{ij}(\theta)\ \ \cdots\ ],\ \ i \neq j, \tag{4.11}$$

Squared TOPS estimates the DOA of wideband signals using the minimum singular value $\sigma_{zi_{min}}(\theta)$ of $\boldsymbol{Z}_i(\theta)$.

$$\hat{\theta} = \arg\max_{\theta} \frac{1}{\sigma_{zi_{min}}(\theta)}. \tag{4.12}$$

4.3 Proposed Method

In this section, we explain our proposed method named weighted squared TOPS (WS-TOPS). WS-TOPS applies the following two approaches to Squared TOPS to improve DOA estimation performance. One is the modified squared matrix method, which is the algorithm to suppress the false peaks in the spatial spectrum of Squared TOPS. To realize the suppression of false peaks, we consider avoiding the undesirable rank decrease of $\boldsymbol{Z}_i(\theta)$ by adding the certain variable to diagonal elements of $\boldsymbol{Z}_i(\theta)$. The other is the selective weighted averaging method, which is the algorithm to improve the DOA estimation accuracy by using the signal subspaces of multiple frequency bands. The details of these algorithms are shown in the following subsections.

4.3.1 Modified Squared Matrix (Algorithm 1)

Although Squared TOPS and TOPS use the projection matrix $\boldsymbol{P}_i(\theta)$ to reduce the signal subspace component leakage in the estimated noise subspace, some false peaks in the spatial spectrum remain. This is the serious disadvantage of TOPS and Squared TOPS. The transformed signal subspace matrix $\boldsymbol{U}'_{ij}(\theta)$ has residual error and it causes the undesirable rank decrease of the matrix $\boldsymbol{Z}_i(\theta)$. Thus, we propose the algorithm to suppress these false peaks by modifying the component of the matrix $\boldsymbol{Z}_i(\theta)$. In particular, we avoid the undesirable rank decrease of $\boldsymbol{Z}_i(\theta)$ by adding $b_j(\theta)$ to diagonal elements of $\boldsymbol{Z}_i(\theta)$.

The steering vector $\boldsymbol{a}_i(\theta)$ is orthogonal to the noise subspaces only when θ is the DOA of the incoming wideband signal sources. Here, we define $b_j(\theta) = \boldsymbol{a}_j^H(\theta)\boldsymbol{W}_j\boldsymbol{W}_j^H\boldsymbol{a}_j(\theta)$. Then, we can avoid the undesirable rank decrease of the matrix $\boldsymbol{Z}_i(\theta)$ by adding the square matrix of which the diagonal elements are $b_j(\theta)$ of the frequency band ω_j. We, however, need to consider how we add $b_j(\theta)$ to the components of the matrix $\boldsymbol{Z}_i(\theta)$, because $b_j(\theta)$ is similar to the components of TOFS and it would cause the degradation of the resolution performance of closely spaced signal sources.

$b_j(\theta)$ is calculated by using a steering vector and noise subspaces. As we can see from eq. (2.22), $\boldsymbol{a}_j^H(\theta)\boldsymbol{a}_j(\theta)$ is M that is the number of antennas. Therefore, $b_j(\theta)$ changes between 0 and M. If the steering vector is orthogonal to all of noise subspaces, $b_j(\theta)$ is 0. If the steering vector is not orthogonal to noise subspaces, $b_j(\theta)$ comes close to M. On the other hand, the elements of $\boldsymbol{U}_{ij}^{'H}(\theta)\boldsymbol{W}_j\boldsymbol{W}_j^H\boldsymbol{U}_{ij}^{'}(\theta)$ are calculated by using the transformed signal subspaces and noise subspaces. Here, we define the lth column of $\boldsymbol{U}_{ij}^{'}(\theta)$ as $\boldsymbol{u}_{ijl}^{'}(\theta)$, which is a transformed signal subspace. As we can also see from eqs. (4.6) and (4.8), $\boldsymbol{u}_{ijl}^{'H}(\theta)\boldsymbol{u}_{ijl}^{'}(\theta)$ is 1, thus each element of $\boldsymbol{U}_{ij}^{'H}(\theta)\boldsymbol{W}_j\boldsymbol{W}_j^H\boldsymbol{U}_{ij}^{'}(\theta)$ changes between 0 and 1. Therefore, we divide $b_j(\theta)$ by M to deal with the elements of $\boldsymbol{U}_{ij}^{'H}(\theta)\boldsymbol{W}_j\boldsymbol{W}_j^H\boldsymbol{U}_{ij}^{'}(\theta)$ and $b_j(\theta)$ as the same range. Based on the discussion, we modify the component of $\boldsymbol{Z}_i(\theta)$ as follows.

First, we obtain the matrix $\boldsymbol{C}_{ij}(\theta)$.

$$\boldsymbol{C}_{ij}(\theta) = \boldsymbol{U}_{ij}^{'H}(\theta)\boldsymbol{W}_j\boldsymbol{W}_j^H\boldsymbol{U}_{ij}^{\prime}(\theta) + \boldsymbol{B}_j(\theta), \tag{4.13}$$

where $\boldsymbol{B}_j(\theta)$ is an $L \times L$ diagonal matrix and it can be expressed as

$$\boldsymbol{B}_j(\theta) = \frac{b_j(\theta)}{M}\boldsymbol{I}, \tag{4.14}$$

where $\boldsymbol{I}$ is an $L \times L$ unit matrix. The matrix $\boldsymbol{C}_{ij}(\theta)$ keeps the full rank except when θ is the DOA of incoming wideband signal sources even if the rank of $\boldsymbol{Z}_i(\theta)$ decreases undesirably. Thus, the algorithm can suppress false peaks in spatial spectrum. Then,

we construct a new matrix $\boldsymbol{Z}'_i(\theta)$ using the matrix $\boldsymbol{C}_{ij}(\theta)$ as follows.

$$\boldsymbol{Z}'_i(\theta) = [\ \cdots\ \ \boldsymbol{C}_{ij}(\theta)\ \ \cdots\ ],\ \ i \neq j. \tag{4.15}$$

Finally, we can estimate the DOA of incoming wideband signal sources using eq. (4.16).

$$\hat{\theta} = \arg\max_{\theta} \frac{1}{\sigma'_{zi_{min}}(\theta)}, \tag{4.16}$$

where $\sigma'_{zi_{min}}(\theta)$ is the minimum singular value of the matrix $\boldsymbol{Z}'_i(\theta)$.

4.3.2 Selective Weighted Averaging (Algorithm 2)

Squared TOPS uses only the single signal subspace $\boldsymbol{F}_i$ of the reference frequency band ω_i, where the difference between the smallest signal eigenvalue $\lambda_{i,L}$ and the largest noise eigenvalue $\lambda_{i,L+1}$ is maximum. This approach is reasonable in terms of computational complexity. However, there are signal subspaces of different frequency bands which could be exploited for further improvement of DOA estimation accuracy. In particular, using several frequency bands simultaneously where SNR are high can improve the DOA estimation performance. Therefore, we introduce an algorithm using the signal subspaces of multiple frequency bands with the consideration on SNR of each frequency band. We define the weight α_i using the smallest signal eigenvalue $\lambda_{i,L}$ and the largest noise eigenvalue $\lambda_{i,L+1}$ of the frequency band ω_i as follows.

$$\alpha_i = \lambda_{i,L}/\lambda_{i,L+1} = \lambda_{i,L}/\sigma_n^2. \tag{4.17}$$

The weight α_i can indicate the reliability of the frequency band ω_i because of the same reason that Squared TOPS selects reference frequency. Then, using the weight α_i, the spatial spectrum of all frequency bands are combined as follows.

$$\hat{\theta} = \arg\max_{\theta} \frac{1}{\frac{1}{K}\sum_{i=1}^{K} \alpha_i \sigma_{zi_{min}}(\theta)}. \tag{4.18}$$

The spatial spectrum obtained from eq. (4.18) is averaged with the weights α_i. Therefore, the algorithm can improve the DOA estimation accuracy of signal sources in

high SNR region. However, the algorithm causes deteriorations of sharpness of spectrum peaks when each frequency band shows different peaks to each other, e.g., in low SNR region. Eventually, the algorithm degrades the resolution performance of closely spaced signal sources in low SNR region.

To prevent the deterioration caused by the process, we propose a selective averaging approach. The point of the approach is that the frequency bands which contain high SNR signal are only used with a weight depending on SNR of its frequency band. By using only the frequency bands ω_i with weight α_i larger than a certain threshold α_{th}, which is reliable frequency bands, we can improve DOA estimation performance and also reduce computational cost.

Finally, we obtain the spatial spectrum based on the algorithm 2 as follows.

$$\hat{\theta} = \arg\max_{\theta} \frac{K'}{\sum_{i=1} \alpha_i \sigma_{zi_{min}}(\theta)}, \{i \mid \alpha_i > \alpha_{th}\}, \tag{4.19}$$

where K' is the number of frequency bands with the weight α_i larger than the threshold α_{th}. If there is no frequency band with weight α_i larger than the threshold α_{th}, we use the signal subspace of the frequency band with the largest weight α_i. For example, there are signal sources with low power and every α_i is smaller than α_{th}.

If we use only single frequency band, the proposed method keeps the same performance as Squared TOPS. In other words, the algorithm can provide better performance than that of Squared TOPS even in the case of all α_i are smaller than the threshold α_{th}. In what follows, we set $\alpha_{th} = 9$, which implies that the signal power of the frequency band is larger than $(3\sigma_n)^2$ based on eq. (4.17). α_{th} in the algorithm 2 determines the frequency bands of which spatial spectra are averaged based on SNR, therefore, the performance of the algorithm 2 depends on SNR of each frequency band.

4.3.3 Weighted Squared TOPS (WS-TOPS)

The algorithm 1 is effective to suppress the undesirable false peaks in the spatial spectrum. The algorithm 2 improves the DOA estimation accuracy in high SNR region.

Table 4.1: Computational complexity.

Algorithm	Complexity	
	Calculation for $\boldsymbol{D}$, $\boldsymbol{Z}$, and $\boldsymbol{Z}'$	Calculation for SVD
TOPS	$O(LM(M-L)(K-1))$	$+O(L^2(M-L)(K-1))$
Squared TOPS	$O(\{2LM(M-L)+L^2(M-L)\}(K-1))$	$+O(L^3(K-1))$
WS-TOPS	$O(\{2LM(M-L)+L^2(M-L)\}(K-1)K')$	$+O(L^3(K-1)K')$

Therefore, we can achieve the further improvement of DOA estimation performance using the two algorithms simultaneously as follows.

$$\hat{\theta} = \arg\max_{\theta} \frac{K'}{\sum_{i=1} \alpha_i \sigma'_{zi_{min}}(\theta)}, \{i \mid \alpha_i > \alpha_{th}\}. \tag{4.20}$$

4.4 Computational Complexity

The number of computations for an $M \times M$ SVD is $O(M^3)$ [86], which is the dominant factor of the computational complexity for the TOPS based method (TOPS, Squared TOPS, and WS-TOPS). For example, the signal processing for TOPS requires an SVD of an $L \times (K-1)(M-L)$ matrix $\boldsymbol{D}''(\theta)$, where $(K-1)(M-L) > L^2$ because $2L \leq M$ and $K \geq L+1$ [43]. The calculation of the evaluation matrix ($\boldsymbol{D}$, $\boldsymbol{Z}$, and $\boldsymbol{Z}'$) for each method should also be in consideration. Table 4.1 lists the dominant factors of the computational complexity of each method and Fig. 4-1 shows examples of the computational cost vs. the system parameters (M, L, and K). The proposed method, WS-TOPS, needs to repeat SVD calculations for several frequency bands. Thus, as we can see in Fig. 4-1, it requires K' times signal processing cost than that of Squared TOPS. However, considering the DOA estimation performance described in the following section, the proposed method can provide enough improvement to be applied.

4.5 Numerical Results

In this section, we evaluate the DOA estimation performance of the proposed method with that of conventional methods described in Section 4.2.

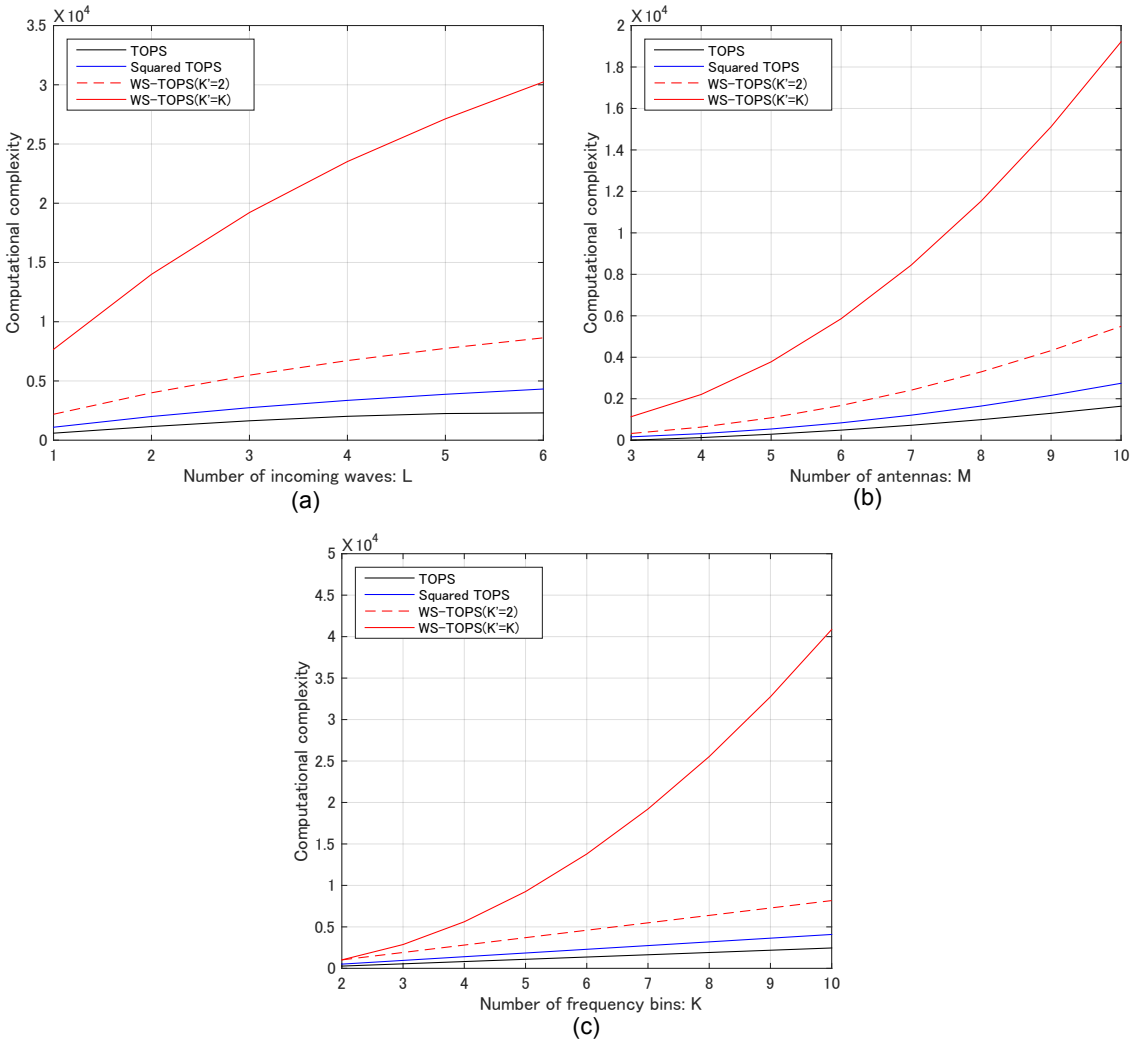

Figure 4-1: Computational complexity, (a) changing the number of waves L, where $M = 10$ and $K = 7$, (b) changing the number of antennas M, where $L = 3$ and $K = 7$, (c) changing the number of frequency bins K, where $M = 10$ and $L = 3$.

4.5.1 Simulation Parameters

The received signals are divided into Q blocks with the number of samples in one block being equal to the number of DFT points. Here, we set Q to 100 and DFT points to 256. We use the frequency bands which are equally spaced K frequency bands between ω_L and ω_H from DFT output. We define the DFT output signal of frequency band ω_i is $\boldsymbol{x}_q(\omega_i), \{i \in 1 \sim K\}$ for the qth block. Then, the estimated

Table 4.2: Simulation parameters.

Item	Symbol	Quantity	Remarks
Antenna spacing	d	$\lambda/2$	Uniform linear array
Frequency ω_L	ω_L	$\pi/3$	The lowest frequency of signal sources (ω domain)
Frequency ω_H	ω_H	$2\pi/3$	The highest frequency of signal sources (ω domain)
Parameter α_{th}	α_{th}	9	

correlation matrix of the frequency band ω_i is

$$\hat{\boldsymbol{R}}(\omega_i) = \frac{1}{Q}\sum_{q=0}^{Q-1} \boldsymbol{x}_q(\omega_i)\boldsymbol{x}_q^H(\omega_i). \tag{4.21}$$

Then, we calculate the signal subspace matrix $\boldsymbol{F}_i$ and the noise subspace matrix $\boldsymbol{W}_i$ from EVD of the correlation matrix $\hat{\boldsymbol{R}}(\omega_i)$, and estimate the DOA of incoming wideband signal sources by using WS-TOPS and each conventional method described in Section 4.2.

The statistical performance was evaluated by performing 500 Monte Carlo runs for each algorithm. The fixed simulation parameters to be used in the simulations are shown in Table 4.2. The number of antennas (M), that of signal sources (L), and that of frequency bands (K) are shown in the caption of each figure. λ is the wavelength corresponding to the highest frequency component of the received wideband signals. Note that the signal power on each frequency between ω_L and ω_H changes randomly for each simulation. This means that the efficient frequency band of each signal sources also changes randomly with each simulation.

4.5.2 Spatial Spectrum

Fig. 4-2 shows the spatial spectrum calculated by each method for four scenarios, where SNR of each incoming signal source is 5 dB. The details of the scenarios are described in the caption of the figure. The spatial spectrum of each method has some sharp peaks at the true directions, which are indicated as dotted lines in the figures.

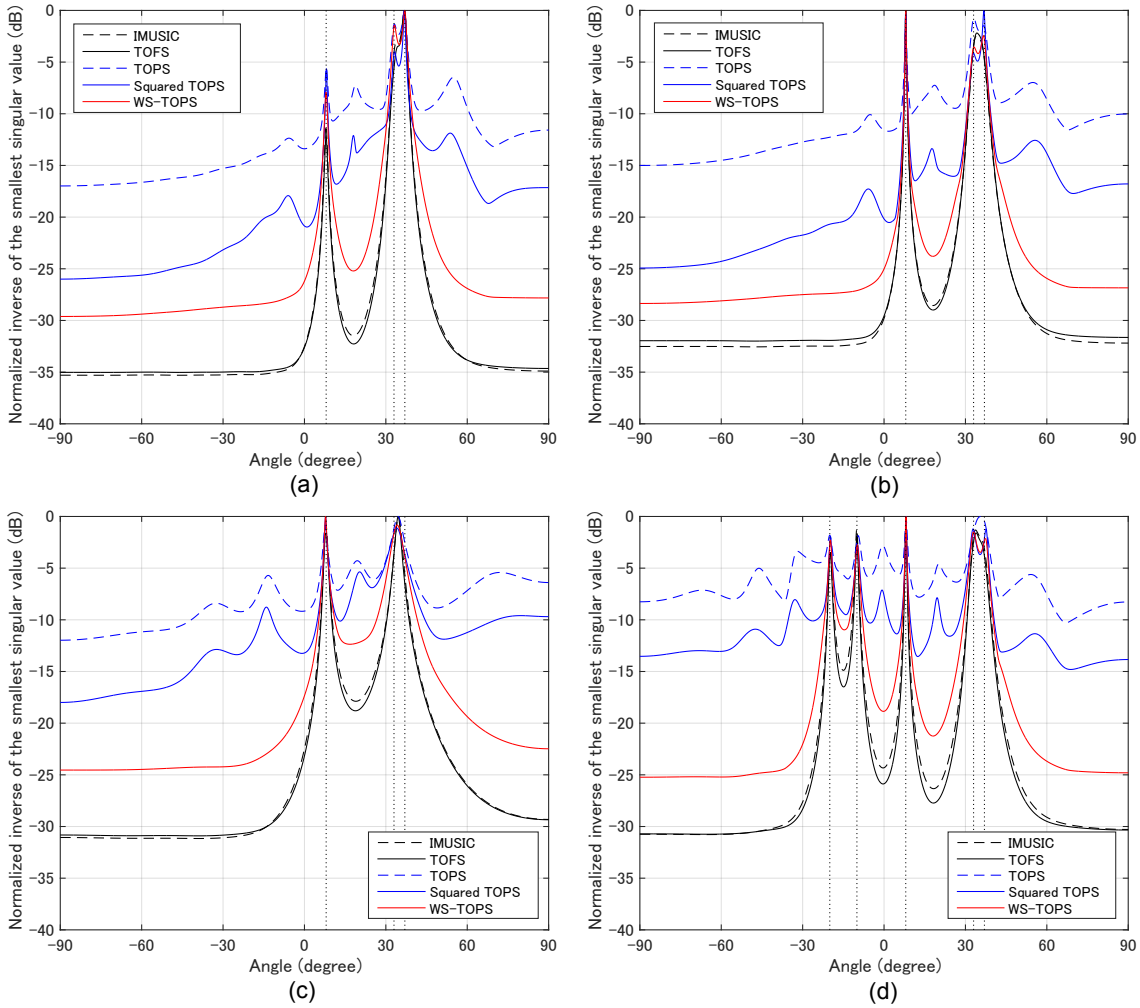

Figure 4-2: Examples of spatial spectrum on (a) $M = 10, K = 7$, and $L = 3$ (8 deg., 33 deg., and 37 deg.), (b) $M = 10, K = 15$, and $L = 3$ (8 deg., 33 deg., and 37 deg.), (c) $M = 6, K = 7$, and $L = 3$ (8 deg., 33 deg., and 37 deg.), and (d) $M = 10, K = 7$, and $L = 5$ (-20 deg, -10 deg, 8 deg., 33 deg., and 37 deg.).

We can see that WS-TOPS can suppress all undesirable false peaks in the spatial spectrum, while the spatial spectrum of TOPS and Squared TOPS have some false peaks. These false peaks in the spatial spectra of TOPS based methods have same peak level as those of true peaks, therefore they cause false detections. From Fig. 4-2, it is also found that WS-TOPS can detect closely spaced signal sources at 33 deg. and 37 deg., while IMUSIC and TOFS cannot.

As shown in Fig. 4-2, WS-TOPS can hold the capability to suppress false peaks for all scenarios. The results prove that the WS-TOPS is robust to the system pa-

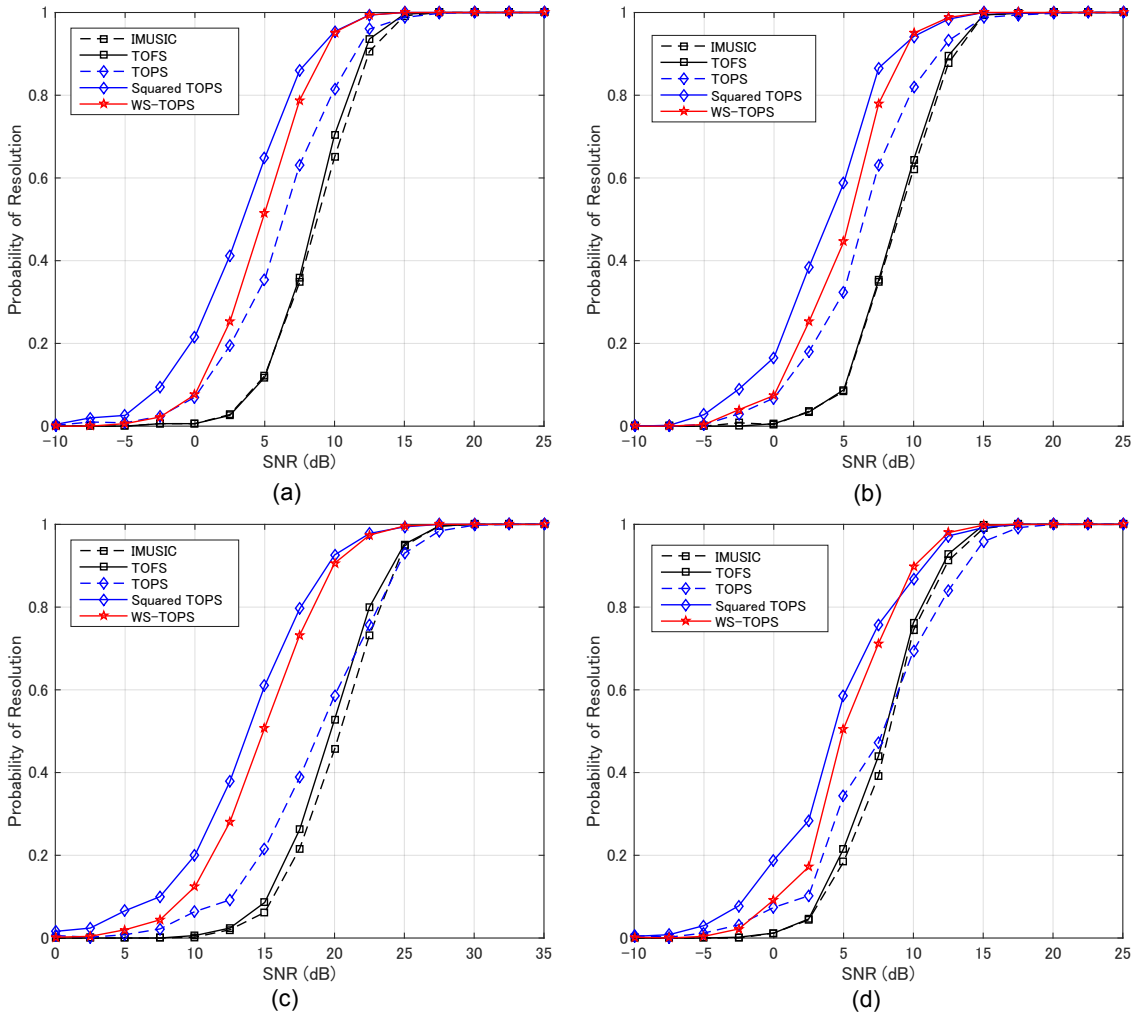

Figure 4-3: Examples of Resolution on (a) $M = 10, K = 7$, and $L = 3$ (8 deg., 33 deg., and 37 deg.), (b) $M = 10, K = 15$, and $L = 3$ (8 deg., 33 deg., and 37 deg.), (c) $M = 6, K = 7$, and $L = 3$ (8 deg., 33 deg., and 37 deg.), and (d) $M = 10, K = 7$, and $L = 5$ (-20 deg, -10 deg, 8 deg., 33 deg., and 37 deg.).

rameters, which are the number of antennas (M), that of sources (L), and that of frequency bins (K).

Regarding the computational complexity of WS-TOPS and TOPS based methods, we calculate the computational costs to obtain an inverse of the minimum singular value of each direction by using MATLAB. In the case of $M = 10$, $L = 3$, and $K = 7$, the averaged computation time of WS-TOPS($K' = 7$) is 2.1 ms, that of WS-TOPS ($K' = 2$) is 0.59 ms, that of Squared TOPS is 0.21 ms, and that of TOPS is 0.17 ms. In the case of $M = 10$, $L = 3$, and $K = 15$, the averaged computation time of

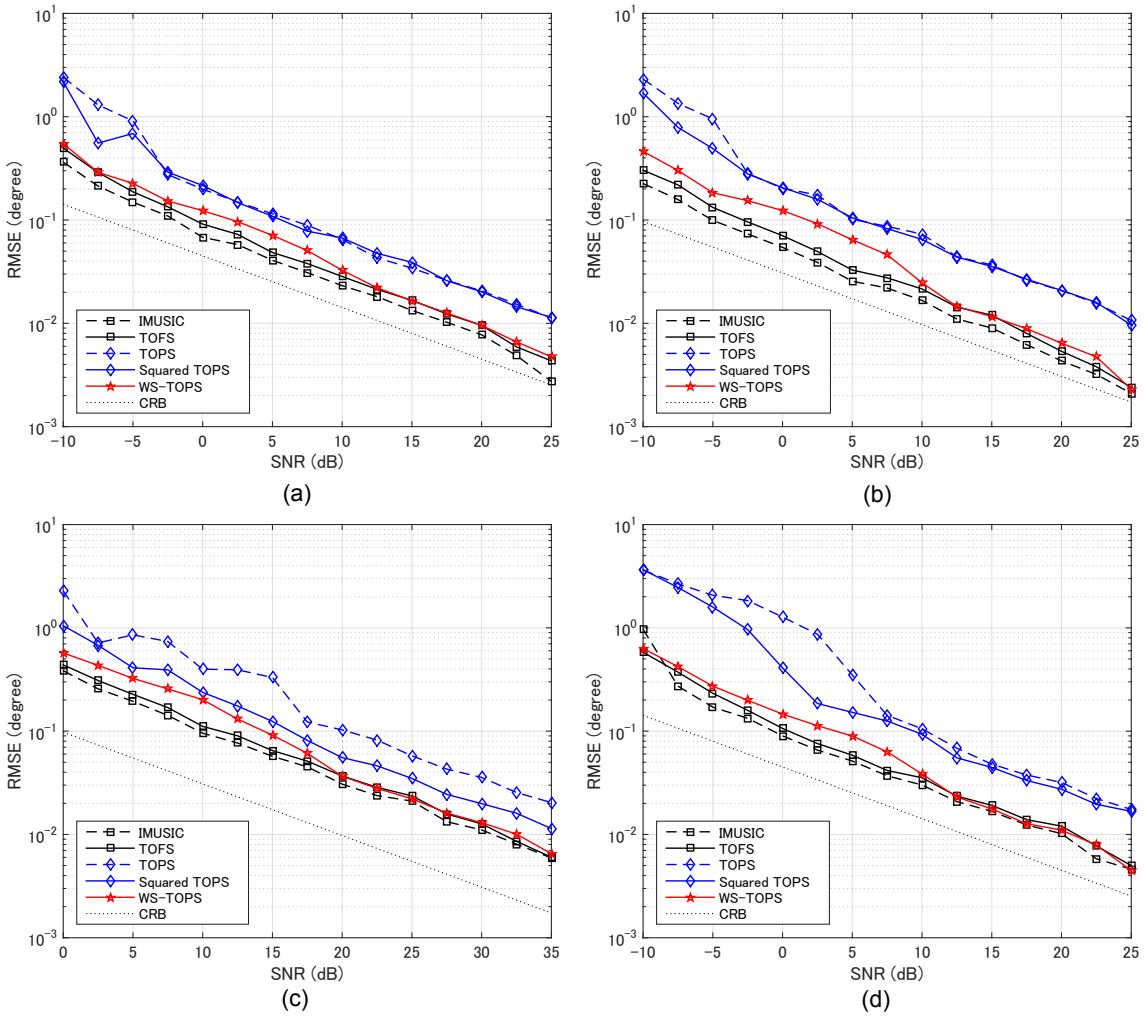

Figure 4-4: Examples of RMSEs of estimated DOA of the signal source from 8 deg. on (a) $M = 10, K = 7$, and $L = 3$ (8 deg., 33 deg., and 37 deg.), (b) $M = 10, K = 15$, and $L = 3$ (8 deg., 33 deg., and 37 deg.), (c) $M = 6, K = 7$, and $L = 3$ (8 deg., 33 deg., and 37 deg.), and (d) $M = 10, K = 7$, and $L = 5$ (-20 deg, -10 deg, 8 deg., 33 deg., and 37 deg.).

WS-TOPS ($K' = 7$) is 5.1 ms, that of WS-TOPS ($K' = 2$) is 1.47 ms, that of Squared TOPS is 0.44 ms, and that of TOPS is 0.42 ms. Although the actual computational times depend on the calculation system, the results show that the effective costs coincide with the computational complexity described in Fig. 4-1.

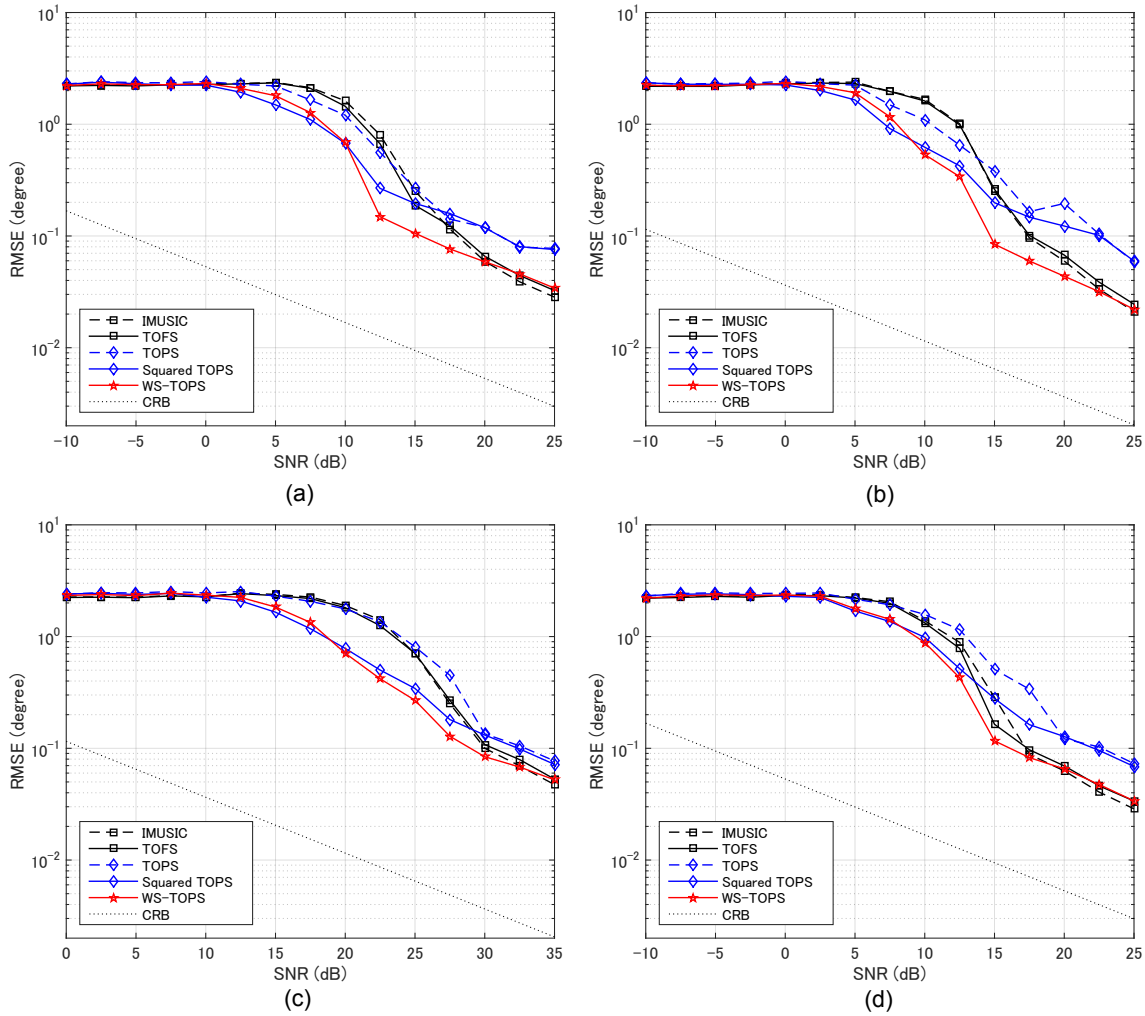

Figure 4-5: Examples of RMSEs of estimated DOA of the signal source from 33 deg. (a) $M = 10, K = 7$, and $L = 3$ (8 deg., 33 deg., and 37 deg.), (b) $M = 10, K = 15$, and $L = 3$ (8 deg., 33 deg., and 37 deg.), (c) $M = 6, K = 7$, and $L = 3$ (8 deg., 33 deg., and 37 deg.), and (d) $M = 10, K = 7$, and $L = 5$ (-20 deg, -10 deg, 8 deg., 33 deg., and 37 deg.).

4.5.3 Probability of Resolution

Fig. 4-3 shows the probability of resolution of WS-TOPS and the conventional methods, where the simulation parameters are shown in the caption of the figure. The probability of resolution denotes the probability of successful detection of all signal sources. In other words, we consider a certain result as a successful detection only when all signal sources are detected. If the number of signal sources we detect is less than the actual number of incoming signal sources, we judge the result as a false

one in terms of successful detection. As we can see from Fig. 4-3, the resolution performance of WS-TOPS is between those of Squared TOPS and TOPS. The results indicate that WS-TOPS can achieve better resolution than that of TOPS, TOFS, and IMUSIC, without dependence on the system parameters.

4.5.4 Root Mean Square Error (RMSE) of Estimated DOA

The RMSEs of the estimated DOA of the signal sources calculated by WS-TOPS and the conventional methods are shown in Figs. 4-4 and 4-5. For comparison purpose, the Cramér-Rao bounds (CRB) [15,16] is also presented in each figure. Fig. 4-4 shows DOA estimation accuracy of the signal source from 8 deg. where there is no closely spaced wideband signal sources. As we can see in Fig. 4-4, WS-TOPS can provide higher DOA estimation accuracy than that of TOPS and that of Squared TOPS in the full range of SNR. It is also found that WS-TOPS shows similar performance to TOFS and IMUSIC in high SNR region. The results that TOPS and Squared TOPS show lower accuracy of DOA estimation than that of IMUSIC coincide with the explanation in [43]. In contrast, the results show that WS-TOPS can improve DOA estimation accuracy and it comes close to that of IMUSIC and TOFS methods in high SNR region.

Fig. 4-5 shows DOA estimation accuracy of the signal source from 33 deg. where there is the closely spaced wideband signal source. From Fig. 4-5, it is found that WS-TOPS yields the best performance of DOA estimation accuracy for closely spaced wideband signal sources in full range of SNR. The results prove that the DOA estimation accuracy of WS-TOPS is better than the conventional methods and also show that the performance of WS-TOPS is robust to the system parameters.

4.6 Conclusion

In this chapter, we have proposed a new DOA estimation method for wideband signals called WS-TOPS based on Squared TOPS. WS-TOPS uses the selective weighted averaging method and the modified squared matrix method to improve DOA estima-

tion performance. The simulation results show that WS-TOPS can suppress all false peaks in the spatial spectrum, while TOPS and Squared TOPS cannot. It is also shown that the DOA estimation accuracy and the resolution performance of WS-TOPS are better than those of the conventional methods. WS-TOPS can achieve the performance without requiring initial estimates. These results prove that WS-TOPS is effective in estimating the DOA of wideband signal sources.

Chapter 5

Low Computational Complexity DOA Estimation of Wideband Signal Sources Based on Squared TOPS

5.1 Introduction

In the previous chapter, we have proposed a DOA estimation method "WS-TOPS" for wideband signal sources. While WS-TOPS can provide high DOA estimation performance, it requires high computational costs. Therefore, in this chapter, we focus on a low computational complexity DOA estimation method based on WS-TOPS. The proposed method can reduce computational complexity with minimizing deterioration on DOA estimation performance. In particular, the method selects two frequency bands and uses the signal subspaces and the noise subspaces. Then, we conduct the orthogonality test of new squared matrix consisting of the weighted signal subspaces and the noise subspaces. Simulation results show that the proposed method can provide good resolution performance and DOA estimation accuracy with low computational complexity. Note that we consider the same system model described

in section 2.4.1.

The rest of chapter is organized as follows. In Section 5.2, the low complexity DOA estimation method for wideband signals is proposed. In Section 5.3, simulation results are presented and conclusions are provided in Section 5.4.

5.2 Proposed Method

Although WS-TOPS can achieve high DOA estimation accuracy without false peaks by using eq. (4.20), it requires high computationaal complexity which depends on the signal processing for construction of the matrix $\boldsymbol{Z}'_i$ and singular value decomposition (SVD) of the matrix $\boldsymbol{Z}'_i$. Moreover, WS-TOPS repeats the construction of the matrix $\boldsymbol{Z}'_i$ and its SVD K' times, thus WS-TOPS should require high computational complexity. In this chapter, we propose a method to realize high DOA estimation performance with low computational complexity.

TOPS based algorithm requires two frequency bands at least, because the method needs to transform the signal subspace of a frequency band to another frequency band using eq. (4.6). The parameter K' in WS-TOPS changes with the SNR as shown in eq. (4.20). Thus, the performance and the computational complexity of WS-TOPS also change with SNR. We can consider, however, that the DOA estimation performance of WS-TOPS mainly depends on the signal subspaces and noise subspaces of the frequency bands with high α_i. Therefore, to reduce the computational complexity we propose the following algorithm. First, we select two frequency bands that have top two α_i defined by eq. (4.17), which are the reliable frequency bands. Let us define them as k_1 for the frequency band with maximum α_i and k_2 for the frequency band with second α_i.

Next, we obtain $\boldsymbol{C}_{k_1k_2}(\theta)$ and $\boldsymbol{C}_{k_2k_1}(\theta)$ using eq. (4.13) and construct the new orthogonality evaluation matrix $\boldsymbol{Q}(\theta)$ as follows.

$$\boldsymbol{Q}(\theta) = \boldsymbol{C}_{k_1k_2}(\theta)\boldsymbol{C}^H_{k_2k_1}(\theta). \tag{5.1}$$

In the case of $K' = 2$, WS-TOPS requires the construction of the matrix $\boldsymbol{Z}'$,

which is an $L \times L(K-1)$ matrix, and its SVD calculation two times as shown in eqs. (4.15) and (4.20), because the signal subspaces of two different frequency bands are selected ($K' = 2$). On the other hand, the proposed method can reduce computational complexity to use only $\boldsymbol{C}_{k_1k_2}(\theta)$ and $\boldsymbol{C}_{k_2k_1}(\theta)$.

Although the proposed method uses only $\boldsymbol{C}_{k_1k_2}(\theta)$ and $\boldsymbol{C}_{k_2k_1}(\theta)$, both of the row and column elements of the matrix $\boldsymbol{Q}(\theta)$, which is obtained by multiplying $\boldsymbol{C}_{k_1k_2}(\theta)$ and $\boldsymbol{C}_{k_2k_1}(\theta)$, are close to zero simultaneously when θ is one DOA of incoming wideband signal sources. Finally, we estimate the DOA of each wideband signal source as follows.

$$\hat{\theta} = \arg\max_{\theta} \frac{1}{\sigma_Q(\theta)}, \tag{5.2}$$

where, σ_Q is the minimum singular value of the matrix $\boldsymbol{Q}(\theta)$.

As we can see in eqs. (4.13) and (5.1), the multiplying process yields the terms including $\boldsymbol{B}_{k_1}(\theta)$ and $\boldsymbol{B}_{k_2}(\theta)$ which are diagonal matrices. The TOPS based term obtained by multiplying $\boldsymbol{U}'^{H}_{k_1k_2}(\theta)\boldsymbol{W}_{k_2}\boldsymbol{W}^{H}_{k_2}\boldsymbol{U}'_{k_1k_2}(\theta)$ and $\boldsymbol{U}'^{H}_{k_2k_1}(\theta)\boldsymbol{W}_{k_1}\boldsymbol{W}^{H}_{k_1}\boldsymbol{U}'_{k_2k_1}(\theta)$ is also produced. The elements of the former terms can improve DOA estimation accuracy of a single source in low SNR regions, because the elements are similar to those of IMUSIC which shows better accuracy than TOPS based methods in low SNR region. The latter one provides improved resolution performance, because the row and column elements have sensitivity to detect the orthogonality of the signal and noise subspaces. Eventually, the process can provide the resolution performance similar to Squared TOPS with improved DOA estimation performance in low SNR regions, although the DOA estimation performance slightly decreases compared to WS-TOPS due to less use of the frequency bands.

Regarding the computational complexity, matrix multiplication operations for calculation are considered. The computing process of the covariance matrix $\boldsymbol{R}_{xx}$ and that of EVD are required for all the methods described in Section 2.4. It is also obvious that the computational complexity of IMUSIC, which does not require the SVD process, is lower than those of the other methods. Therefore, we focus on the

computational complexity of TOPS, Squared TOPS, and WS-TOPS. The dominant factors of the computational complexity of TOPS based algorithms are the computing processes of constructing the orthogonality evaluation matrices and SVD of them. Since it is known that the number of computations for an $M \times M$ SVD is $O(M^3)$ and that for multiplication of $M \times L$ matrix and $L \times K$ matrix is $O(MLK)$ [86], the computational complexity of each method is obtained as shown in Table 5.1. Figures 5-1 and 5-2 show the computational complexity vs. the number of signal sources and the number of antennas, respectively. As we can see in Figs. 5-1 and 5-2, the proposed method can reduce computational complexity considerably, in particular the computational complexity of the proposed method is lower than that of the original TOPS.

Table 5.1: Computational complexity.

Algorithm	Complexity	
	Calculation for $\boldsymbol{D}$, $\boldsymbol{Z}$, $\boldsymbol{Z}'$ and $\boldsymbol{Q}$	Calculation for SVD
TOPS	$O(LM(M-L)(K-1))$	$+O(L^2(M-L)(K-1))$
Squared TOPS	$O(\{2LM(M-L)+L^2(M-L)\}(K-1))$	$+O(L^3(K-1))$
WS-TOPS	$O(\{2LM(M-L)+L^2(M-L)\}(K-1)K')$	$+O(L^3(K-1)K')$
Proposed method	$O(2\{2LM(M-L)+L^2(M-L)\}+2M(M-L)+(M-L)+L^3)$	$+O(L^3)$

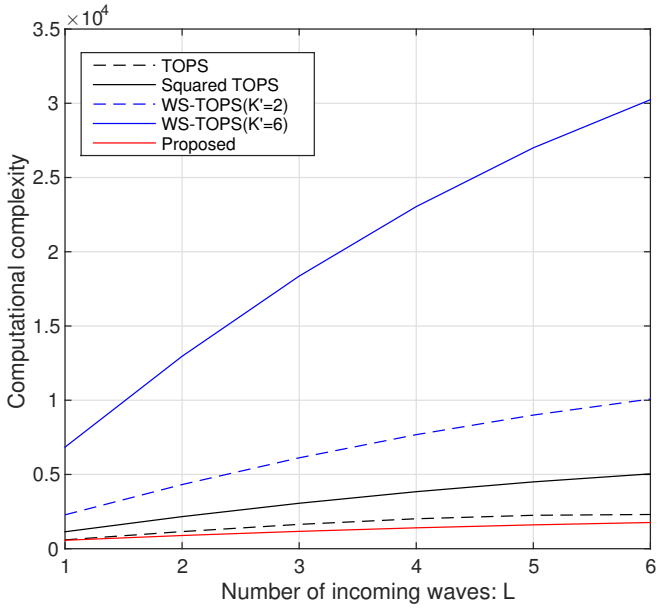

Figure 5-1: Computational Complexity vs. the number of incoming waves L, where $M = 10$ and $K = 7$.

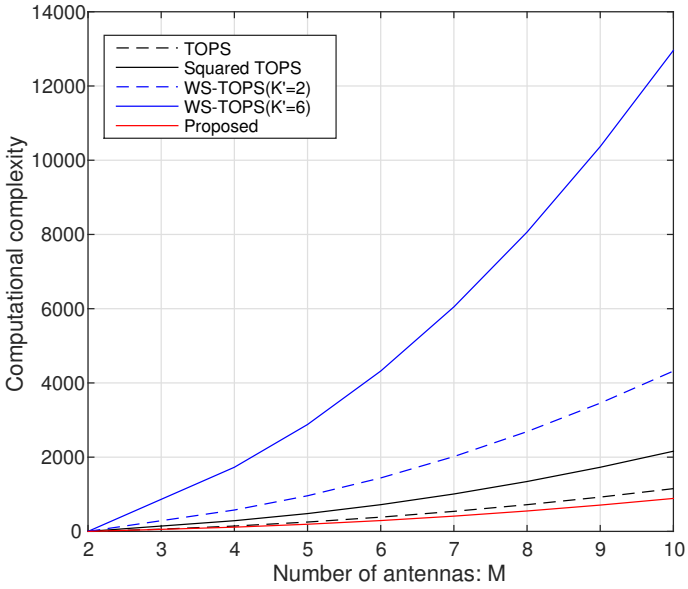

Figure 5-2: Computational Complexity vs. the number of antennas M, where $L = 2$ and $K = 7$.

5.3 Numerical Results

The proposed method has been evaluated through numerical simulation by performing 300 Monte Carlo runs with the other conventional methods described in Section 2.4. Regarding WS-TOPS, we also calculated WS-TOPS with fixed K' to evaluate the performance of proposed method with WS-TOPS in a certain K' condition.

5.3.1 Simulation Parameters

Here, we select WS-TOPS with $K' = 2$ for comparison, because the proposed method uses two frequency bands. We consider uniform liner array with ten antennas. The received signals are divided into Q blocks with the number of samples in one block being equal to that of DFT points. In this chapter, we set Q to 100 and DFT points to 256. We use the frequency bands which are equally spaced K frequency bands between ω_L and ω_H from DFT output. We define the DFT output signal of frequency band ω_i as $\boldsymbol{x}_q(\omega_i), \{i \in 1 \sim K\}$ for the qth block. Then, the estimated

Table 5.2: Simulation parameters.

Item	Symbol	Quantity	Remarks
Number of antennas	M	10	Uniform linear array
Antenna spacing	d	$\lambda/2$	
Number of sources	L	4	
Direction of sources 1	θ_1	-10 deg	
Direction of sources 2	θ_2	12 deg	
Direction of sources 3	θ_3	33 deg	
Direction of sources 4	θ_4	37 deg	
Frequency ω_L	ω_L	$\pi/3$	The lowest frequency of signal sources (ω domain)
Frequency ω_H	ω_H	$2\pi/3$	The highest frequency of signal sources (ω domain)
Bandwidth of each source	Bw	$\pi/3$	$\pi/3 \sim 2\pi/3$ (ω domain)
Parameter α_{th}	α_{th}	10	for WS-TOPS
Parameter β	β	40	for WS-TOPS and the proposed method
Number of frequency bands	K	7	

correlation matrix of the frequency band ω_i is

$$\hat{\boldsymbol{R}}(\omega_i) = \frac{1}{Q}\sum_{q=0}^{Q-1} \boldsymbol{x}_q(\omega_i)\boldsymbol{x}_q^H(\omega_i). \tag{5.3}$$

Then, we calculate the signal subspace matrix $\boldsymbol{F}_i$ and the noise subspace matrix $\boldsymbol{W}_i$ from EVD of the correlation matrix $\hat{\boldsymbol{R}}(\omega_i)$, and estimate the DOA of incoming wideband signal sources by using the proposed method and each conventional method described in Section 2.4.

To demonstrate the DOA estimation accuracy and the resolution performance of the proposed method, we assume that there are four wideband siganal sources. The simulation parameters to be used in the simulations are listed in Table 5.1. λ is the wavelength corresponding to the highest frequency component of the received wideband signals. The parameters α_{th} and β are determined based on pre-simulations.

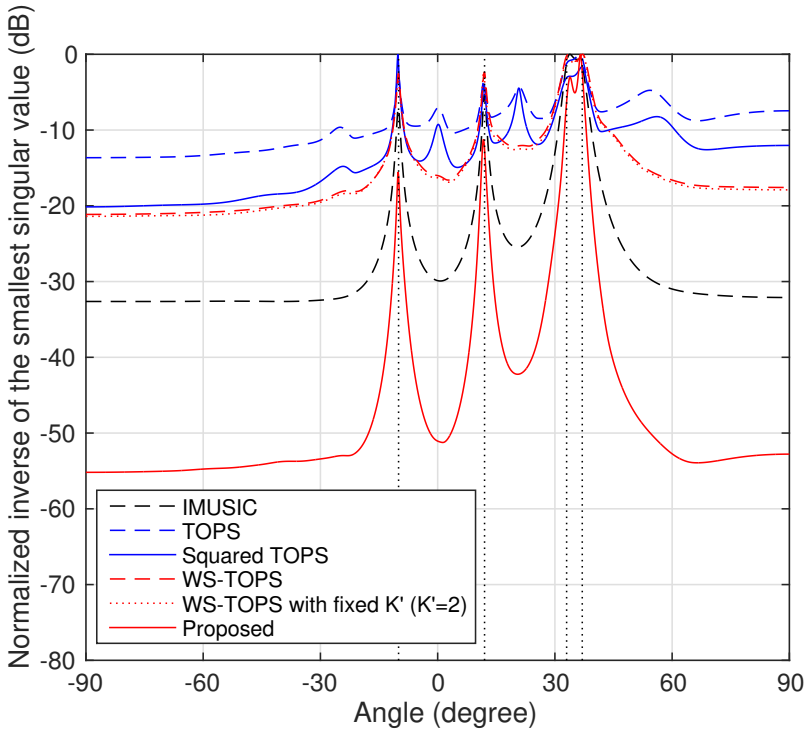

Figure 5-3: Examples of the spatial spectrum of the proposed method and the conventional methods, where SNR of each incoming signal sources is 5 dB.

5.3.2 DOA Estimation Performance

Figure 5-3 shows the spatial spectrum of each method, where SNR of each incoming signal source is 5 dB. The normalized inverse of the smallest singular value shows that each spectrum has some sharp peaks at the true directions, which indicated as dotted lines in the figure. It is found that the proposed method and WS-TOPS can suppress all false peaks while TOPS and Squared TOPS have some false peaks. It is also shown that the TOPS based method, the proposed method, WS-TOPS and Squared TOPS, can detect closely spaced signal sources at 33 deg. and 37 deg., while IMUSIC cannot. It means that the proposed method can keep resolution performance with low computational complexity.

Figure 5-4 shows the resolution performances of each method. The probability of resolution denotes the probability that all signal sources are resolved. As we can see in the figure, the proposed method achieves the same resolution performance as WS-TOPS, WS-TOPS ($K' = 2$), and Squared TOPS. The figure also shows that

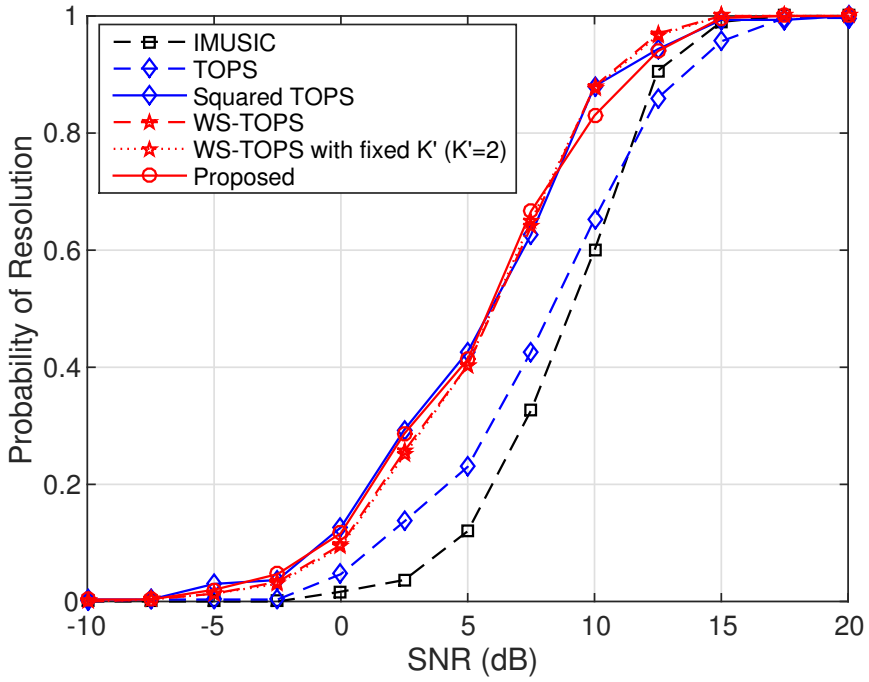

Figure 5-4: Resolution performance of the proposed method and the conventional methods.

the resolution performance of the proposed method is better than those of the other conventional methods: TOPS and IMUSIC.

Figures 5-5 and 5-6 show root mean square errors (RMSE) of the estimated DOA of the signal sources 1 and 2, respectively. $RMSE_l$ which is the RMSE of the l th signal source is calculated by the following equation.

$$RMSE_l = \sqrt{\frac{1}{T}\sum_{t=1}^{T}(\hat{\theta}_{l,t} - \theta_l)^2}, \tag{5.4}$$

where T is the number of simulation runs and θ_l denotes the true direction of the l th signal source, and $\hat{\theta}_{l,t}$ denotes the estimated one of the t th simulation run, which is the direction of the nearest peak to the true direction. Even if we detect less signals than the actual number of signal sources, we use the nearest direction as the estimated one. This means that the calculations to obtain the RMSE of closely spaced signals use the same direction when they cannot be resolved each other. As we can see in Figs. 5-5 and 5-6, IMUSIC shows the best performance and WS-TOPS shows the

second best in terms of DOA estimation accuracy. The performance of WS-TOPS ($K' = 2$) is as good as that of WS-TOPS except for high SNR region. It indicates that the DOA estimation performance of WS-TOPS mainly depends on the frequency bands with high α_i as we mentioned in Section 2.4. The DOA estimation accuracy of the proposed method is almost same as that of WS-TOPS and WS-TOPS ($K' = 2$) except for high SNR region. In particular, the RMSEs of the proposed method at low SNR region is lower than that of WS-TOPS owing to elements of $\boldsymbol{B}_{k_1}(\theta)\boldsymbol{B}_{k_2}^H$.

Figures 5-7 and 5-8 show that the RMSEs of the estimated DOAs of signal sources 3 and 4, respectively. From these figures, it is found that the proposed method yields the better performance of DOA estimation accuracy for closely spaced wideband signal sources than those of Squared TOPS, TOPS, and IMUSIC. It is also found that the DOA estimation accuracy of the proposed method deteriorates compared to that of WS-TOPS, because the proposed method only uses two frequency bands to reduce the computational complexity.

The simulation results prove that the proposed method can achieve good performance of DOA estimation compared to those of other conventional methods with low computational complexity.

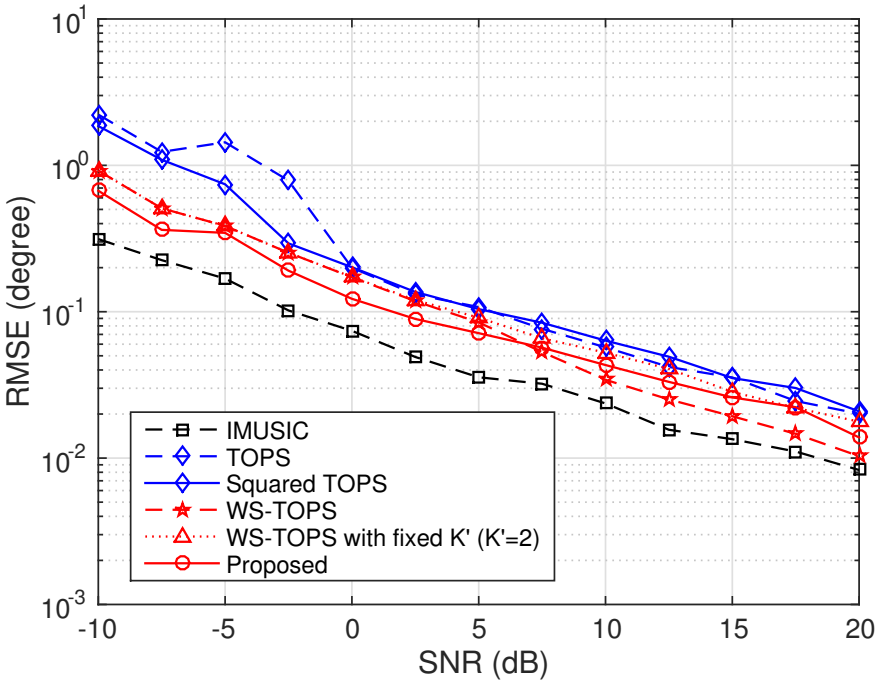

Figure 5-5: RMSEs of the estimated DOA of the signal source 1 (-10 deg.) calculated by the proposed method and the conventional methods.

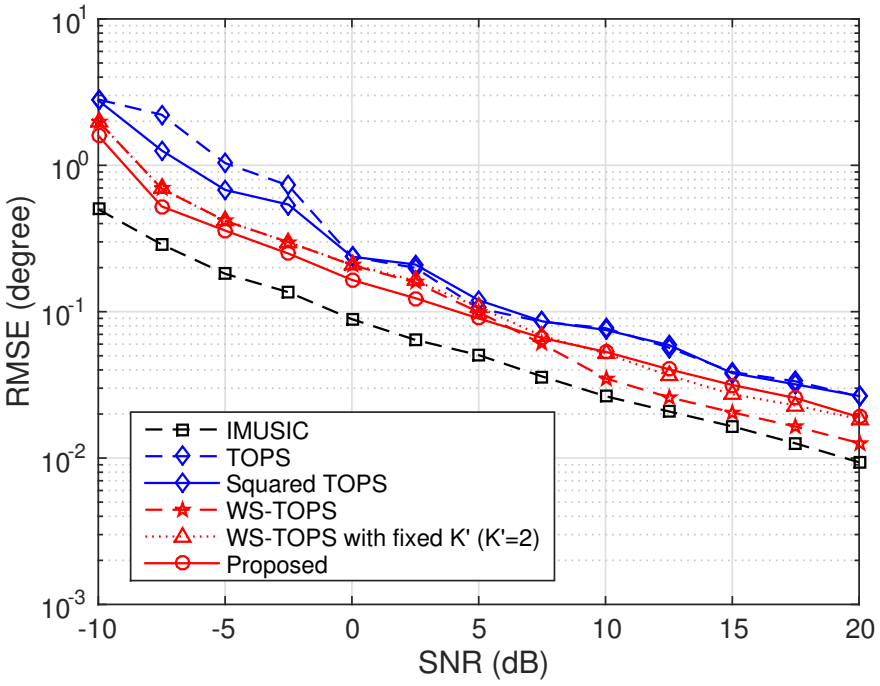

Figure 5-6: RMSEs of the estimated DOA of the signal source 2 (12 deg.) calculated by the proposed method and the conventional methods.

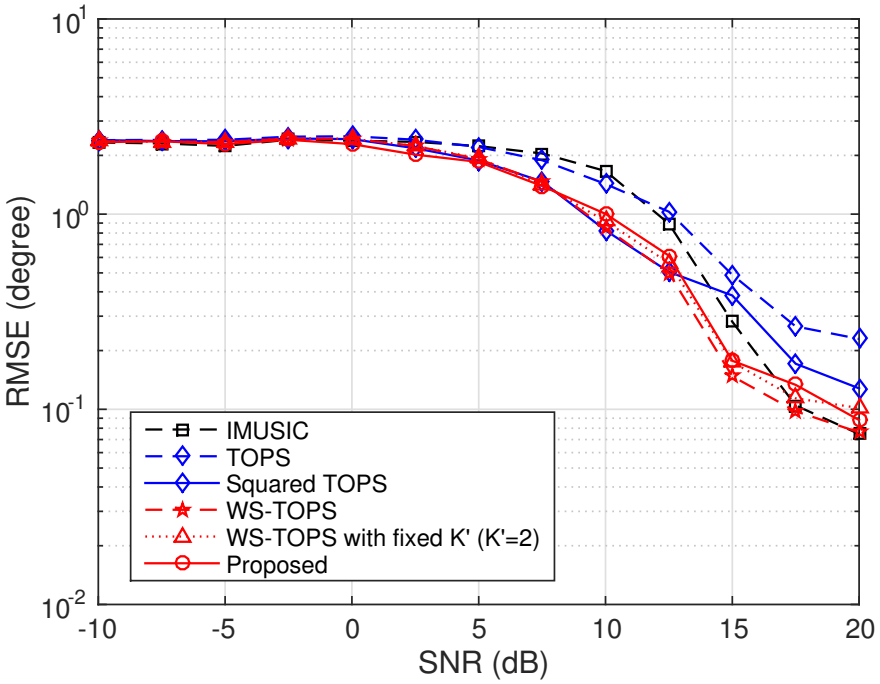

Figure 5-7: RMSEs of the estimated DOA of the signal source 3 (33 deg.) calculated by the proposed method and the conventional methods.

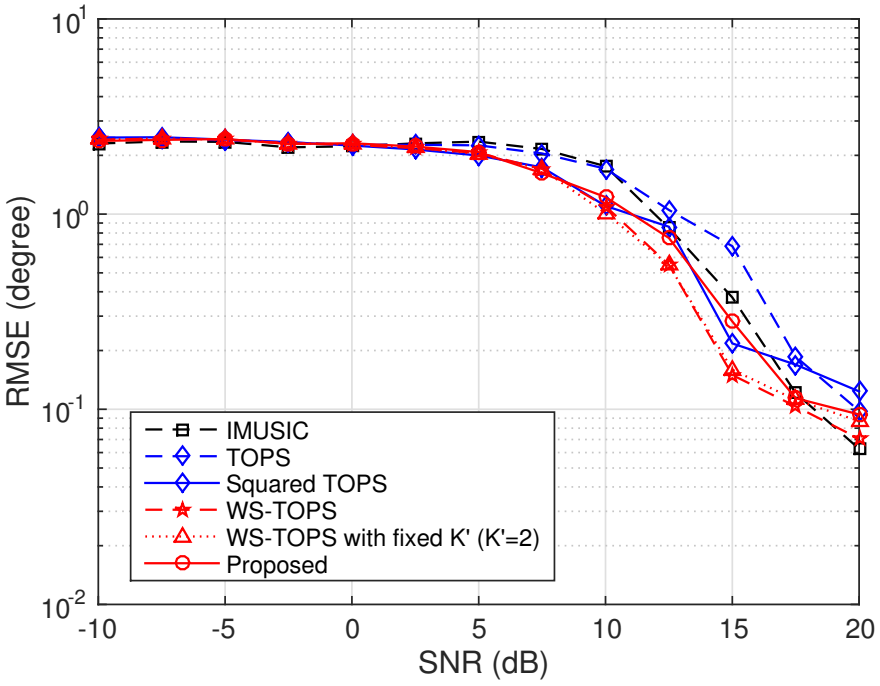

Figure 5-8: RMSEs of the estimated DOA of the signal source 4 (37 deg.) calculated by the proposed method and the conventional methods.

5.4 Conclusion

In this chapter, we have proposed a new DOA estimation method for wideband signal sources. The proposed method employs the new orthogonality evaluation matrix consisting of the signal subspaces and the noise subspaces of the two selected frequency bands to reduce the computational complexity. The numerical results show that our proposed method can provide the improved spatial spectrum without false peaks and estimate DOA of each source accurately even if multiple signal are close to each other. These results prove that the proposed method can provide high resolution performance and high accuracy of DOA estimation with low computational complexity.

Chapter 6

Conclusion

This dissertation has discussed a study on high-resolution DOA estimation method for array antenna systems. With the emergence and improvement of RF sensor systems with array antennas e.g., communication system, radar systems and electronic surveillance systems, these systems have provided remarkable improvement of performance. Therefore, as we described in Introduction, the improvement of the RF sensor systems have been attracting much attention for decades. Based on the background, we focused on the improvement of the DOA estimation performance with array antenna for multiple signal sources. In this dissertation, we proposed DOA estimation methods which can achieve the better performance in terms of DOA estimation accuracy than that of the conventional DOA estimation methods. The contribution of this dissertation is summarized as follows:

In Chapter 3, we proposed a new DOA estimation method by using the temporal spatial virtual array based on Doppler shift with adaptive PRI control. The numerical results show that our proposed method can provide the improved spatial spectrum for each target and estimate the DOA of each target accurately even if multiple moving targets exist in the search area. The simulation results also prove that the proposed method can achieve high accuracy of DOA estimation without dependence on the parameters of the targets even if the initial estimation errors exist. Although the proposed method can estimate the DOA of moving targets accurately, it requires high computational complexity cased by the iteration of spatial spectrum calculation

for each target. As a future work, we will consider the low complexity approach to estimate the DOA of moving targets with the temporal spatial virtual array.

In Chapter 4, we proposed a new DOA estimation method for wideband signals called WS-TOPS based on Squared TOPS. WS-TOPS uses the selective weighted averaging method and the modified squared matrix method to improve DOA estimation performance. The simulation results show that WS-TOPS can suppress all false peaks in the spatial spectrum, while TOPS and Squared TOPS cannot. It is also shown that the DOA estimation accuracy and the resolution performance of WS-TOPS are better than those of the conventional methods. WS-TOPS can achieve the performance without requiring initial estimates. These results prove that WS-TOPS is effective in estimating the DOA of wideband signal sources. Since the proposed method can detect any kinds of wideband signal sources, it can be applied to many types of application. For example, we can avoid the wideband interference signal with beam forming technique based on the accurate DOA of the signal source detected by the proposed method.

In chapter 5, we proposed a low computational complexity DOA estimation method for wideband signal sources. The method employs the new orthogonality evaluation matrix consisting of the signal subspaces and the noise subspaces of the two selected frequency bands to reduce the computational complexity. The numerical results prove that the proposed method can provide high resolution performance and high accuracy of DOA estimation with low computational complexity.

References

[1] L. C. Godara, "Application of antenna arrays to mobile communications. II. Beam-forming and direction-of-arrival considerations," *Proceedings of the IEEE*, vol. 85, no. 8, pp. 1195–1245, 1997.

[2] H. Krim and M. Viberg, "Two decades of array signal processing research: the parametric approach," *IEEE Signal processing magazine*, vol. 13, no. 4, pp. 67–94, 1996.

[3] M. I. Skolnik, *Introduction to radar systems*. McGraw-Hill., 2001.

[4] R. J. Mailloux, *Phased array antenna handbook*. Artech House, MA, 1994.

[5] R. Nitzberg, *Radar signal processing and adaptive systems*. Artech House, MA, 1999.

[6] W.-D. Wirth, *Radar techniques using array antennas*. IET, 2001, vol. 10.

[7] N. J. Willis, *Bistatic radar*. SciTech Publishing, 2005, vol. 2.

[8] Z. Chen, G. Gokeda, and Y. Yu, *Introduction to Direction-of-arrival Estimation*. Artech House, 2010.

[9] J. Capon, "High-resolution frequency-wavenumber spectrum analysis," *Proceedings of the IEEE*, vol. 57, no. 8, pp. 1408–1418, 1969.

[10] R. Schmidt, "Multiple emitter location and signal parameter estimation," *IEEE transactions on antennas and propagation*, vol. 34, no. 3, pp. 276–280, 1986.

[11] A. Barabell, "Improving the resolution performance of eigenstructure-based direction-finding algorithms," in *Acoustics, Speech, and Signal Processing, IEEE International Conference on ICASSP'83.*, vol. 8. IEEE, 1983, pp. 336–339.

[12] R. Roy and T. Kailath, "ESPRIT-estimation of signal parameters via rotational invariance techniques," *IEEE Transactions on Acoustics, Speech, and Signal Processing*, vol. 37, no. 7, pp. 984–995, 1989.

[13] S. A. Vorobyov, A. B. Gershman, and K. M. Wong, "Maximum likelihood direction-of-arrival estimation in unknown noise fields using sparse sensor arrays," *IEEE Transactions on Signal Processing*, vol. 53, no. 1, pp. 34–43, 2005.

[14] A. L. Swindlehurst and P. Stoica, "Maximum likelihood methods in radar array signal processing," *Proceedings of the IEEE*, vol. 86, no. 2, pp. 421–441, 1998.

[15] P. Stoica and R. L. Moses, *Spectral analysis of signals*. Pearson Prentice Hall Upper Saddle River, NJ, 2005, vol. 452.

[16] P. Stoica, E. G. Larsson, and A. B. Gershman, "The stochastic CRB for array processing: a textbook derivation," *IEEE Signal Processing Letters*, vol. 8, no. 5, pp. 148–150, 2001.

[17] D. Bliss and K. Forsythe, "Multiple-input multiple-output (MIMO) radar and imaging: degrees of freedom and resolution," in *Signals, Systems and Computers, 2004. Conference Record of the Thirty-Seventh Asilomar Conference on*, vol. 1. IEEE, 2003, pp. 54–59.

[18] F. C. Robey, S. Coutts, D. Weikle, J. C. McHarg, and K. Cuomo, "MIMO radar theory and experimental results," in *Signals, Systems and Computers, 2004. Conference Record of the Thirty-Eighth Asilomar Conference on*, vol. 1. IEEE, 2004, pp. 300–304.

[19] J. Li and P. Stoica, "MIMO radardiversity means superiority," in *Proceedings of the 14th adaptive sensor array processing workshop (ASAP06)*. Lincoln Lab, 2006, pp. 1–6.

[20] ——, "MIMO radar with colocated antennas," *IEEE Signal Processing Magazine*, vol. 24, no. 5, pp. 106–114, 2007.

[21] N. H. Lehmann, E. Fishler, A. M. Haimovich, R. S. Blum, D. Chizhik, L. J. Cimini, and R. A. Valenzuela, "Evaluation of transmit diversity in MIMO-radar direction finding," *IEEE transactions on signal processing*, vol. 55, no. 5, pp. 2215–2225, 2007.

[22] A. M. Haimovich, R. S. Blum, and L. J. Cimini, "MIMO radar with widely separated antennas," *IEEE Signal Processing Magazine*, vol. 25, no. 1, pp. 116–129, 2008.

[23] H. Godrich, A. M. Haimovich, and R. S. Blum, "Target localization accuracy gain in MIMO radar-based systems," *IEEE Transactions on Information Theory*, vol. 56, no. 6, pp. 2783–2803, 2010.

[24] I. Bekkerman and J. Tabrikian, "Target detection and localization using MIMO radars and sonars," *IEEE Transactions on Signal Processing*, vol. 54, no. 10, pp. 3873–3883, 2006.

[25] Y. Okamoto and T. Ohtsuki, "Human activity classification and localization algorithm based on temporal-spatial virtual array," in *2013 IEEE International Conference on Communications (ICC)*. IEEE, 2013, pp. 1512–1516.

[26] J. D. Taylor, *Introduction to ultra-wideband radar systems*. CRC press, 1994.

[27] F. Ahmad and M. G. Amin, "Through-the-wall human motion indication using sparsity-driven change detection," *IEEE Transactions on Geoscience and Remote Sensing*, vol. 51, no. 2, pp. 881–890, 2013.

[28] K.-T. Kim, D.-K. Seo, and H.-T. Kim, "Efficient radar target recognition using the MUSIC algorithm and invariant features," *IEEE Transactions on Antennas and Propagation*, vol. 50, no. 3, pp. 325–337, 2002.

[29] X. Zhang, L. Xu, L. Xu, and D. Xu, "Direction of departure (DOD) and direction of arrival (DOA) estimation in MIMO radar with reduced-dimension MUSIC," *IEEE communications letters*, vol. 14, no. 12, pp. 1161–1163, 2010.

[30] J. Li, Y. Xie, P. Stoica, X. Zheng, and J. Ward, "Beampattern synthesis via a matrix approach for signal power estimation," *IEEE Transactions on Signal Processing*, vol. 55, no. 12, pp. 5643–5657, 2007.

[31] P. Pal and P. Vaidyanathan, "Nested arrays: A novel approach to array processing with enhanced degrees of freedom," *IEEE Transactions on Signal Processing*, vol. 58, no. 8, pp. 4167–4181, 2010.

[32] W. Roberts, L. Xu, J. Li, and P. Stoica, "Sparse antenna array design for MIMO active sensing applications," *IEEE Transactions on Antennas and Propagation*, vol. 59, no. 3, pp. 846–858, 2011.

[33] X. H. Wu, A. A. Kishk, and A. W. Glisson, "Antenna effects on a monostatic MIMO radar for direction estimation, a Cramer-Rao lower bound analysis," *IEEE Transactions on Antennas and Propagation*, vol. 59, no. 6, pp. 2388–2395, 2011.

[34] M. N. El Korso, R. Boyer, A. Renaux, and S. Marcos, "Statistical resolution limit for source localization with clutter interference in a MIMO radar context," *IEEE Transactions on Signal Processing*, vol. 60, no. 2, pp. 987–992, 2012.

[35] R. Boyer, "Performance bounds and angular resolution limit for the moving colocated MIMO radar," *IEEE Transactions on Signal Processing*, vol. 59, no. 4, pp. 1539–1552, 2011.

[36] G. Su and M. Morf, "The signal subspace approach for multiple wide-band emitter location," *IEEE Transactions on Acoustics, Speech, and Signal Processing*, vol. 31, no. 6, pp. 1502–1522, 1983.

[37] M. Wax, T.-J. Shan, and T. Kailath, "Spatio-temporal spectral analysis by eigenstructure methods." DTIC Document, Tech. Rep., 1984.

[38] H. Wang and M. Kaveh, "Coherent signal-subspace processing for the detection and estimation of angles of arrival of multiple wide-band sources," *IEEE Transactions on Acoustics, Speech, and Signal Processing*, vol. 33, no. 4, pp. 823–831, 1985.

[39] M. A. Doron and A. J. Weiss, "On focusing matrices for wide-band array processing," *IEEE Transactions on Signal Processing*, vol. 40, no. 6, pp. 1295–1302, 1992.

[40] F. Sellone, "Robust auto-focusing wideband DOA estimation," *Signal Processing*, vol. 86, no. 1, pp. 17–37, 2006.

[41] D. N. Swingler and J. Krolik, "Source location bias in the coherently focused high-resolution broad-band beamformer," *IEEE Transactions on Acoustics, Speech, and Signal Processing*, vol. 37, no. 1, pp. 143–145, 1989.

[42] E. D. Di Claudio and R. Parisi, "WAVES: weighted average of signal subspaces for robust wideband direction finding," *IEEE Transactions on Signal Processing*, vol. 49, no. 10, pp. 2179–2191, 2001.

[43] Y.-S. Yoon, L. M. Kaplan, and J. H. McClellan, "TOPS: new DOA estimator for wideband signals," *IEEE Transactions on Signal Processing*, vol. 54, no. 6, pp. 1977–1989, 2006.

[44] K. Okane and T. Ohtsuki, "Resolution improvement of wideband direction-of-arrival estimation "Squared-TOPS"," in *Communications (ICC), 2010 IEEE International Conference on*. IEEE, 2010, pp. 1–5.

[45] H. Yu, J. Liu, Z. Huang, Y. Zhou, and X. Xu, "A new method for wideband DOA estimation," in *2007 International Conference on Wireless Communications, Networking and Mobile Computing*. IEEE, 2007, pp. 598–601.

[46] W.-K. Ma, T.-H. Hsieh, and C.-Y. Chi, "DOA estimation of quasi-stationary signals with less sensors than sources and unknown spatial noise covariance: a Khatri-Rao subspace approach," *IEEE Transactions on Signal Processing*, vol. 58, no. 4, pp. 2168–2180, 2010.

[47] D. Feng, M. Bao, Z. Ye, L. Guan, and X. Li, "A novel wideband DOA estimator based on Khatri-Rao subspace approach," *Signal Processing*, vol. 91, no. 10, pp. 2415–2419, 2011.

[48] P. Stoica, P. Babu, and J. Li, "SPICE: A sparse covariance-based estimation method for array processing," *IEEE Transactions on Signal Processing*, vol. 59, no. 2, pp. 629–638, 2011.

[49] P. Stoica and P. Babu, "SPICE and LIKES: Two hyperparameter-free methods for sparse-parameter estimation," *Signal Processing*, vol. 92, no. 7, pp. 1580–1590, 2012.

[50] Z.-M. Liu, Z.-T. Huang, and Y.-Y. Zhou, "Direction-of-arrival estimation of wideband signals via covariance matrix sparse representation," *IEEE Transactions on Signal Processing*, vol. 59, no. 9, pp. 4256–4270, 2011.

[51] J.-A. Luo, X.-P. Zhang, and Z. Wang, "A new subband information fusion method for wideband DOA estimation using sparse signal representation," in *2013 IEEE International Conference on Acoustics, Speech and Signal Processing*. IEEE, 2013, pp. 4016–4020.

[52] H. Hayashi and T. Ohtsuki, "DOA estimation in MIMO radar using temporal spatial virtual array with music algorithm," in *Signal Processing and Communication Systems (ICSPCS), 2015 9th International Conference on*. IEEE, 2015, pp. 1–6.

[53] ——, "DOA estimation using temporal spatial virtual array based on doppler shift with adaptive PRI control," *IEICE Transactions on Communications*, vol. E99-B, no. 09, pp. 2009–2018, Sep. 2016.

[54] ——, "DOA estimation for wideband signals based on weighted squared TOPS," *EURASIP Journal on Wireless Communications and Networking*, vol. 2016, Isuue 1, 2016:243.

[55] ——, "Low computational complexity direction-of-arrival estimation of wideband signal sources based on squared TOPS," *IEICE Transactions on Communications*, vol. E100-A, no. 01, pp. 1–8, Jan. 2017.

[56] O. L. Frost, "An algorithm for linearly constrained adaptive array processing," *Proceedings of the IEEE*, vol. 60, no. 8, pp. 926–935, 1972.

[57] H. L. Van Trees, *Detection, estimation, and modulation theory, optimum array processing*. John Wiley & Sons, 2004.

[58] B. Porat and B. Friedlander, "Direction finding algorithms based on high-order statistics," *IEEE Transactions on Signal Processing*, vol. 39, no. 9, pp. 2016–2024, 1991.

[59] P. Chevalier, L. Albera, A. Ferréol, and P. Comon, "On the virtual array concept for higher order array processing," *IEEE Transactions on Signal Processing*, vol. 53, no. 4, pp. 1254–1271, 2005.

[60] S. U. Pillai, Y. Bar-Ness, and F. Haber, "A new approach to array geometry for improved spatial spectrum estimation," *Proceedings of the IEEE*, vol. 73, no. 10, pp. 1522–1524, 1985.

[61] Y. I. Abramovich, D. A. Gray, A. Y. Gorokhov, and N. K. Spencer, "Positive-definite toeplitz completion in DOA estimation for nonuniform linear antenna arrays. I. Fully augmentable arrays," *IEEE Transactions on Signal Processing*, vol. 46, no. 9, pp. 2458–2471, 1998.

[62] Y. I. Abramovich, N. K. Spencer, and A. Y. Gorokhov, "Positive-definite toeplitz completion in DOA estimation for nonuniform linear antenna arrays. II. Partially augmentable arrays," *IEEE Transactions on Signal Processing*, vol. 47, no. 6, pp. 1502–1521, 1999.

[63] D. H. Johnson and D. E. Dudgeon, *Array signal processing: concepts and techniques*. Simon & Schuster, 1992.

[64] D. Pearson, S. U. Pillai, and Y. Lee, "An algorithm for near-optimal placement of sensor elements," *IEEE Transactions on Information Theory*, vol. 36, no. 6, pp. 1280–1284, 1990.

[65] J. Li, L. Xu, P. Stoica, K. W. Forsythe, and D. W. Bliss, "Range compression and waveform optimization for MIMO radar: a Cramer-Rao bound based study," *IEEE Transactions on Signal Processing*, vol. 56, no. 1, pp. 218–232, 2008.

[66] A. Khabbazibasmenj, A. Hassanien, S. A. Vorobyov, and M. W. Morency, "Efficient transmit beamspace design for search-free based DOA estimation in MIMO radar," *IEEE Transactions on Signal Processing*, vol. 62, no. 6, pp. 1490–1500, 2014.

[67] G. Cui, H. Li, and M. Rangaswamy, "MIMO radar waveform design with constant modulus and similarity constraints," *IEEE Transactions on Signal Processing*, vol. 62, no. 2, pp. 343–353, 2014.

[68] M. Wax and T. Kailath, "Detection of signals by information theoretic criteria," *IEEE Transactions on Acoustics, Speech, and Signal Processing*, vol. 33, no. 2, pp. 387–392, 1985.

[69] E. Fishler, M. Grosmann, and H. Messer, "Detection of signals by information theoretic criteria: general asymptotic performance analysis," *IEEE Transactions on Signal Processing*, vol. 50, no. 5, pp. 1027–1036, 2002.

[70] P.-J. Chung, J. F. Bohme, C. F. Mecklenbrauker, and A. O. Hero, "Detection of the number of signals using the Benjamini-Hochberg procedure," *IEEE Transactions on Signal Processing*, vol. 55, no. 6, pp. 2497–2508, 2007.

[71] J. Xin, N. Zheng, and A. Sano, "Simple and efficient nonparametric method for estimating the number of signals without eigendecomposition," *IEEE Transactions on Signal Processing*, vol. 55, no. 4, pp. 1405–1420, 2007.

[72] S. Kritchman and B. Nadler, "Non-parametric detection of the number of signals: Hypothesis testing and random matrix theory," *IEEE Transactions on Signal Processing*, vol. 57, no. 10, pp. 3930–3941, 2009.

[73] J. Li, P. Stoica, and Z. Wang, "On robust Capon beamforming and diagonal loading," *IEEE Transactions on Signal Processing*, vol. 51, no. 7, pp. 1702–1715, 2003.

[74] D. H. Johnson, "The application of spectral estimation methods to bearing estimation problems," *Proceedings of the IEEE*, vol. 70, no. 9, pp. 1018–1028, 1982.

[75] T.-J. Shan, M. Wax, and T. Kailath, "On spatial smoothing for direction-of-arrival estimation of coherent signals," *IEEE Trans. Acoust. Speech Signal Process*, vol. 33, no. 4, pp. 806–811, 1985.

[76] S. U. Pillai and B. H. Kwon, "Forward/backward spatial smoothing techniques for coherent signal identification," *IEEE Transactions on Acoustics, Speech, and Signal Processing*, vol. 37, no. 1, pp. 8–15, 1989.

[77] R. T. Williams, S. Prasad, A. Mahalanabis, and L. H. Sibul, "An improved spatial smoothing technique for bearing estimation in a multipath environment," *IEEE Transactions on Acoustics, Speech, and Signal Processing*, vol. 36, no. 4, pp. 425–432, 1988.

[78] M. Viberg and B. Ottersten, "Sensor array processing based on subspace fitting," *IEEE Transactions on signal processing*, vol. 39, no. 5, pp. 1110–1121, 1991.

[79] M. Viberg, B. Ottersten, and T. Kailath, "Detection and estimation in sensor arrays using weighted subspace fitting," *IEEE transactions on Signal Processing*, vol. 39, no. 11, pp. 2436–2449, 1991.

[80] Y. Bresler and A. Macovski, "Exact maximum likelihood parameter estimation of superimposed exponential signals in noise," *IEEE Transactions on Acoustics, Speech, and Signal Processing*, vol. 34, no. 5, pp. 1081–1089, 1986.

[81] I. Ziskind and M. Wax, "Maximum likelihood localization of multiple sources by alternating projection," *IEEE Transactions on Acoustics, Speech, and Signal Processing*, vol. 36, no. 10, pp. 1553–1560, 1988.

[82] O. Besson, F. Vincent, P. Stoica, and A. B. Gershman, "Approximate maximum likelihood estimators for array processing in multiplicative noise environments," *IEEE Transactions on Signal Processing*, vol. 48, no. 9, pp. 2506–2518, 2000.

[83] M. Wax, "Detection and localization of multiple sources via the stochastic signals model," *IEEE Transactions on Signal Processing*, vol. 39, no. 11, pp. 2450–2456, 1991.

[84] P. Stoica and K. C. Sharman, "Novel eigenanalysis method for direction estimation," in *IEE Proceedings F-Radar and Signal Processing*, vol. 137, no. 1. IET, 1990, pp. 19–26.

[85] ——, "Maximum likelihood methods for direction-of-arrival estimation," *IEEE Transactions on Acoustics, Speech, and Signal Processing*, vol. 38, no. 7, pp. 1132–1143, 1990.

[86] G. H. Golub and C. F. Van Loan, *Matrix computations*. JHU Press, 2012, vol. 3.

Appendix A

Publication List

A.1 Journals

[1] H. Hayashi and T. Ohtsuki, "Low Computational Complexity Direction-of-Arrival Estimation of Wideband Signal Sources Based on Squared TOPS," *IEICE Transactions on Communications*, Vol.E100-A, No.1, pp.219-226, Jan. 2017.

[2] H. Hayashi and T. Ohtsuki, "DOA estimation for Wideband Signals Based on Weighted Squared TOPS," *EURASIP Journal on Wireless Communications and Networking*, Vol.2016, Issue 1, 2016:243.

[3] H. Hayashi and T. Ohtsuki, "DOA Estimation Using Temporal Spatial Virtual Array Based on Doppler Shift with Adaptive PRI Control," *IEICE Transactions on Communications*, Vol.E99-B, No.09, pp.2009-2018, Sep. 2016.

A.2 Conferences Proceedings (peer-reviewed)

[1] C. Tamba, H. Hayashi, and T. Ohtsuki, "Improvement of Blink Detection Using a Doppler Sensor Based on CFAR Processing," in *IEEE Global Communications Conference (GLOBECOM)*, Washington DC, USA, Dec. 2016.

[2] H. Hayashi and T. Ohtsuki, "DOA Estimation in MIMO Radar Using Temporal Spatial Virtual Array with MUSIC algorithm," in *International Conference on*

Signal Processing and Communication Systems (ICSPCS), Cairns, Australia, Dec. 2015.

[3] H. Hayashi and T. Ohtsuki, "Performance of DOA Estimation Using Temporal Spatial Virtual Array," in *International Workshop on Vision, Communications and Circuits (IWVCC)*, Yokohama, Japan, Oct-Nov, 2015.

A.3 Conferences Proceedings (Japanese, without peer-review)

[1] H. Hayashi and T. Ohtsuki, "Improvement Method of DOA Estimation Algorithm Squared TOPS," in Proc. IEICE General Conf., Fukuoka, Japan, Mar. 2016. (in Japanese.)

[2] C. Tamba, H. Hayashi, and T. Ohtsuki, "Improvement of Blink Detection Using a Doppler Sensor Based on CFAR Processing," in Proc. IEICE Tech. Rep., Tokyo, Japan, Feb. 2016. (in Japanese.)

[3] C. Tamba, H. Hayashi, and T. Ohtsuki, "Blink Detection Using a Doppler Sensor Based on CFAR Processing," in Proc. IEICE General Conf., Fukuoka, Japan, Mar. 2016. (in Japanese.)

[4] H. Hayashi and T. Ohtsuki, "DOA Estimation for Wideband Signals by Using Weighted Squared-TOPS," in Proc. IEICE Tech. Rep., Fukuoka, Japan, Aug. 2015. (in Japanese.)

[5] H. Hayashi and T. Ohtsuki, "DOA Estimation Using Temporal-Spatial Virtual Array Based on Doppler Shift," in Proc. IEICE Tech. Rep., Tokyo, Japan, Mar. 2015. (in Japanese.)

[6] H. Hayashi and T. Ohtsuki, "Direction-of-Arrival Estimation by Using Temporal-Spatial Virtual Array Based on Doppler Shift," in Proc. IEICE General Conf., Tokyo, Japan, Mar. 2015. (in Japanese.)

[7] H. Hayashi and T. Ohtsuki, "Temporal-Spatial Virtual Array Based on Adaptive PRI Control," in Proc. IEICE Society Conf., Tokushima, Japan, Sept. 2014. (in Japanese.)

[8] H. Hayashi and T. Ohtsuki, "Temporal-Spatial Virtual Array Based on Adaptive PRI Control," in Proc. IEICE Tech. Rep., Kochi, Japan, Aug. 2014. (in Japanese.)